University of Groningen

Kapteyn Astronomical Institute

Master research project report

Determination of stellar atmospheric parameters for the X-shooter Spectral Library

Author:
Anke Arentsen

Supervisor:
Prof. dr. Scott C. Trager

September 8, 2016

Abstract

In this work, we derive stellar atmospheric parameters for the new X-shooter Spectral Library (XSL, Chen et al. 2014a,b). The spectra in XSL will be used in stellar population modeling, therefore the stars need accurate and uniform stellar atmospheric parameters. We investigate two different methods to determine these parameters, using the current version of the spectra in the library. The first method is Starfish (Czekala et al. 2015), a Bayesian inference full spectrum fitting code that extensively samples the parameter space. We find that Starfish is not suitable for the automatic determination of stellar atmospheric parameters for a few hundred stars because of its long run-time and the need for user interaction. The second method is ULySS (Koleva et al. 2009), a full spectrum fitting software that performs a relatively simple χ^2 fitting. We find that it is suitable for the mass-production of stellar atmospheric parameters and that it can produce a uniform set of parameters for XSL. We test different settings and decide to use an empirical interpolator made from the MILES spectra (Sánchez-Blázquez et al. 2006, Prugniel et al. 2011) over a wavelength range of $4000 - 5500$ Å to determine the final stellar atmospheric parameters for XSL. A new version of XSL will be available soon, and we discuss possible improvements of the current method for the final determination of the parameters.

Contents

Chapter 1

Introduction

Galaxy formation and evolution is a large field of research in astronomy, and many approaches are used to study galaxies and their origin. A very successful approach is the study of stellar populations in galaxies, because the stars in a galaxy reveal much about its formation and evolution. It is possible to apply the knowledge we have gained from the detailed study of stars in our own galaxy to the stellar populations in other galaxies. Preferably we would study the stars of another galaxy one by one, but it is frequently the case that those galaxies are too far away to obtain resolved spectroscopy of individual stars. One could, however, use the integrated light of a galaxy to study its stellar population.

The assumption can be made that the integrated light of a galaxy is the sum of the light of all its individual stars (Tinsley 1972). If there is a way to decompose the observed integrated light into the contributions from individual stars, it is possible to study the stellar content of a galaxy using its integrated light. Stellar population synthesis (SPS) models are built to do exactly this. These SPS methods fit an observed spectrum with a model spectrum that consists of a combination of spectra of different types of stars. Into these fits go many assumptions about, for example, the initial mass function, stellar evolution, dust in the galaxy and star formation history. A model galaxy spectrum can be created using these assumptions in combination with a large library of stellar spectra of different types of stars. The work described in this Thesis is a contribution to a new spectral library that is to be used in SPS modelling.

1.1 Stellar spectral libraries

A galaxy has stars of many different masses, metallicities and evolutionary stages, and all these different types have their own distinct influence on a galaxy spectrum. In order to be able to model a galaxy properly, it is important to have spectra of as many different types of stars as possible. Specific stellar spectral libraries are made for use in SPS modelling, and there are currently already several libraries available. Most of these libraries are empirical, and consist of a collection of observed stellar spectra. There are however also some theoretical libraries, which are collections of spectra produced by spectral synthesis codes. Both types of spectral libraries can be used in SPS, and each has its advantages and disadvantages.

1.1.1 Theoretical libraries

Theoretical spectra are convenient to use since it is known exactly to what type of star they belong. Spectra can be computed for any desired combination of stellar parameters, so also for rare types of stars. This is an advantage over empirical libraries, because these contain mainly stars from the Milky Way and only a few stars from close-by neighboring galaxies. Our Milky

Way has a unique star formation and metallicity history, and stars carry the imprints of this. Some combinations of metallicity and stellar mass barely occur in the Milky Way, for example very massive metal-poor stars. These stars could exist in other galaxies that have different star formation histories to the Milky Way. If we model such a galaxy using an empirical library, we can never find the right combination of Milky Way stars to fit the model because spectra for stars with different abundances than those that occur in the Milky Way are also needed. This is possible with theoretical libraries. Additional advantages of using synthetic spectra are that these spectra are usually extremely high in resolution, and they can be computed for almost any desired wavelength range. Observed spectra always suffer from a finite instrumental resolution and wavelength coverage of the spectrograph.

A disadvantage of synthetic spectra is that the spectra are not real. Stellar evolutionary models and codes have become better over the years and synthetic spectra are starting to look more and more like real spectra, but there are still problems with them. Synthetic models are limited by how well the inserted spectral line lists are, and some numerical assumptions need to be made to be able to calculate the models for example in the assumption of sphericity, the choice between local thermodynamic equilibrium (LTE) or non-LTE or simplifying to fewer than three dimensions. Using synthetic spectra to do SPS modelling is challenging; some features that are in an observed galaxy spectrum are not correctly represented by any reasonable combination of synthetic stellar spectra because some regions in the spectra are simply not recreated well (Coelho 2014). Another disadvantage is that it is computationally very expensive to run a complete stellar evolutionary code, calculate stellar interiors and atmospheres and make spectra of them. Synthetic spectra are usually calculated for a grid of different parameters, and this grid cannot be sampled very densely if there are many parameters. Therefore there are large gaps between neighbouring points in parameter space. If a spectrum in between these points is needed in SPS modelling, interpolation is necessary and interpolation is a challenging task. Interpolation is also necessary when using empirical libraries, but there are usually more stars closer to each other in the relevant parameter space.

1.1.1.1 PHOENIX library

Examples of collections of model spectra are ATLAS9 by Castelli and Kurucz (1997, 2004), the models by Coelho et al. (2005) and the new PHOENIX models[1] (Husser et al. 2013). This last library is based on the PHOENIX stellar atmosphere code. We will use this library later in this Thesis. The synthetic spectra produced by this code cover the wavelength range 500 Å-5.5μm, at extremely high resolutions of $R \approx 500\ 000$ in the optical and NIR, $R \approx 100\ 000$ in the IR and $\Delta\lambda = 0.1$ Å in the UV ($R = \frac{\lambda}{\Delta\lambda}$). It covers the stellar atmospheric parameter space from $T_{\rm eff} = 2300$ K to 12 000 K, from $\log g = 0.0$ to 6.0 and from [Fe/H] $= -4.0$ to $+1.0$. The separation of the grid points is 100 K at the lower temperatures, and 200 K above 7000 K. The surface gravity points are separated by 0.5 dex. [Fe/H] also has steps of 0.5 dex for the highest [Fe/H] values, and steps of 1.0 dex below -2.0.

1.1.2 Empirical libraries

Empirical libraries are the libraries that are most often used in SPS modelling, mainly because we prefer to use real stellar spectra to model a galaxy spectrum that is made up of spectra of real stars. Many observational programs have therefore been executed to create such libraries. Examples of existing empirical libraries are presented in Table 1.1, where for each we give the

[1]http://phoenix.astro.physik.uni-goettingen.de/

Table 1.1. Empirical stellar spectral libraries

Spectral Library (Reference)	Spectral range (nm)	Number of Stars	Resolving Power
Lick/IDS (Worthey & Ottaviani 1997)	400 – 640	460	8 – 10 Å(FWHM)
Pickles Atlas (Pickles 1998)	115 – 2500	138	500 Å(FWHM)
Lançon & Wood (2000)	500-2500	100	1100
ELODIE (Prugniel & Soubiran 2001)	390-680	1388	42000/10000
UVES-POP (Bagnulo et al. 2003)	307-1030	300	80000
STELIB (Le Borgne et al. 2003)	320-930	249	2000
CFLIB/INDO-US (Valdes et al. 2004)	346-946	1237	5000
MILES (Sánchez-Blázquez et al. 2006)	352-750	985	2000
NGSL (Gregg et al. 2006)	167-1025	374	1000
IRTF-SpeX (Rayner et al. 2009)	800-5000	210	2000

spectral range, the number of stars and the mean resolving power $R = \frac{\lambda}{\Delta\lambda}$. We will describe two of these libraries in more detail in the next sections.

1.1.2.1 ELODIE

At the time the first version of the ELODIE library (Prugniel & Soubiran 2001) was created, existing stellar spectral libraries all had low resolution or were restricted to a limited area in the stellar atmospheric parameter space. The ELODIE library aimed to improve these things in comparison to the existing libraries, and was made for two purposes. The first is for use in SPS modelling, the second for automated parametrization of stellar spectra. The ELODIE library consists of spectra of stars obtained with the ELODIE echelle spectrograph at the Observatoire de Haute-Provence. There was already an early version of the library with only FGK stars (Soubiran et al 1998), and for the full ELODIE library this FGK library was supplemented with stars from other observing programs with the same spectrograph.

The first version of the new ELODIE library had 908 spectra of 709 stars. The spectra have a resolution $R \approx 42\,000$ and cover the wavelength range $\lambda = 4100-6800$ Å. An updated version of the library is described in Prugniel et al. (2007b). This version (3.1) has better data-reduction, has been supplemented with more spectra so that the library consists of 1962 spectra of 1388 stars, and now also covers $\lambda = 3900 - 4100$ Å. There are two versions of the library, a high resolution version at $R = 42\ 000$ which is normalized to its pseudo-continuum, and the low resolution version at $R = 10\ 000$, which is given in physical flux normalized at $\lambda = 5550$ Å.

The ELODIE library has been used to create the PEGASE-HR SPS models (Le Borgne et al. 2004), which are synthetic model spectra of galaxies with a very high resolution ($R = 10\ 000$). The library has also been used to create a polynomial interpolator for the determination of stellar atmospheric parameters (Prugniel & Soubiran 2001, Wu et al. 2011).

1.1.2.2 MILES

In 2006, the new stellar spectral library MILES (Sánchez-Blázquez et al. 2006) was presented because there were still some shortcomings in the existing stellar spectral libraries. For example, the range in stellar atmospheric parameters in ELODIE was still limited, and the flux calibration for ELODIE was not excellent because of the use of an echelle spectrograph. Another existing library in the visible was CFLIB, but they could not obtain good spectrophotometry for their spectra.

MILES was made to have simultaneous moderate spectral resolution, good atmospheric parameter coverage, a wide spectral range and accurate flux calibration. The stars are observed with the Isaac Newton Telescope at La Palma. MILES has 998 stars covering 3500-7500 Å in wavelength at a mean resolution of $R \approx 2000$. This is a lower resolution than ELODIE, but it covers more of the stellar atmospheric parameter space and has increased flux calibration quality.

MILES has been used to create the Vazdekis-MILES SPS models (Vazdekis et al. 2010) and it has been used in a similar way to ELODIE for the determination of stellar atmospheric parameters (Prugniel et al. 2011).

1.1.2.3 A new spectral library

Trager (2012) reviewed all modern stellar spectral libraries that were designed for SPS modelling, and identified some points that could use some improvement. He describes five points that a good empirical stellar spectral library should have:

- Good calibrations: very good flux and wavelength calibrations are needed to create the best stellar population models. Well-derived stellar atmospheric parameters are also important.
- Lots of stars: it is important to cover the whole parameter space for stars. Stars of all different temperatures, surface gravities, metallicities and different evolutionary phases are needed.
- Moderate-to-high spectral resolution: a higher resolution makes it possible to not only model massive galaxies but also individual stellar clusters.
- Broad wavelength coverage: stars of different evolutionary phases contribute to different parts of the spectrum. To get a full view of the types of stars in a stellar population, coverage of as large a part of the spectrum as possible is preferred.
- Simultaneous observations at all wavelengths of interest: if one can observe all parts of the spectrum at the same time, the problem of variable stars is smaller.

On the basis of these points, a team began the X-shooter Spectral Library (XSL) project. This library would cover a larger part of the spectrum and at higher resolution than previously available for $\sim$ 700 stars. The X-shooter instrument (Vernet et al. 2011) makes it possible to take moderate resolution ($R \approx 10000$) spectra simultaneously over a very large wavelength range with three arms: the UVB, VIS and NIR together ranging from $3000 - 24800$ Å. We will describe XSL in more detail in the next chapter, because this Thesis is part of the XSL project.

1.2 Deriving stellar atmospheric parameters

In order to use spectra in stellar population models, it is important that the stars have good determinations of their stellar atmospheric parameters effective temperature T_{eff}, surface gravity $\log g$ and overall metallicity [Fe/H] (Prugniel et al. 2007a, Percival & Salaris 2009). Changing the three parameters has an effect on many of the indices used in stellar population modelling. For example, if the temperatures of the stars in the giant branch change, the fit of an isochrone for the stellar population will be different, which then has a strong effect on the age determination of that stellar population.

The spectrum of a star can be used to determine the stellar atmospheric parameters. Each of the three stellar atmospheric parameters has a different identifiable effect on the spectrum of a star. The effective temperature mainly shapes the continuum, but also has a large effect on the strength of the spectral lines present in the spectrum. The surface gravity mainly has an effect on the shape of spectral lines, but this effect is relatively small and temperature and metallicity also affect the shape of spectral lines (albeit in a different way). The metallicity mainly determines which spectral lines there are and how strong they are. Determining these stellar atmospheric parameters is not straightforward since a stellar atmosphere does not change linearly as a function of these parameters and there are degeneracies between the parameters.

Many different methods exist to derive stellar atmospheric parameters and each of these methods has its advantages and disadvantages. The variations of the stellar flux with wavelength can be linked to the three stellar atmospheric parameters, therefore it is possible to use photometry of stars to estimate their parameters if there are flux measurements at different wavelengths. Using photometry it is possible to determine the effective temperature very well (Infrared Flux Method, Blackwell & Lynas-Gray 1998) but the other parameters are more difficult. To get better results, one could use spectrophotometry to determine the stellar parameters. In spectrophotometry, the stellar flux is measured in many narrow photometric bands, spanning a large range in wavelength, so it is similar to very low resolution spectroscopy.

These days spectroscopy is generally used to determine stellar atmospheric parameters. With spectroscopy, the individual lines in a spectrum can be studied and used for the determination of the stellar atmospheric parameters, which increases the sensitivity to all three parameters. There is a wide variety of spectroscopic fitting methods. A common technique uses subsets of the data that are known to have useful information in them. A combination of several of these sets can be sensitive to a specific parameter. An example of such a code is `MOOG` (Sneden 1973). Another approach compares an observed spectrum with a set of model template spectra and optimizes a set of parameters, where some weighting is usually applied to specific spectral regions. Examples are the `SPC` code (Buchhave et al. 2012) and the `pPXF` code (Cappellari & Emsellem 2004). Template model spectra in these codes could be created using, for example, theoretical or empirical stellar spectral libraries. It is also possible to incorporate a complete spectral synthesis back-end into the parameter determination code. This is done in `SME` (Valenti & Piskunov 1996) for restricted wavelength ranges.

The determined stellar atmospheric parameters depend on many assumptions and model choices. Among other things, the result depends on the spectral range that is used, which model spectra are used, on the manner of interpolating these models, on whether or not the models are synthetic or empirical, on which spectral line lists are used when the models are synthetic and on the way of minimizing the difference between data and model spectrum. Taking a spectrum and analyzing it with x different spectroscopic methods will usually result in x different values for each of the three parameters. For example Jofré et al. (2010) compare stellar atmospheric parameters from the SEGUE Stellar Parameter Pipeline (SSPP: Lee et al. 2008a,b; Allende Prieto et al. 2008) with results from several other methods that use different synthetic model grids and sometimes different spectral ranges. In their Figure 7 and Table 2, they show the scatter and the offsets of the different methods with respect to each other. The scatter in the parameters ranges from 101 to 195 K for $T_{\rm eff}$, from 0.23 to 0.48 dex for $\log g$ and from 0.14 to 0.33 dex for [Fe/H]. Offsets between different determinations of the parameters range from -159 to 244 K for $T_{\rm eff}$, from -0.27 to 0.63 dex for $\log g$ and from -0.41 to 0.17 dex for [Fe/H]. These scatters and offsets represent systematic uncertainties introduced by the methods. Within a specific method it is possible to derive an internal uncertainty of the derived parameters, which mainly describes how well the method worked for a specific spectrum. It does not say anything about how close the stellar atmospheric parameters are to their physical values and about possibly present biases. The final uncertainty on the stellar atmospheric parameters of a star is a combination of the internal and systematic uncertainties.

1.3 In this Thesis

In this Thesis, we aim to find stellar atmospheric parameters for the stars in XSL. These parameters need to be good, but they also need to be uniform. The quality of the parameters clearly influences the results of the stellar population models, because when the parameters are not correct, wrong combinations of stars will be used to model stellar populations. Uniformity means that the parameters are derived with the same method for all of the stars. This is important because within one method the derived stellar atmospheric parameters are consistent with each other, whereas different methods each have their own biases and problems. It is difficult to keep track of possible biases when using stellar atmospheric parameters that are derived using different methods. If the stellar atmospheric parameters of the stars in a library are uniform, the stellar population models created from the spectra will be consistent.

Many of the stars in XSL have previously been studied, so it is possible to do a literature search for the stars in XSL and look for the best determinations of the parameters per star. This is a lot of work and requires human judgement of what the "best value" is. Furthermore, such a method would not result in a uniform sample of parameters because many different methods for the derivation of the parameters are used in the literature. Preferably we would use a method that can easily calculate the stellar atmospheric parameters for all of the stars in the same way. In this Thesis we will describe several methods and we test whether they can be used to derive uniform stellar atmospheric parameters for XSL.

We will first describe XSL in more detail in Chapter 2, then we describe two different pieces of software that can be used for the determination of stellar atmospheric parameters in Chapters 3 and 4, with a discussion of results for XSL with these methods. In Chapter 5 we present a sample of stellar atmospheric parameters for XSL and we end with a summary and conclusions in Chapter 6.

Chapter 2

The X-shooter Spectral Library

The X-shooter Spectral Library (XSL) team is making a new stellar spectral library. Improvements over existing libraries are the larger wavelength coverage, the higher resolution than many of them and a goal of very good wavelength and flux calibrations. The X-shooter instrument (Vernet et al. 2011) at UT3 of the VLT is perfect for creating a good stellar spectral library. It has the ability to simultaneously cover wavelengths from 300-2480 nm in three spectral arms (UVB, VIS, NIR), it has a resolution $R \approx 10\ 000$ and it is possible to perform good flux and wavelength calibrations of the spectra. It can also target faint stars in, for example, the Galactic Bulge and the Magellanic Clouds.

2.1 Observations

The stars in XSL were selected to cover the Hertzsprung-Russell (HR) diagram as much as possible (see Figure 2.1). The stars were observed in a "Pilot Program" and a "Large Program". The Pilot Program focused mainly on stars currently lacking in existing libraries, such as long-period variable stars, cool bright stars and carbon stars, but also had many other stars spread over the HR diagram. The Large Program filled the rest of the HR diagram with hundreds of more stars. The observations started in 2009 and were finished in 2014. A first Data Release (DR1) was published in Chen et al. (2014a,b). They describe the configuration for which the stars were observed, which resulted in the resolutions being $R \approx 7000 - 9000$ for the UVB, $R \approx 11000$ for the VIS and $R \approx 8000$ for the NIR. Every star was observed in two modes, a narrow-slit nodding mode to take the spectra and a wide-slit staring mode for the flux calibration. In the narrow-slit observations there is always some light that is lost, which results in difficulties for the flux calibration. The wide-slit observations however do have all the flux, and can be used to calibrate the flux of the nodding frames.

Every single observation of a star results in three final spectra. The UVB spectra cover $3000 - 6000$ Å, the VIS spectra cover $5500 - 10200$ Å and the NIR spectra start at 10000 Å and go up to 24800 Å. Spectra of stars of various stellar types are shown in Figure 2.2. These spectra are combined spectra from the UVB and VIS arms. Because of the way the X-shooter instrument splits the light over the three spectral arms, there are dichroic features at the edge of the individual arm spectra. These appear as strong absorption features. In the overlap region between the UVB and VIS, this usually occurs around 5700 Å; some of the spectra in the figure show gaps in this region if the feature was really strong.

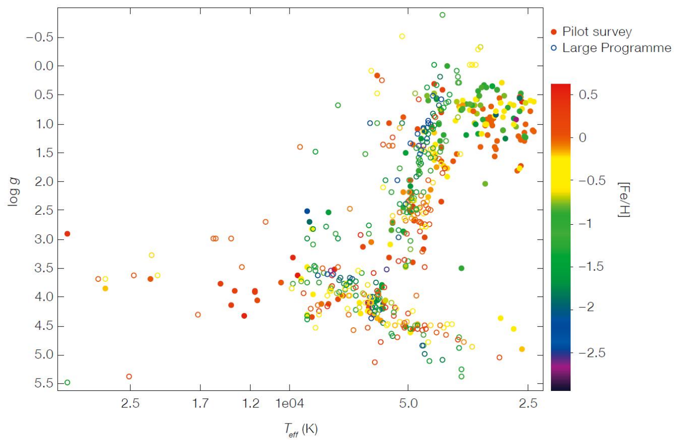

Figure 2.1 - Coverage of the HR diagram of XSL stars (image taken from Chen et al. 2014a).

Spectra of the Pilot Program were released in Data Release 1 (DR1), and contains 258 UVB and VIS spectra of 237 stars (with some stars observed multiple times to probe variability). A new version of the data reduction and calibration is currently being implemented, and will result in Data Release 2 (DR2). DR2 will have 911 observations of 679 unique stars in the UVB, VIS and NIR arms. Separate spectra for the three arms will be released, as well as merged spectra of the three arms at a common resolution. DR2 is scheduled to be released in 2017.

2.2 Subset used in this Thesis

Between DR1 and DR2 there has been an internal data release (P3). This contains the Pilot Program spectra from DR1 plus UVB, VIS and NIR spectra from stars in the Large Program that went through an intermediate version of the automatic data reduction without problems and were checked visually to have a good spectrum. We use the UVB and VIS spectra from P3 in this Thesis. P3 consists of 411 UVB (359 VIS) Large Program spectra and 198 UVB (184 VIS) Pilot Program spectra. This results in 609 UVB (543 VIS) spectra of 564 UVB (510 VIS) unique stars that could be used for stellar atmospheric parameter determination. Some of these spectra have not had absolute flux calibration applied, but these can still be used if we find a method that does not require absolute flux calibration.

2.3 Literature parameter compilation

It is useful to compare computed stellar atmospheric parameters to literature values, or use these literature values as initial guesses. We therefore compiled a list of stellar atmospheric parameters from the literature. We queried the MILES, ELODIE and PASTEL databases in VizieR[1] and as input we gave it a list of names (recognized by Simbad[2]) of all the stars in XSL.

The stellar atmospheric parameters for the MILES library are published by Cenarro et al. (2007), who present a homogenized set of literature stellar atmospheric parameters that has been corrected for systematic deviations. They corrected their literature parameters by comparing them to a reference system by Soubiran, Katz & Cayrel (1998), which has homogeneously

[1] http://vizier.u-strasbg.fr/viz-bin/VizieR
[2] http://simbad.u-strasbg.fr/simbad/

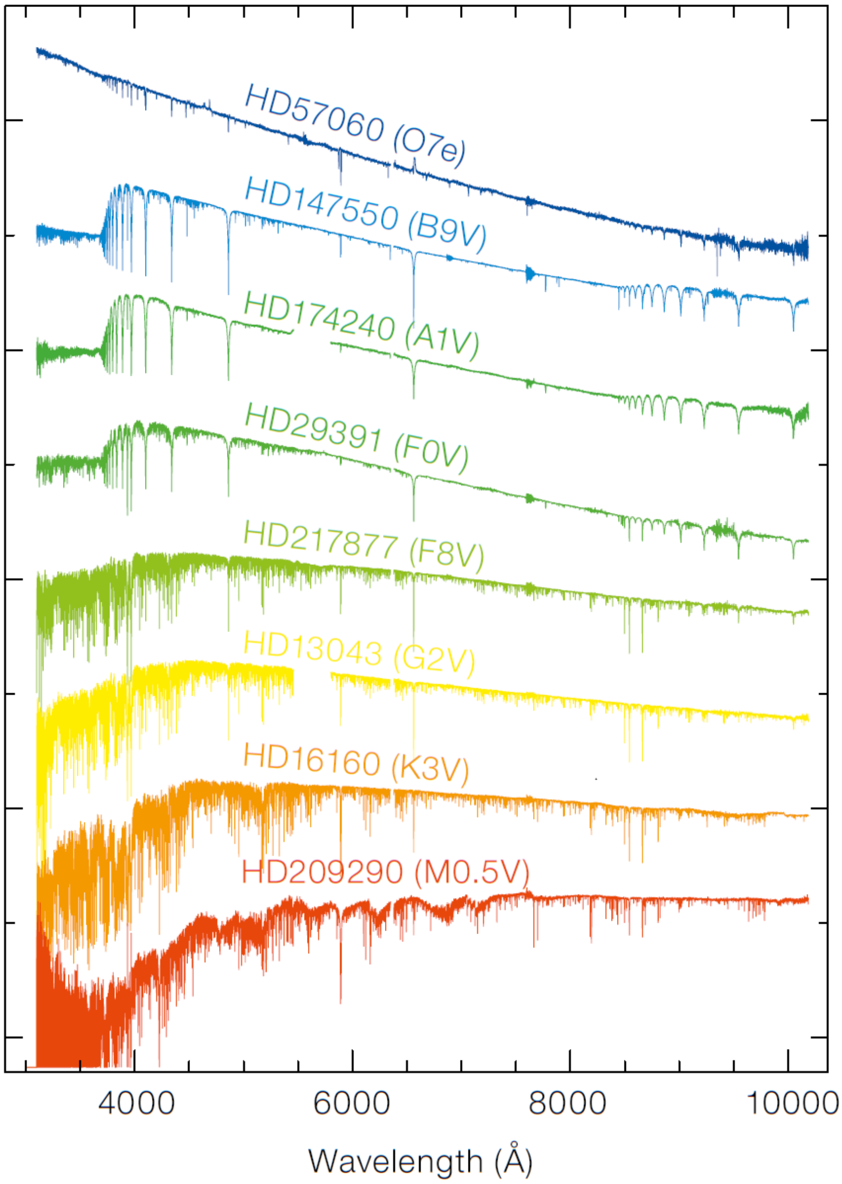

Figure 2.2 - The classic OBAFGKM temperature sequence as represented in XSL (image taken from Chen et al. 2014a).

derived stellar atmospheric parameters. For the XSL stars that overlap with this library, we adopt literature stellar atmospheric parameters from this set.

The literature parameters for the ELODIE library (Prugniel & Soubiran 2001) are derived by averaging a set of multiple literature parameters, giving less weight to old determinations and more weight to effective temperatures calculated with the Infrared Flux Method (Blackwell & Lynas-Gray 1998). If stars are not in the MILES library but are in the ELODIE library, we adopt literature stellar atmospheric parameters from this compilation.

PASTEL is a database with stellar atmospheric parameters collected from all over the literature for tens of thousands of stars. The PASTEL database has most of the XSL stars in it, but the values for the stellar atmospheric parameters are simply a collection from the literature and they are inhomogeneous. We only used the parameters from PASTEL if a star did not overlap with the MILES or ELODIE library. From PASTEL, we selected the most recently published set of all three stellar atmospheric parameters. If there was no complete set in any of the publications, we selected the most recent parameters that were present. The parameters of a few stars were added by A. Lançon (AL), when they were from references in PASTEL that were already used for some other stars.

This procedure resulted in effective temperatures from the literature for 447 stars, surface gravities for 434 stars and metallicities for 426 stars. The literature parameters are not necessarily the "correct" values, but we use this list for guesses of the parameters and to make global comparisons between our results and the literature. The literature parameters are given in the second, third and fourth column of Table 6.1 in the Appendix.

2.4 DR1 parameters

Chen (2013) describes how she derived the stellar atmospheric parameters for DR1 (presented in Figure 2.1) using two different methods. For the warm stars (O-K types) she used ULySS (Koleva et al. 2007) with the MILES interpolator (Prugniel et al. 2011). For the cool stars (M, long-period-variable stars, L, S types) she used pPXF (Cappellari & Emsellem 2004) with an interpolated theoretical grid of BT-SETTL[3] (Allard et al. 2011) models. The DR1 parameters are not uniform, have not been studied in much detail and they encompass just the Pilot Program. In this Thesis we aim to derive the parameters again, but this time for a much larger part of the XSL sample and in a uniform way for all stars.

[3]http://phoenix.ens-lyon.fr/Grids/BT-Settl/

Chapter 3

Method I: Starfish

The first software package we tested for the derivation of stellar atmospheric parameters for XSL is Starfish (Czekala et al. 2015, henceforth C15). It is a Bayesian inference code that uses full-spectrum fitting to determine (among other things) stellar atmospheric parameters. It compares the full observed spectrum to a model spectrum and not just in a few specific regions, and therefore uses as much of the information in the spectrum as possible. There are a few points in which Starfish tries to be more rigorous in its determination than previously existing codes. First, Starfish includes a spectral emulator that can create interpolated spectra from a coarsely sampled synthetic spectral library grid. Interpolating within these grids can be challenging, and this emulator approach makes it possible to keep track of the errors produced in the interpolation. A second development is that when fitting data to the models, Starfish makes use of a nontrivial covariance matrix with global and local kernels, which is more rigorous and much better at describing the residuals of the fits than simple χ^2 fitting. We briefly describe the methodology of Starfish here, and after that we describe a recipe to fit a spectrum and apply this to some XSL spectra. We end with a discussion about the results and the usefulness of Starfish for the mass-production of stellar atmospheric parameters.

3.1 Methodology

In this section we give a short description of the way Starfish works, summarizing the key parts of C15.

3.1.1 Generating a model spectrum

To fit an observed spectrum with any method, a comparison spectrum is needed. Such a spectrum is usually an interpolated spectrum from a stellar library. Starfish is built to work well with synthetic spectral libraries at its back-end, for example the previously described PHOENIX library (Husser et al. 2013). Interpolation is challenging and introduces uncertainties in the created spectrum, because spectra do not change in a straightforward way as a function of effective temperature, surface gravity and metallicity. If the interpolation mechanism is not working properly, parameters closer to grid points will be favored over values in between grid points, because the interpolation error in the latter is too large.

Czekala et al. developed an *emulator* for Starfish that can properly do this interpolation and keep track of the uncertainty. It is not necessary to go into much detail here, as it is described in detail in the Appendix of C15. In short, first spectra in a sub-region of the model library are decomposed into eigenspectra using principal component analysis (PCA). At each point in this sub-grid of the library, the spectrum can be recreated by a linear combination of the PCA eigenspectra. The weights of the eigenspectra are smooth functions of the stellar atmospheric parameters. In between the grid points, an interpolated spectrum can be created using the eigenspectra and their interpolated weights. The emulator does not produce just one spectrum for a certain combination of parameters but gives a distribution over possible interpolated spectra. By marginalizing over the distribution, Starfish includes the uncertainty in the interpolated spectrum. It keeps the information from the emulator in a covariance matrix to be used later in its likelihood calculations (Section 3.1.3).

3.1.2 Post-processing

The emulator produces model spectra f_λ that only depend on $T_{\rm eff}$, $\log g$ and [Fe/H]. They are extremely high resolution, at zero redshift, with no instrumental or physical broadening of the spectra, and they have perfect flux calibration. Real spectra are often at lower resolution, can be redshifted, have broadening of their spectral lines because of stellar rotation and instrumental resolution and they have non-perfect flux calibrations. This means that the model spectra need to be post-processed before it is possible to compare them with observed spectra.

First the interpolated spectrum is convolved with three kernels $\mathcal{F}$ that contribute to the broadening and location of spectral lines. These treat the instrumental spectral broadening (σ_v), the broadening induced by stellar rotation ($v \sin i$) and the radial velocity through a Doppler shift (v_r). After convolution, it is necessary for the model spectrum to be resampled to the number of pixels of the observed spectrum. After that there are still differences in the flux between model and data. Two of the parameters involved are Ω, which is the subtended solid angle, and the extinction A_λ. Ω is needed because synthetic spectra typically give the flux measured at the stellar surface instead of the flux measured by the observer. A_λ is needed because it alters the amount of flux at different wavelengths that reaches us from the star. The model spectrum is multiplied by a function of Ω and A_λ. In the fit in Starfish, $v \sin i$, v_r and Ω are determined simultaneously with the atmospheric parameters, and a constant is assumed for A_λ. Together these seven parameters are represented by Θ.

Furthermore there are also some imperfections in the flux calibration of the data. Starfish deals with flux calibration uncertainties by using a set of Chebyshev polynomials, where the coefficients of the polynomials are included in the overall fit as nuisance parameters. This polynomial P is multiplied with the model spectrum. Each of the spectral orders has its own coefficients ϕ_P, because the flux calibration can be dependent on wavelength and therefore differ between orders. The presence of this polynomial means that it is not necessary to have observed spectra with absolute flux calibration.

The final model spectrum is described in the next equation, where RES indicates the re-sampling operator:

$$M(\Theta, \phi_P) = RES\left(f_\lambda(T_{\rm eff}, \log g, [\mathrm{Fe/H}]) * \mathcal{F}_v^{\rm inst} * \mathcal{F}_v^{\rm rot} * \mathcal{F}_v^{\rm dop}\right) \times \Omega \times 10^{-0.4 A_\lambda} \times P\left(\phi_P\right) \quad (3.1)$$

3.1.3 Model evaluation

Now we can start to compare the post-processed model spectra with the data. The goodness of the fit between data and model is assessed by calculating a pixel-by-pixel likelihood function. Starfish adopts a multidimensional Gaussian likelihood function

$$p\left(D|M\right) = \frac{1}{\left[(2\pi)^{N_{\rm pix}} \det(C)\right]^{\frac{1}{2}}} exp\left(-\frac{1}{2} R^T C^{-1} R\right), \quad (3.2)$$

where N_{pix} is the number of pixels in the data spectrum D, M is the (post-processed) model spectrum from Equation 3.1, R are the residuals $D-M$ and C is the covariance matrix. Through this likelihood function, Starfish gives the most weight to the spectra that have the smallest residuals, and it can account for covariances in the residual spectrum through the matrix C. If the covariance matrix is diagonal (when all the pixels are independent), minimizing the above likelihood function reduces to simple χ^2 minimization. It is usually not the case that the pixels are independent and it is wise to use a more complicated covariance matrix.

In Starfish this covariance matrix consists of a number of contributions. They are given in Equation 3.3, where C_{ij} describes the covariance between two pixels i and j:

$$C_{ij} = b\ \delta_{ij}\ \sigma_i^2 + K_{ij}^G\left(\phi_{C,G}\right) + K_{ij}^L\left(\phi_{C,L}\right) + K_{ij}^E\left(\mathbf{w}\right) \tag{3.3}$$

The first term in this equation describes the Poisson noise in the pixels, scaled up by a factor of b to account for any additional data or reduction uncertainties. There is no covariance between pixels in this term. The second term is a global covariance kernel that accounts for a sort of average correlation between neighboring pixels throughout the whole spectrum. This global covariance is, among other things, produced by the oversampling of a spectrum. This kernel introduces a few hyperparameters $\phi_{C,G}$ (parameters that we are not actually interested in but need to be fitted) into the model. These hyperparameters are the amplitude and the scale of the kernel, and the functions described by them can be interpreted as many realizations of covariant residuals from a fit between model and data. The third term in Equation 3.3 is a local covariance kernel (or actually several kernels), which accounts for small regions of highly correlated residuals. These could for example be produced by spectral features that are wrong in the models. To parametrize these highly correlated regions, the hyperparameters $\phi_{C,L}$ are introduced. They describe the location, the amplitude and the width of each patch with a high local covariance. The last term is the covariance kernel coming from the emulator (Section 3.1.1), which describes the uncertainties coming from the interpolation of the models. Its hyperparameters are the different weights $\mathbf{w}$ of the eigenspectra of the PCA decomposition of the spectral library.

The way these kernels work together is shown in Figure 5 of C15, which is also included here as Figure 3.1. It shows the contributions of the first three terms of the covariance matrix, but the emulator kernel can be added on top of this in a similar manner.

3.1.4 Priors

In this Bayesian framework, it is possible to incorporate prior knowledge of parameters in the fit. The authors of Starfish generally recommend using uniform priors. They do say that it is necessary in many cases to put a prior on the surface gravity. For the local covariance kernels they adopt a prior for the widths that is flat below the combination of instrumental and physical broadening of the spectrum and smoothly tapers to zero for larger values. This ensures that the local covariance kernels cannot go to very large widths and low amplitudes, which is where the global covariance kernel should work.

3.1.5 Exploring the posterior

Now everything is ready to start the exploration of the parameter space to look for the best fit. We have three groups of parameters that need to be explored in the fitting procedure, these are

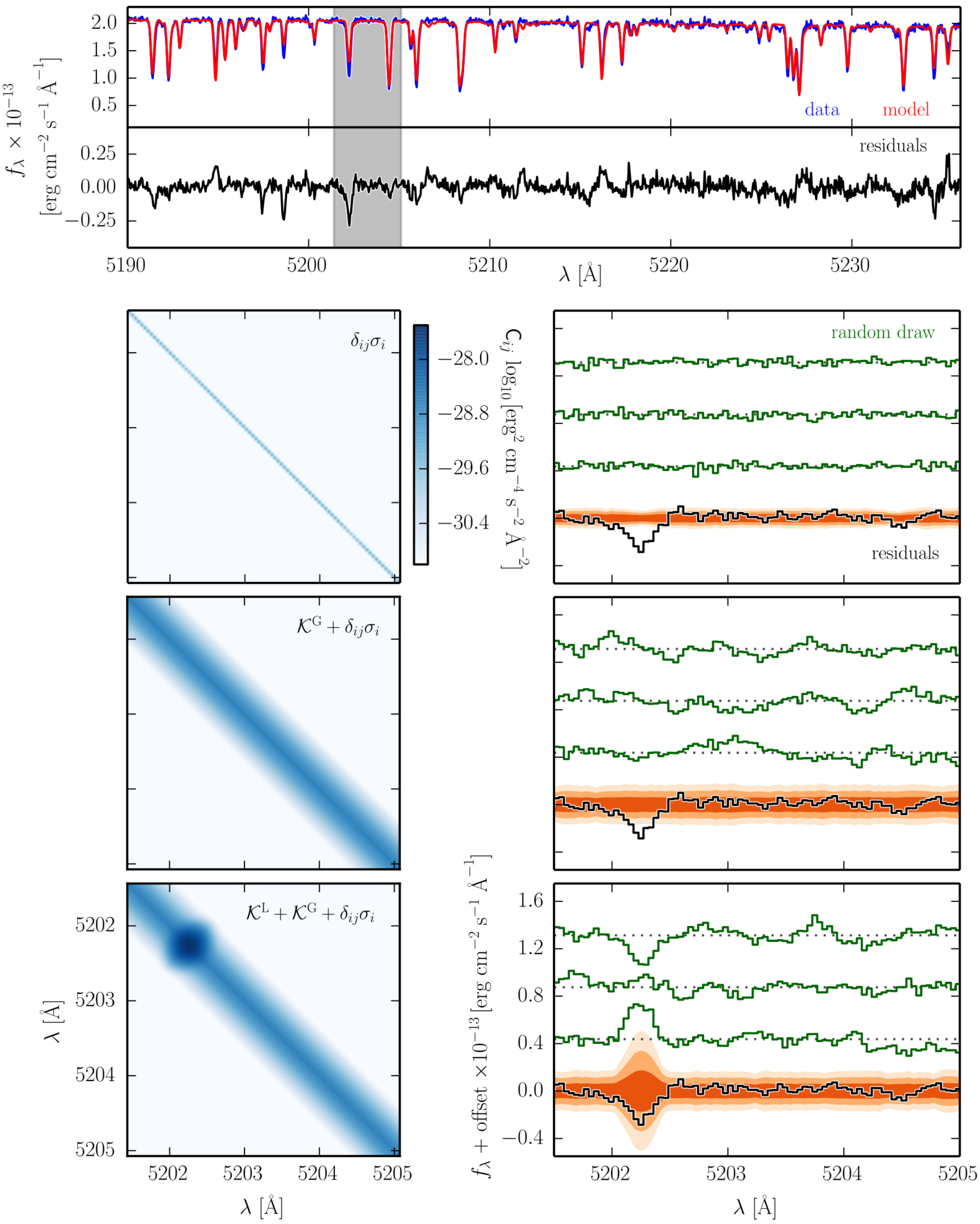

Figure 3.1 - Figure 5 from C15. In the top panel, an observed spectrum and a model spectrum are shown in blue and red respectively, and in black the residuals of the fit. The grey region indicates the region shown in subsequent panels. The left column shows the covariance matrix. Plotted in the top panel is the trivial noise matrix, in the middle panel the global covariance matrix is added and in the bottom panel a local covariance kernel is plotted on top of the others. In the right column the zoomed-in residual spectrum is plotted in black, together with example random draws from the covariance matrix shown in the left column. The orange contours represent 200 draws from the covariance matrix, with 1σ, 2σ and 3σ dispersions. It is clear that a combination of the different covariance terms is able to reproduce all of the important residual features.

the parameters that we are actually interested in knowing the values of ($\Theta = T_{\rm eff}$, $\log g$, [Fe/H], σ_v, v_z and Ω), the nuisance parameters describing the flux calibration (ϕ_P) and the covariance hyperparameters (ϕ_C). All of these parameters appear in the posterior distribution function described by Bayes' theorem

$$p(\Theta, \phi_P, \phi_C|D) \propto p(D|\Theta, \phi_P, \phi_C)p(\Theta, \phi_P, \phi_C), \tag{3.4}$$

where $p(D|\Theta, \phi_P, \phi_C)$ is the likelihood function described in Equation 3.2.

The posterior is explored and sampled in the Starfish machinery by performing Markov Chain Monte Carlo (MCMC) simulations using a blocked Gibbs sampler. In MCMC, a walk through the parameter space is performed, taking random steps (Monte Carlo) that are not dependent on the previous steps (Markov Chain). The algorithm used for this is the blocked Gibbs sampler, which can sample blocks of parameters at the same time while keeping other blocks fixed. In the Gibbs sampler, values for the parameters in each block are drawn from a multivariate distribution. These blocks are in our case the Θ, ϕ_P and ϕ_C sets of parameters. Whether or not a drawn value will be accepted is determined by the Metropolis-Hastings algorithm. If the value of the log-posterior is larger with the new parameter than with the old parameter, the new value is accepted. If the log-posterior is smaller than the previous one, the new parameter is sometimes accepted based on a random process but is usually discarded. All the parameters are then updated in blocks, and a walk through the parameter space is performed to explore the posterior. This walk should end up around the best values for the parameters and explore the region around it. The first steps in the chain are not a good representation of the underlying distribution; this is the burn-in period, which is thrown out at the end. To ensure the independence of each step in the chain, the final chain can be thinned to keep every nth value.

Step by step the exploration proceeds as follows:

1. Give initial values for the parameters Θ. Assume constant ϕ_P. Assume only the trivial noise spectrum and the spectral emulator kernel contribute to C.

2. Start Gibbs sampler. Sample Θ using the Metropolis-Hastings algorithm while keeping ϕ_P and ϕ_C constant. Update Θ.

3. For each spectral order separately: sample ϕ_P and ϕ_C while keeping Θ constant. Update ϕ_P and ϕ_C.

4. Repeat steps 2 and 3 for a large number of samples (for example 20000).

5. Repeat complete procedure with different initializations. Compute convergence diagnostic, to ensure that all of the chains have converged to the posterior distribution.

In the first few thousand iterations, ϕ_C consists only of the global kernel parameters. After the parameters have been sampled a bit, local kernels can be instantiated using an average of residual spectra from the burn-in period. This average is examined iteratively to locate the regions where a local covariance kernel is needed. The adopted threshold for inserting a local kernel is when the local residual is larger than $4 \times$ the standard deviation in the average residual spectrum. Once the locations of these kernels have been set, the Gibbs sampler is started again.

The full algorithm can be parallelized a lot. The only step that needs synchronization is the proposal of stellar parameters (step 2), the other steps can happen simultaneously for different orders of the spectrum. This makes the code a lot faster.

3.2 A per-star cookbook

We have described the method to make a model, make it ready for comparison with real data, make the fit to the data and explore the posterior of the distribution of parameters. After carefully studying the documentation and the cookbook on the Starfish page[1] and experimenting a bit, we adopted the method and steps described in this section to actually derive the stellar atmospheric parameters of a star. Here are the practical steps we follow:

1. Set up the configuration file. This file contains the paths to the models and the data spectrum, the range of the parameter space in which the model PCA grid needs to be made, the wavelength range and which orders to use, initial guesses for the Θ parameters and a first guess for the global covariance parameters.

2. Create the PCA grid, optimize and store it.

3. Perform a preliminary optimization of the Θ parameters.

4. Update configuration file with best parameters.

5. Perform a preliminary optimization of the ϕ_P parameters. A general ϕ configuration file is created.

   (intermediate step) Generate a spectrum to check if the first steps have gone well.

6. Update configuration file with the current best parameters.

7. Start sampling. First sample Θ, ϕ_P and only the global part of ϕ_C. Take for example 5000 samples.

8. Update configuration files with the new best parameters Θ. ϕ_P and ϕ_C are automatically written to a separate configuration file.

9. Generate a spectrum and residuals.

10. Instantiate local covariance kernels using residuals from fits with the burned-in and thinned chain of samples from step 7.

    (optional step) Compute the 'optimal' jump matrix, which gives the preferred size of the steps in parameter space to be taken during the sampling, derived from the samples of step 7.

11. Final sampling, which includes Θ, ϕ_P, the global and the local parts of ϕ_C. Take for example 20000 samples.

12. Repeat previous steps for different initial values in the configuration file.

13. Examine the resulting chains using walker and corner plots, and compute a convergence diagnostic. Determine final stellar atmospheric parameters and their uncertainty.

[1] `http://iancze.github.io/Starfish/current/index.html`

Table 3.1. Literature stellar atmospheric parameters for the four stars we use to test Starfish

Name	$T_{\rm eff}$ (K)	$\log g$ (dex)	[Fe/H] (dex)
CD-4911404	4676	2.88	+0.23
HD005544	4655	2.26	−0.04
HD005857	4520	2.80	−0.30
HD014625	4513	2.42	−0.00

3.3 Running Starfish on XSL stars

We test Starfish on the UVB spectra of a few stars in XSL using the method we described above. We run Starfish with the PHOENIX spectral library. We specify the XSL instrumental resolution by putting the FWHM of the instrumental profile in the UVB to 29.5 km/s in one of the configuration files. We use the standard settings of the main configuration file, if we do not describe otherwise below.

We selected the set of stars to test Starfish on to be located roughly in the same area of parameter space, so it would be possible to use the same PCA grid for all of them. These stars are given with their literature atmospheric parameters in Table 3.1. The final PCA range we chose for set of four stars was $\mathrm{T_{eff}} = [4300, 5000]$, $\log g = [1.5, 3.0]$ and $\mathrm{[Fe/H]} = [-0.5, 0.5]$.

Starfish works by fitting multiple orders of a spectrum in parallel. We did not have access to the reduced separate orders of the spectra, so we split the spectra artificially into chunks of 160 Å(1000 pixels). We also convert the fits files of the spectra to *hdf*5 files, which is the input format that Starfish uses. For optimal speed of fitting, there should be one available core on the machine per order that is fitted. In the testing phase, we had a computer with 4 cores, so we fit 4 chunks of spectrum simultaneously. We use the red part of the UVB in four chunks, covering 4800-5400 Å (artificial orders 12-15). We describe some of our results in the next section. For the sampling, we decided to take 10000 samples in step 7 and 50000 samples in step 11 of Section 3.2 to make sure we sample the parameter space well enough. We did not run Starfish multiple times on a single star with different initializations, because running it once took many hours. We used the optimal jump matrix in step 11 calculated from the 10000 samples from step 7.

3.4 Results

We present results for one star as an example. In Figures 3.2 and 3.3 we show the final corner plot and walker plot for a fit on the UVB spectrum (orders 12-15) of HD014625, produced from the chains of samples coming out of step 13 in the cookbook. We took a burn-in period of 10000 to create these images, but we did not thin the chain so that the plot would be clearer. In Figure 3.2 it is clearly seen that Starfish finds that the $T_{\rm eff}$, $\log g$ and [Fe/H] (or Z) are all degenerate with each other. It can also be seen for [Fe/H] and $\log g$ that the edge of the grid was hit while sampling (the edges were $\mathrm{[Fe/H]} = -0.5$ and $\log g = 1.5$). If we compute the Gelman-Rubin convergence diagnostic (Gelman et al. 2013) with the chain burned-in by 10000 and thinned to every $50^{\rm th}$ sample, we find that only $\log \Omega$ has not converged, which could also be seen by eye from Figure 3.3. The resulting parameters using the same burn-in and thinning are given in Table 3.2. The fit for these parameters is shown in Figure 3.4 for one of the orders.

Table 3.2. Resulting parameters for HD016425 with Starfish

Parameter	Result	Unit
$T_{\rm eff}$	4608 ± 40	K
$\log g$	1.8 ± 0.1	dex
[Fe/H]	-0.40 ± 0.05	dex
v_z	36.3 ± 0.1	km/s
$v \sin i$	7.0 ± 0.7	km/s
$\log \Omega$	-11.421 ± 0.003	

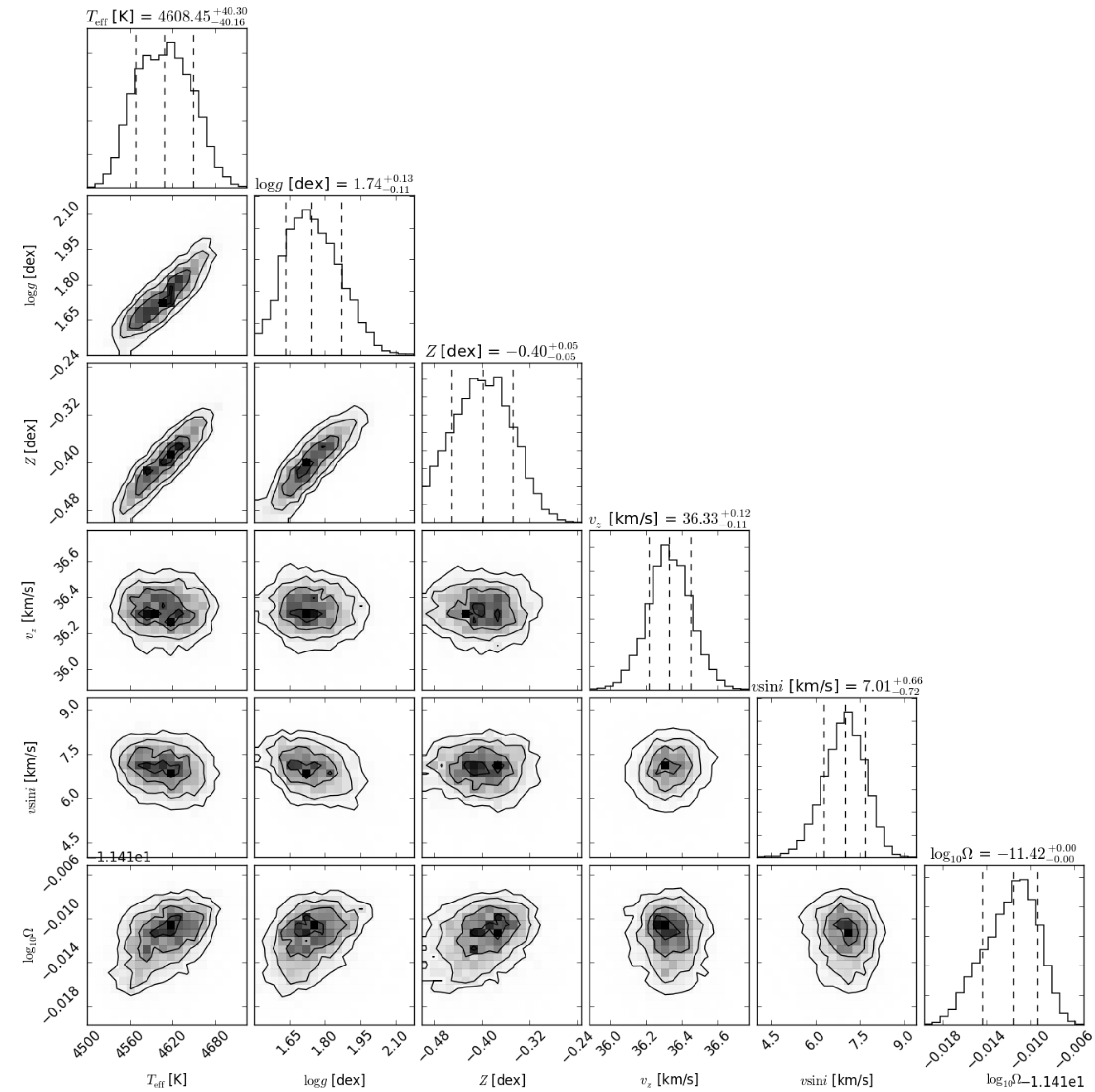

Figure 3.2 - Corner plot for HD014625 after burn-in of 10000 and no thinning. Dashed lines in the histogram plots show 1 sigma quantiles away from the mean, also represented by the numbers in the titles of the columns (rounded to two decimal places). In the surface plots, 1, 2 and 3 sigma contours are overplotted.

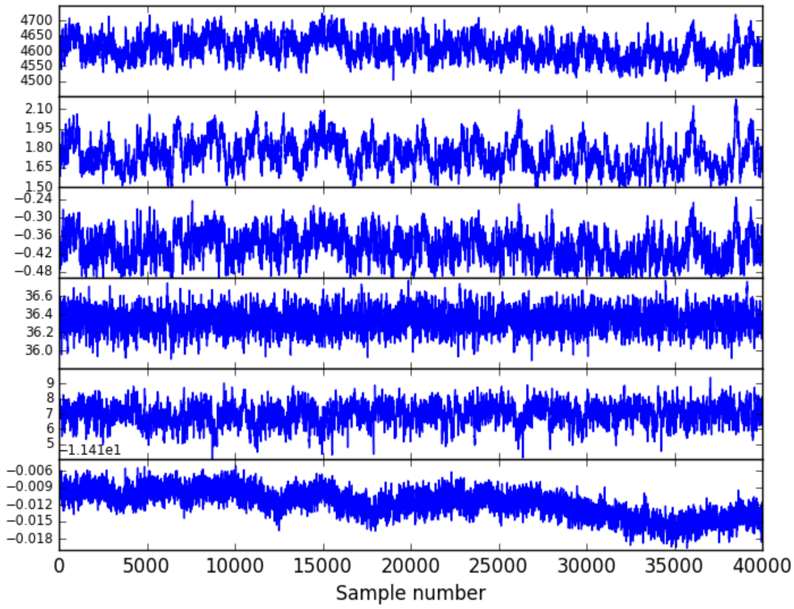

Figure 3.3 - Walker plot for HD014625 after burn-in of 10000 and no thinning. This shows the values of all six parameters in every step of the sampling. From top to bottom are $T_{\rm eff}$, $\log g$ and [Fe/H], v_z, $v \sin i$ and $\log \Omega$.

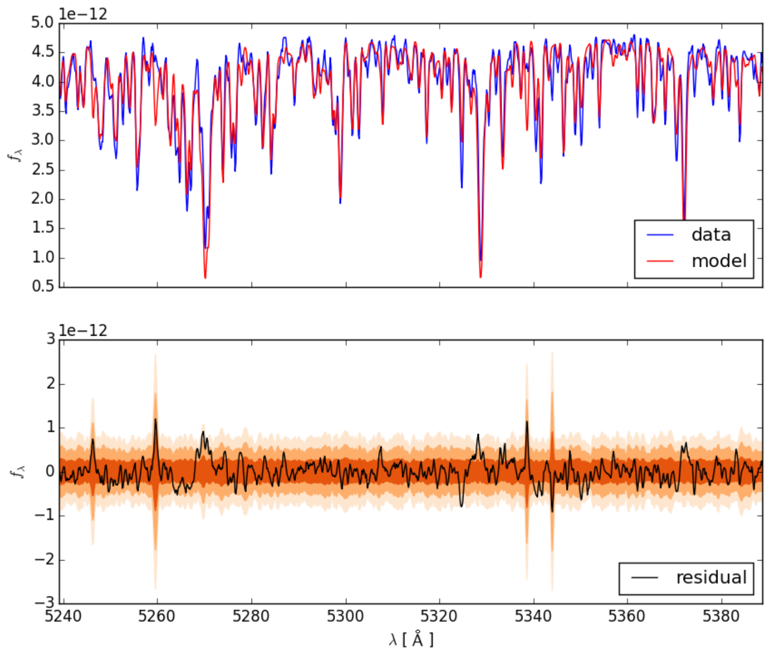

Figure 3.4 - Fit of artificial order 15 for the spectrum of HD014625, using the parameters from Table 3.4. The orange contours represent 50 draws from the covariance matrix, with 1σ, 2σ and 3σ dispersions.

3.5 Discussion

We have run Starfish on a few stars and presented detailed results for one of these. For HD014625 we do not reproduce any of the three literature stellar atmospheric parameters within the given uncertainty. It is generally the case that fitting codes for stellar atmospheric parameters underestimate errors, but Starfish is built to have a more robust determination of the errors. Even though Starfish takes out some of the systematic uncertainties because it employs a non-trivial covariance matrix, many other systematic uncertainties still remain. C15 mention three other important sources of error that should be considered but are not in Starfish: (1) data calibration; (2) the relatively small effect $\log g$ has on the spectrum; (3) assumptions about the models. For our determination this means that potential issues with the current data calibration in XSL are not influencing the errors that Starfish finds. To deal with the second problem, one could fix $\log g$ while fitting the other parameters. This is what they do in C15. When they do not fix $\log g$, they find a shift of ~ 0.9 dex to lower $\log g$ (and accompanying shifts in T_{eff} and [Fe/H]). We also find a significantly lower value for $\log g$, which could be the result of the weak dependence of the spectrum on $\log g$. The final issue is one of the models that are used. C15 performed a test in which they fitted the same star with PHOENIX and a different synthetic library (the customized Castelli & Kurucz 2004 grid). They found shifts of 150 K (higher) and 0.15 dex (higher) in [Fe/H] compared to PHOENIX. This shows that the results are highly dependent on which library is used.

One way that we could potentially improve the fit of our spectra at this point is by putting a strong prior $\log g$ or by fixing it. Unfortunately we can not do this for all our stars because we do not always have a good determination for $\log g$ from the literature, or we have no literature value at all.

3.5.1 Disadvantages of Starfish

Starfish is in theory very interesting because of its thorough treatment of model interpolation and its use of an elaborate covariance matrix. Unfortunately we have experienced several disadvantages of using Starfish to derive stellar atmospheric parameters for many stars. These disadvantages are long computation times for the PCA grid and the parameter sampling, sensitivity to initial parameter guesses and the occurrence of errors when running the code. We describe them in more detail below.

3.5.1.1 PCA grid

A first disadvantage is that the computation of the PCA grid (the first step in fitting a star) takes several hours. The optimization of the PCA is performed in a Bayesian manner involving large MCMC simulations, which are computationally quite expensive. The size of the grid that we used had a range of 700 K, 1.5 dex in $\log g$ and 1.5 dex in [Fe/H], and for such a range the optimization of the PCA grid takes approximately 3 hours. In our experience, this grid size is on the small side and one would preferably use a larger grid. Experimentation with different grid sizes was difficult because of these long computation times.

Furthermore, the sampling of the stellar atmospheric parameters will take longer in a larger PCA grid. This is because a larger PCA grid is described by more eigenspectra and therefore is harder to work with than a smaller grid. Therefore, it is not wise to fit all the stars in XSL using just one large PCA grid, and it would be better to compute a separate PCA grid for every star (or small groups of stars). If we were to divide the parameter space that is covered by XSL into chunks of 500 K, 1.5 dex in $\log g$ and 1.5 dex in [Fe/H], we would need $\sim$100 PCA grids (assuming that the XSL range is [3000,10000] K, [0.0,6.0] dex in $\log g$ and [-2.0, +1.0] in [Fe/H]). But some of the stars will fall close the edge of these grids and cannot be fit well. Therefore we should create one PCA grid per star, which significantly increases the necessary time per fit of a star.

3.5.1.2 Optimization

Guesses of $T_{\rm eff}$, $\log g$, [Fe/H], $v \sin i$ and v_z are needed to have a good starting point for the optimization and/or sampling of the parameters. For a large sample of XSL stars we do not have any literature stellar atmospheric parameters, and in particular there are no values for any of the stars for $v \sin i$ and v_z (although the latter could be computed or found in Simbad for many stars). The optimization module seems to work reasonably well for the stellar atmospheric parameters, but only if the guesses for $v \sin i$ and v_z are good. We found that the optimization of v_z and $v \sin i$ did not work properly, and only resulted in reasonable values if the original guess was already close to the final value. An example of a fit with badly optimized parameters (especially v_z) is shown in Figure 3.5. In this optimization, the initial guess for v_z was close to the optimized value, which is clearly not the correct value. For the mass-production of stellar atmospheric parameters, it is inconvenient if the automatic optimization of the parameters does not work properly.

3.5.1.3 Sampling

Performing the sampling of the parameter space (steps 7-11 in Section 3.2) is computationally very expensive. Luckily the MCMC algorithm is parallelized, but to make full use of this parallelization for a fit of a full spectrum of more than 30 orders, access to a computer cluster or supercomputer is needed. C15 claim that a full fit of just the stellar atmospheric parameters (and not completely sampling the covariances) of > 30 orders of a $R \approx 40000$ spectrum takes 2 hours. If the full posteriors for the nuisance parameters also need to be fully explored, the computation might take an order of magnitude longer. In our experience, it takes about 1.5 hours to run 10000 samples on an XSL spectrum with $R \approx 10000$ for 4 orders (on a machine with 4 cores), including a full sampling of the covariance. This cannot directly be compared to the time that C15 find since we have different resolutions and order sizes.

In combination with the optimization issue mentioned earlier, these long computation times are problematic. If the resulting "optimized" values are far away from the actual value, the

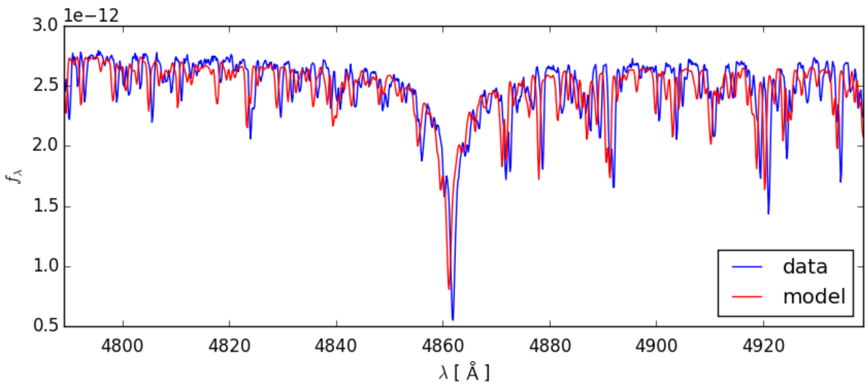

Figure 3.5 - Fit of HD19019, with the Θ parameters that result from the optimization.

sampling step will need tens of thousands of MCMC simulation steps to converge to the best value. This means a very long time of burn-in for the sampling step and fewer useful samples. One should increase the total number of samples to fully sample the underlying posterior distribution, which increases the computing time per star.

During the sampling we ran into an additional issue. There is a Cholesky decomposition of the covariance matrix performed in the code to speed up the sampling, but sometimes this decomposition results in an error. There are different sources of this error discussed on the Starfish Github page[2]. In an earlier version of the code (that we used), it was possible that the scaling factor for the global covariance level would jump to negative values, which would cause negative eigenvalues in the Cholesky decomposition of the covariance matrix. When that happened, the code would crash. Forcing this scaling factor to be positive by putting a prior on it fixed the problem. There can also be an additional cause of the Cholesky error, namely an error in numerical precision in the Cholesky decomposition of the covariance matrix. This can also result in negative eigenvalues, which then again crashes the code. We have run into this issue a few times, but there is not yet a clear solution to it.

3.6 Conclusion

The long computation times (in combination with the large number of stars and their spread throughout the parameter space) for the PCA grids and MCMC simulations, the need for good initial parameter estimates and a prior on $\log g$ and the problems with the Cholesky error are some of the difficulties for the mass-production of stellar atmospheric parameters. Additionally, sometimes there is a need for a visual inspection of the fits of the stars before starting the sampling to check whether the optimization was approximately correct. Human judgement is then needed to change the parameters in the configuration file. For fitting individual stars these things can be dealt with, but if we want to automate the process the above points make it quite complicated.

Besides these things, we also see that we do not need our stellar parameters to the precision that Starfish gives. It is not worth the time to derive stellar atmospheric parameters to such high precision if it is not necessary. Additionally, the high precision given by Starfish is partially artificial.

All these things together made us decide not to use Starfish as the main inference method for the stellar atmospheric parameters of XSL.

[2] `https://github.com/iancze/Starfish/issues/26`

Chapter 4

Method II: ULySS

The second piece of software for the determination of stellar atmospheric parameters we tested is ULySS. ULySS is short for University of Lyon Spectroscopic Software, a full spectrum fitting software package presented by Koleva et al. (2009). The software was created for two purposes: (i) the determination of stellar atmospheric parameters and (ii) the determination of star formation and metal enrichment histories of galaxies. We use ULySS to determine the stellar atmospheric parameters for XSL. It has been used for this purpose before for the stellar atmospheric parameters of the MILES, ELODIE and CFLIB spectral libraries (Prugniel et al. 2011, Wu et al. 2011). First we describe its general methodology and some interpolators, after that we describe how we run ULySS on XSL stars, then we present results for different interpolators, and we end with a discussion of these results.

4.1 Methodology

ULySS performs a χ^2 minimization between observed spectra and template spectra built from a comparison spectral library. ULySS has the option to automatically reject regions of the fit where there are large spikes in the residuals, due to for example cosmic rays, emission lines, telluric lines or bad sky subtraction (`/CLEAN` option).

The model for the template spectra is

$$Obs(\lambda) = P_n(\lambda) \times G(v_{\rm sys}, \sigma) \otimes \mathrm{TGM}(\mathrm{T_{eff}}, \log g, [\mathrm{Fe/H}], \lambda), \tag{4.1}$$

where $Obs(\lambda)$ is the observed spectrum approximated by a linear combination of several non-linear components, $P_n(\lambda)$ is an nth order Legendre polynomial and $G(v_{\rm sys}, \sigma)$ is a Gaussian broadening function parametrized by the systemic velocity $v_{\rm sys}$ and the dispersion σ. The TGM (temperature, gravity, metallicity) component is a model of a stellar spectrum for given atmospheric parameters created by interpolating a given reference spectral library.

$P_n(\lambda)$ is a polynomial that takes out the uncertainties in the shape of the spectrum and the flux calibration. The polynomial is included in the fitted model (and not done beforehand) and therefore does not bias the results for the atmospheric parameters. A test can be made to show that large values of n almost do not affect the parameters (Wu et al. 2011). See also Section 4.3.1 for our determination for the optimal value of n. Because of this polynomial, it is also possible to fit spectra that are not flux-calibrated.

$G(v_{\rm sys}, \sigma)$ is a Gaussian broadening function that is convolved with the interpolated model spectrum. $v_{\rm sys}$ represents the radial velocity of a star, and σ has both the effects of broadening caused by the instrumental resolution and physical broadening caused by the rotation of stars.

ULySS has the possibility to calculate and use the Line Spread Function (LSF), which in the simplest form is $v_{\rm sys}$ and σ as a function of wavelength. This LSF calculation can be done separately from the determination of the stellar atmospheric parameters, using the `uly_lsf` command. We need to use the LSF because there is a wavelength dependent radial velocity and broadening in our spectra.

The TGM component is described in more detail in the next section.

4.2 The interpolators

The TGM component in Equation 4.1 is produced by a spectral interpolator. An interpolator creates an interpolated spectrum from a reference spectral library. This could in principle be any empirical or theoretical library with enough stars to cover most of the parameter space. The interpolator approximates each wavelength bin of a spectrum with a polynomial function of $T_{\rm eff}$, $\log g$ and [Fe/H]. It is described by 19 to 26 terms, depending on which version of the interpolator is used. The coefficients of these terms should describe the full reference library. As an example, the first ten terms of the interpolators that we used are (Prugniel et al. 2011):

$$\begin{aligned} TGM(T_{\rm eff}, \log g, [\mathrm{Fe/H}], \lambda) =& a_0(\lambda) + a_1(\lambda) \times \log T_{\rm eff} + a_2(\lambda) \times [\mathrm{Fe/H}] \\ &+ a_3 \times \log g + a_4(\lambda) \times (\log T_{\rm eff})^2 \\ &+ a_5(\lambda) \times (\log T_{\rm eff})^3 + a_6(\lambda) \times (\log T_{\rm eff})^4 \\ &+ a_7(\lambda) \times \log T_{\rm eff} \times [\mathrm{Fe/H}] + a_8(\lambda) \times \log T_{\rm eff} \times \log g \\ &+ a_9(\lambda) \times (\log T_{\rm eff})^2 \times \log g \\ &+ a_{10}(\lambda) \times (\log T_{\rm eff})^2 \times [\mathrm{Fe/H}] \end{aligned} \tag{4.2}$$

The interpolation done with such a polynomial is generally a global interpolation, using the same interpolator for a large part of parameter space. But it is difficult to make a completely global interpolator for many stars if they range from spectral types M to O and have large differences in effective temperature. The temperature is the stellar atmospheric parameter with the largest impact on the shape of a spectrum. One would need many terms in the interpolator to make a completely global interpolator work, but adding many more terms could result in an unstable interpolator. The interpolator is therefore not a completely global interpolator but it is split into three parts, each of which has its own coefficients. The regions overlap enough so that linear interpolation between the regions is possible. The three temperature regions are (Prugniel et al. 2011):

$$\begin{aligned} &\text{OBA regime} : T_{\rm eff} > 7000K \\ &\text{FGK regime} : 4000 < T_{\rm eff} < 9000K \\ &\text{M regime} : T_{\rm eff} < 4550K \end{aligned}$$

The interpolators can be built using different types of spectral libraries. Empirical libraries have the advantage that they are made of real stars and therefore observed spectra are compared with spectra of real stars (although interpolated). The disadvantages are that these empirical libraries and thus the interpolators cover only a small part in wavelength, and they have a much lower resolution than theoretical models. Theoretical models have extremely high resolution and cover a much larger part of the full wavelength regime. But they are synthetic and not real, and it is not yet fully clear how well these models represent real stars. The question is then whether or not we can trust an interpolator made from these theoretical spectra.

We will describe three examples of interpolators below, two empirical and one theoretical.

4.2.1 Empirical interpolators: ELODIE and MILES

Two libraries that are similar to XSL are ELODIE and MILES. As described in the Introduction, these libraries are made for a similar purpose to XSL, and they have optical spectra at respectively high and medium resolution for hundreds of stars. ULySS contains spectral interpolators for both of these libraries.

The most recent version of the ELODIE interpolator is described in Wu et al. (2011). It is based on version 3.2 of the ELODIE library, which is not yet published. This new version of the library is based on the same set of stars as ELODIE 3.1 (Prugniel et al. 2007b), but there are several improvements with respect to version 3.1. The interpolator was made from the $R = 10000$ version of the library, in a few steps. A first interpolator was made using a sub-sample of stars in ELODIE 3.1 and their literature atmospheric parameters. The literature sample is inhomogeneous and often inaccurate, so this first version of the interpolator is just a starting point. With this interpolator, the observed spectra are fitted and parameters are derived for stars that did not have any spectroscopic parameters in the literature. From this, a more homogenized sample was made and a second interpolator was computed. This interpolator was used iteratively to find homogeneous atmospheric parameters for the full library. Then from these parameters and their spectra, the final internal interpolator was computed. New to this version of the ELODIE interpolator is that it is also possible to make interpolated models of stars in sparsely populated regions in the library, and it is even possible to extrapolate to regions where there are no ELODIE stars. To be able to do this, some semi-empirical spectra were created in these regions, as described in Wu et al. (2011).

A similar interpolator for MILES is described in Prugniel et al. (2011), and an updated version improved for cool stars is described in Sharma et al. (2016). In Prugniel et al. (2011) the atmospheric parameters for most of the stars in the MILES library (Sánchez-Blázquez et al. 2006) are computed using the ELODIE v3.2 interpolator. From these parameters and the MILES spectra, an interpolator was computed. This interpolator was iteratively examined by looking at the residuals of observed stellar spectra and their interpolated spectra, in this way reducing the effect of some of the outlier stars. The final interpolator is the MILES v1 interpolator. Sharma et al. (2016) correct the parameters from Prugniel et al. (2011) for detected systematics and supplement the list of parameters with parameters for the coolest stars. After carefully checking and correcting for biases, they built the new MILES v2 interpolator.

Both the ELODIE v3.2 and the MILES v2 interpolator have 26 terms in the FGK and M regimes, and 19 terms in the OBA regime. Both interpolators cover the wavelength range that is given for them in Table 1.1 in the Introduction.

4.2.2 PHOENIX interpolator

There are no existing polynomial interpolators for synthetic spectral libraries. We wanted to be able to use the PHOENIX models in ULySS, so an interpolator was made for us by P. Prugniel (private communication) using the high resolution PHOENIX spectra. This interpolator uses the same polynomial decomposition as the most recent MILES and ELODIE interpolators, except that the PHOENIX interpolator also has 26 terms in the OBA regime. Making the interpolator is partly simpler for synthetic libraries than for empirical libraries, since there is no difficult procedure to derive the atmospheric parameters for the library spectra. The synthetic spectra by definition have known parameters because they are made from models.

4.3 Running ULySS on XSL stars

In this section we describe the details of the method we apply to determine atmospheric parameters for XSL stars using ULySS. First we describe how we determine the optimal value for the order of the multiplicative polynomial and how we determine the LSF, then we describe our final procedure and different settings we use.

4.3.1 Multiplicative polynomial

In ULySS the order n of the multiplicative polynomial $P_n(\lambda)$ used in the fit can be set by hand. The optimal value of n depends on the wavelength range used in the fit, the resolution of the observed spectra and the accuracy of the wavelength calibration of those spectra. To determine the optimal order of this Legendre polynomial, we follow the method described in Koleva et al. (2009). We selected a few stars of different spectral type and analyzed them with different values of n. For this test, we used the MILES interpolator in the spectral range $4000 - 5500$ Å. In Figure 4.1 we show the variation of the χ^2 and the stellar atmospheric parameters with n, and we use this to select a value of n for which the results become independent of n. Based on this plot, we adopt $n = 70$. This is comparable to the value adopted by Wu et al. (2011) for ELODIE who adopt $n = 70$, and the value adopted for MILES in Prugniel et al. (2011) who adopt $n = 40$. We did the same test in the spectral range $4700 - 5500$ Å with the MILES and ELODIE interpolators, and in both cases $n = 70$ is fine as well.

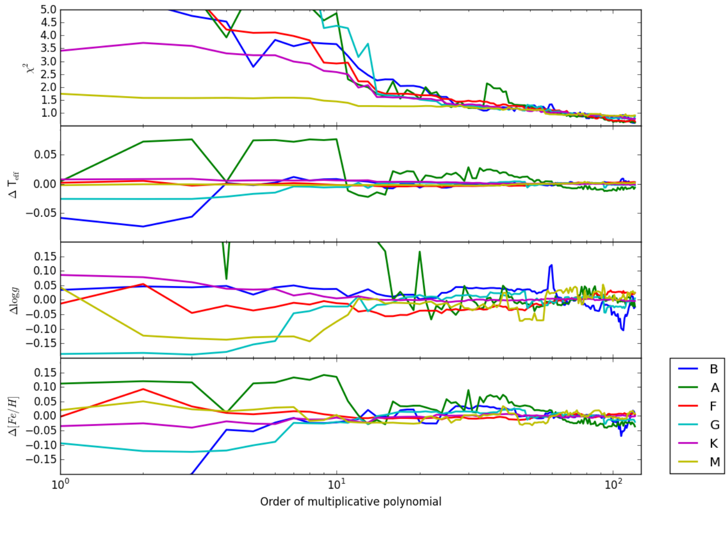

Figure 4.1 - Evolution of χ^2, $\log \mathrm{T_{eff}}$, $\log g$ and [Fe/H] with increasing multiplicative polynomial degree n. The plot shows the χ^2 divided by its asymptotic value (defined here as the mean of the solutions for $n > 25$), and the atmospheric parameters as differences between the calculated parameters and their asymptotic values.

4.3.2 LSF

We determine the LSF ($v_{\rm sys}$ and σ) separately from the stellar atmospheric parameters using the `uly_lsf` command. The variation of the LSF with wavelength has only a small influence on the determined atmospheric parameters (Wu et al. 2011), but we implement it anyway to be complete. One could study LSFs independently to learn more about, for example, the stellar rotation of the stars. However, in our case the resolution of the interpolators is generally lower than the resolution of our observed spectra, which makes it difficult to interpret the σ part of the LSF. There are also some strange unphysical wavelength shifts in parts of the spectra present in v_z. By first determining the LSF and then inserting it when determining the stellar atmospheric parameters, we can hopefully take out these problems with σ and v_z in the final fit. We determine the LSF in chunks of 300 Å, and we shift the center of the region by 100 Å every time so there is some overlap between neighboring LSF points. After the determination, we smooth the LSF using the `uly_lsf_smooth` command, because it should be a smooth function of wavelength.

4.3.3 Fitting a spectrum

To determine the parameters of a star, the final sequence is as follows. We decide which interpolator to use (PHOENIX, MILES or ELODIE), we select a wavelength range over which we want to fit the spectrum, we convolve the XSL spectrum to the resolution of the chosen interpolator in this wavelength range if necessary, and we run ULySS with the `/CLEAN` option turned on. In the first run with ULySS we give it no input parameters but we let ULySS find a first guess for the stellar atmospheric parameters $T_{\rm eff}$, $\log g$ and [Fe/H] of a star. We then use these parameters with the `uly_lsf` command to determine the relative LSF between the observed spectrum and a spectrum produced by the interpolator. After that we run ULySS again to find the atmospheric parameters, but this time inserting the previously determined LSF. The parameters we find in this last run are the final atmospheric parameters coming out of ULySS. There is a small difference in this procedure if we use the PHOENIX interpolator. We skip the first step (running ULySS with no input parameters) because for an unknown reason it does not work with the PHOENIX interpolator. Instead of the ULySS first guess we use values for the stellar atmospheric parameters from the literature for the determination of the LSF.

4.3.4 Different settings

We test different interpolators and wavelength ranges. The results for the PHOENIX interpolator give a rough indication of how good the interpolator is and whether or not this first version of the interpolator can be used or not. For the MILES and ELODIE interpolators we already know that they should work properly, because they have been used and tested before. We therefore investigate these interpolators in a bit more detail by comparing the resulting stellar atmospheric parameters from the two interpolators with each other, and for a single interpolator we compare the resulting stellar atmospheric parameters for different wavelength ranges. The spreads we measure in these comparisons also give an indication of the uncertainties in ULySS.

The wavelength ranges we can use depend on the available, usable part of the XSL spectra and on the interpolators. First of all we need ranges in the spectra that have a lot of spectral information, and do not have much telluric absorption. Above ∼6800 Å, telluric lines start to become more present, so we prefer not to use this part of the spectrum. We also cannot use the VIS spectrum below 6000 Å, because there the dichroic feature between the UVB and VIS arm dominates the spectrum. In the UVB arm the spectra start to have enough flux to be useful above 3500 Å, but between 3900 Å and 4000 Å many stars have strong Ca H and K lines. Therefore it could be wise to not use this region because these strong lines could strongly influence the results. The UVB spectra can be used until ~ 5500 Å, after that the dichroic feature between the UVB and VIS dominates the spectrum again. Additionally, the interpolators that we use also have a limited wavelength coverage. MILES covers $3500 - 7500$ Å (the PHOENIX interpolator too, because it has the same format), while ELODIE covers $3900 - 6800$ Å. Based on the spectra and the interpolators, we choose four different wavelength ranges to run ULySS on. The main range we will use is $4000 - 5500$ Å, which covers as much of the UVB as possible but excludes the Ca H and K lines. We also select three ranges of 800 Å, the UV from $3900 - 4700$ Å, the VB from $4700 - 5500$ Å and the VIS from $6000 - 6800$ Å.

4.4 Results

In this section we present the results from the methods described in the previous section. We compute stellar atmospheric parameters for the Large Program stars in XSL, which is the largest sample of spectra which has gone through the most recent data reduction cycle. First we show results from the PHOENIX interpolator, and after that we show results from the MILES and ELODIE interpolators and perform a test at different wavelengths.

4.4.1 PHOENIX

We computed the stellar atmospheric parameters for the Large Program stars in our XSL sample with the PHOENIX interpolator using the wavelength range $4000 - 5500$ Å. We show the results together with the literature values on an HR-diagram-type plot in Figure 4.2. In Figure 4.3, we present the difference between all computed parameters and their corresponding literature values.

4.4.2 ELODIE & MILES: 4000–5500 Å

We also computed the stellar atmospheric parameters for the Large Program stars with the ELODIE and MILES interpolators using the wavelength range from $4000 - 5500$ Å. We present the resulting effective temperatures and surface gravities together with their literature values (if there are any) on HR-diagram-type plots in Figures 4.4 (ELODIE) and 4.6 (MILES). We also present the differences of each of the three computed stellar atmospheric parameters with their literature values in Figures 4.5 (ELODIE) and 4.7 (MILES). There are some measurements that do not show on the difference plots because they are further away than 3000 K from the literature T_{eff}, 4 dex from the literature $\log g$ or 3 dex from the literature [Fe/H]. The mean differences and dispersions are given in Table 4.1.

In Figure 4.8 we present the computed stellar atmospheric parameters from the two interpolators against each other (a zoomed-in version of this is presented in Figure 4.9). These plots show the size of the differences when using the exact same method, but with a different empirical model interpolator. The mean difference and dispersion for the comparison are given in Table 4.1.

4.4.3 MILES: UV, VB and VIS

For the MILES interpolator, we compute the stellar atmospheric parameters again in three smaller wavelength ranges. By doing this, we can determine how much the resulting parameters change when we use a different wavelength range. The results for the dispersions and average differences are given in Table 4.1.

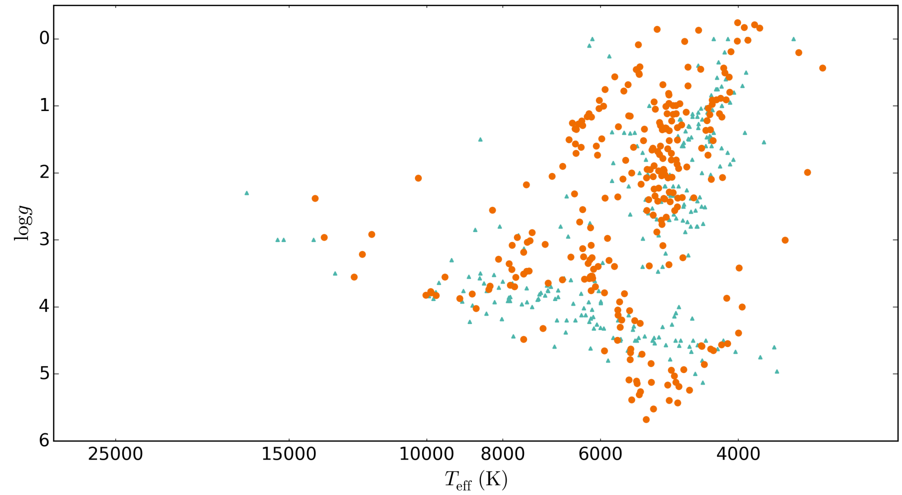

Figure 4.2 - Comparison of $T_{\rm eff}$ and $\log g$ for XSL from the literature (cyan triangles) with the results from ULySS with the PHOENIX interpolator (orange circles).

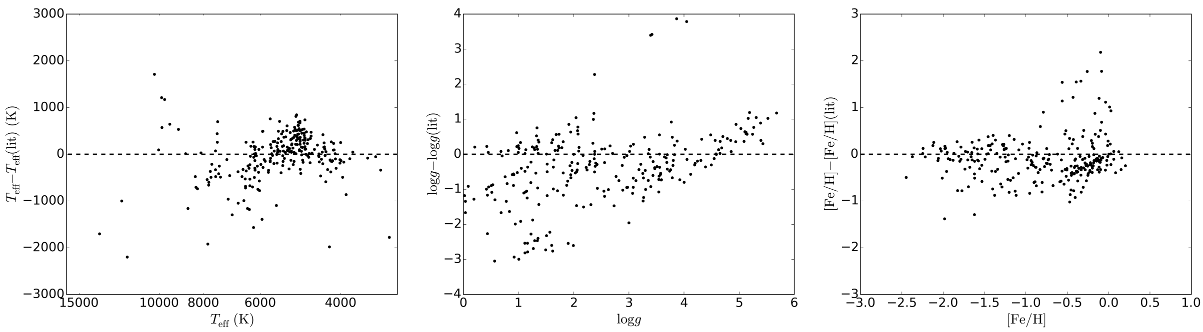

Figure 4.3 - Comparison of $T_{\rm eff}$, $\log g$ and [Fe/H] for XSL from the literature with the results from ULySS with the PHOENIX interpolator.

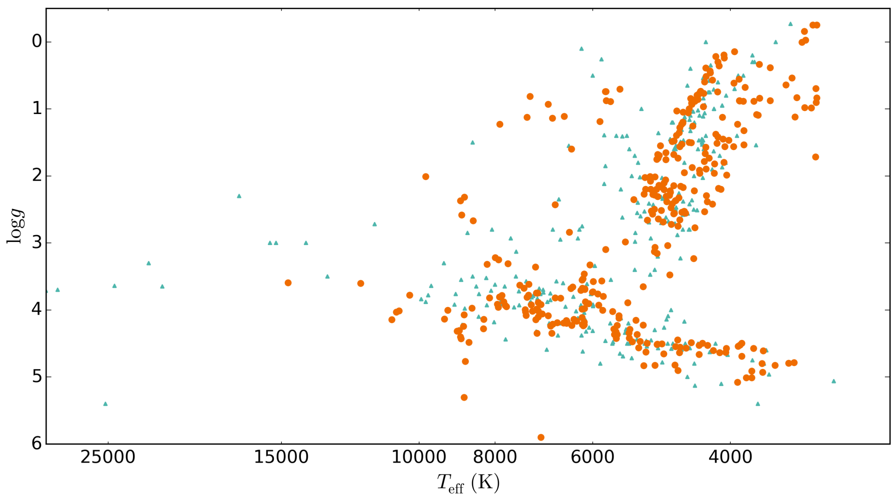

Figure 4.4 - Comparison of $\log g$ and $T_{\rm eff}$ for XSL from the literature (cyan triangles) with the results from ULySS with the ELODIE interpolator (orange circles).

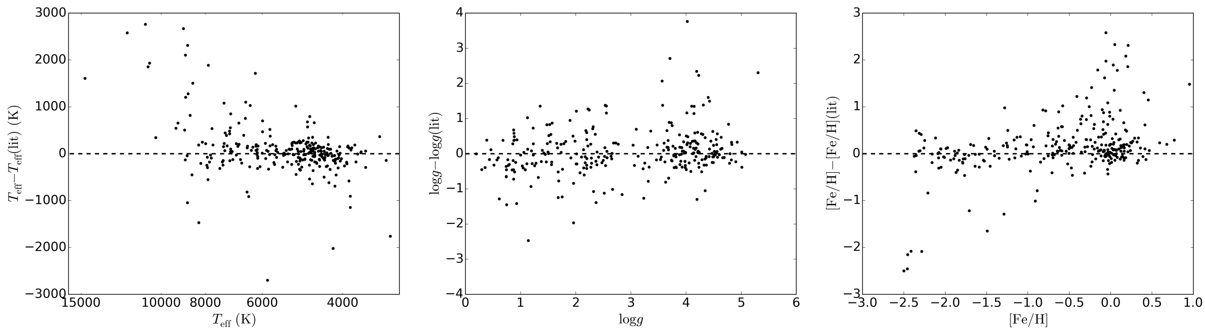

Figure 4.5 - Comparison of $T_{\rm eff}$, $\log g$ and [Fe/H] for XSL from the literature with the results from ULySS with the ELODIE interpolator.

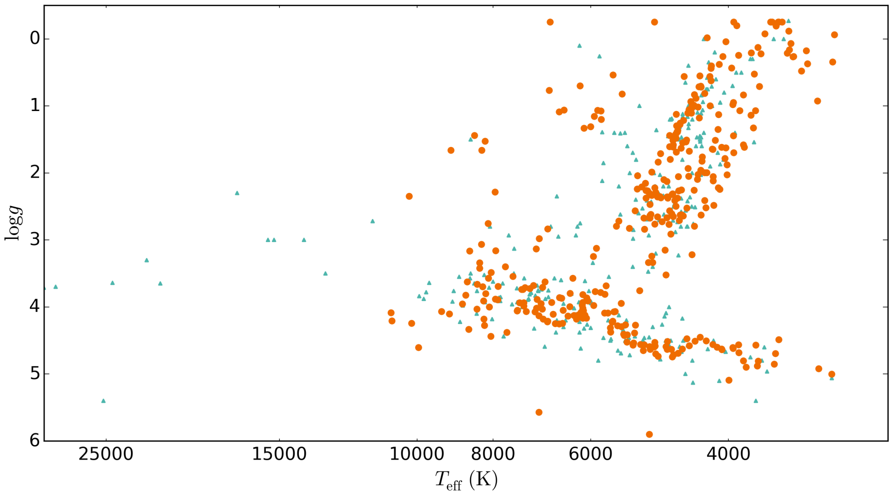

Figure 4.6 - Comparison of $\log g$ and $T_{\rm eff}$ for XSL from the literature (cyan triangles) with the results from ULySS with the MILES interpolator (orange circles).

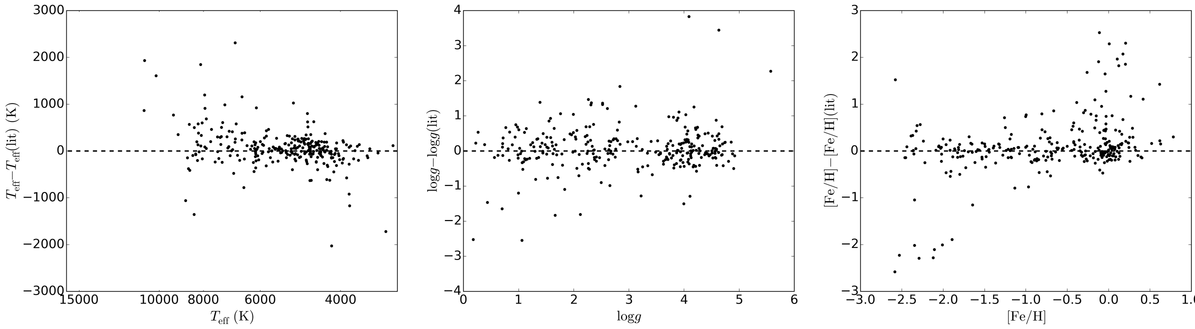

Figure 4.7 - Comparison of $T_{\rm eff}$, $\log g$ and [Fe/H] for XSL from the literature with the results from ULySS with the MILES interpolator.

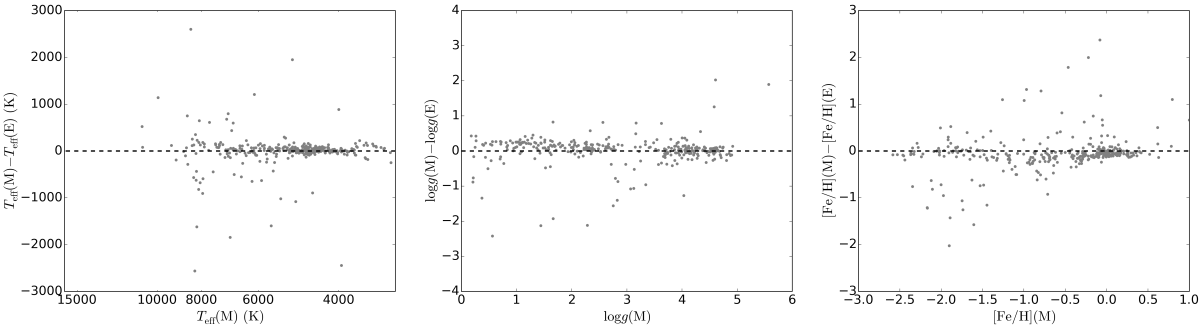

Figure 4.8 - Comparison of $T_{\rm eff}$, $\log g$, and [Fe/H] for XSL from the MILES interpolator with the results from ULySS with the ELODIE interpolator.

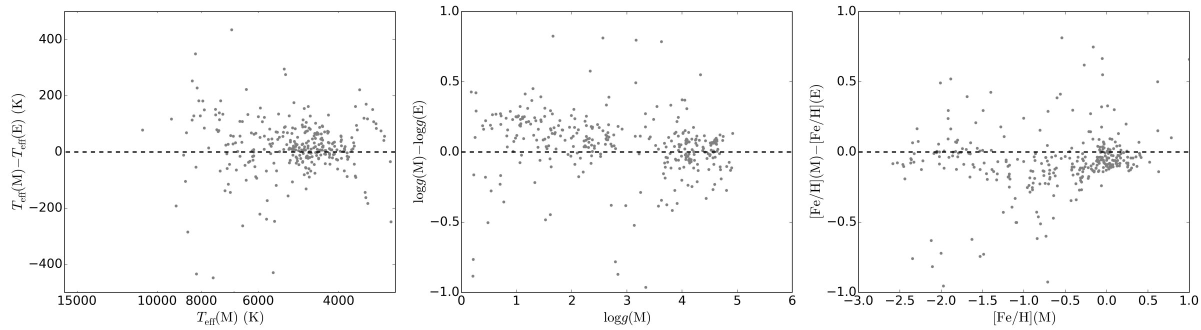

Figure 4.9 - Same as Figure 4.8 but zoomed in.

Table 4.1. Comparison of the atmospheric parameters with different interpolators and wavelength ranges.

Comparison	N^{a}	T_{eff} (K)		$\log g$ (dex)		[Fe/H] (dex)	
		Δ	σ	Δ	σ	Δ	σ
UVB: MILES - literature	295/292/285	48	260	0.07	0.46	0.06	0.28
UVB: ELODIE - literature	292/289/282	25	281	0.03	0.53	0.14	0.32
UVB: MILES - ELODIE	338	22	84	0.06	0.19	−0.06	0.13
MILES: UV - VB	352	19	111	−0.02	0.21	0.01	0.10
MILES: UV - VIS	279	−12	171	−0.07	0.36	−0.07	0.20
MILES: VB - VIS	280	−34	136	−0.07	0.30	−0.10	0.18

Note. — For each parameter, the Δ column gives the mean difference between the two samples in the first column. The σ column gives the dispersion between the two. Both were computed with the IDL command `BIWEIGHT_MEAN` to discard outliers.

[a]Number of compared stars. If there is more than one number, a different number of stars is used for every parameter.

4.5 Discussion

We have run ULySS with different settings to test several interpolators and wavelength regimes. These multiple tests were possible because running ULySS on the complete sample of Large Program stars takes only ~ 2 hours. In this section we will discuss the results. We start with the results from the PHOENIX interpolator, and we describe the results of a further test of this interpolator. After that we discuss the results from the two empirical interpolators.

4.5.1 PHOENIX results

When we look at the results from ULySS with the PHOENIX interpolator in Figure 4.2, it is clear that there are many problematic regions on this plot. First of all there is the region of the dwarf stars with effective temperatures between 3000 and 6000 K, where compared to the literature the interpolator finds extremely low surface gravities for the lowest effective temperatures, and a bump to higher surface gravities between 4500 and 5500 K. A second problematic region seems to be the region of the dwarf stars with effective temperatures above 6000 K. Almost all computed surface gravities are (much) lower than their literature values, and together with that the interpolator also seems to shift the stars towards lower effective temperatures. The third problematic region is the giant branch, where most of the stars seem to be shifted towards higher effective temperatures with respect to the literature. These three problematic regions can also be recognized in Figure 4.3.

If we compare Figure 4.2 with Figures 4.4 and 4.6, we clearly see that the PHOENIX interpolator is performing much worse than the ELODIE and MILES interpolators. There can be several reasons for this, but two of the most obvious are (1) the PHOENIX models do not describe the stars well enough, and (2) the interpolator does not work properly with the PHOENIX models. There have not been many tests with polynomial interpolators for synthetic libraries yet, so we performed a test ourselves to see whether the problem could be with the interpolator or with the models themselves. We performed a self-inversion test with the interpolator to check how well it could reproduce the stellar atmospheric parameters of its own models.

4.5.1.1 Test of the PHOENIX interpolator

In the self-inversion test, we ran ULySS with the PHOENIX interpolator on the PHOENIX model spectra themselves. On the PHOENIX website[1], there is a download of the full library at a resolution of $R = 10000$, which is similar to the resolution of XSL. We downloaded this $R = 10000$ library so that we could feed those spectra to the interpolator and see how well the stellar atmospheric parameters are reproduced. In theory, if the interpolator would be perfect, the atmospheric parameters ULySS gives should be the same as the real values of the models (which are known). But it can never be perfect, because the interpolator provides a global description of the full library (so it does not describe each section of the library perfectly), and also a stellar spectrum cannot be completely described by a polynomial of the three stellar atmospheric parameters. However, with the polynomial interpolation method it should be possible to describe a spectrum well enough to determine atmospheric parameters with small uncertainties from a given spectrum.

First we calculate the LSF of the $R = 10000$ model with respect to the interpolated model. This should not really be necessary, but we will do the same when using real spectra so this is done for the sake of comparability. We then ran ULySS on the UVB part from $4000 - 5500$ Å, also turning on the `/CLEAN` command. Results of the self-inversion tests are shown in HR-diagram-type plots in Figures 4.10 and 4.11 for models with [Fe/H] = 0.0 and −1.0 respectively. It is clear that there are large differences between the atmospheric parameters computed by the PHOENIX interpolator and the real model values. Differences in temperature are not so clear in these plots because there are many points close together, so for clarity we show the differences in $T_{\rm eff}$ in Figures 4.12 and 4.13. The deviations in $T_{\rm eff}$ are of the order of 200 K, except at temperatures larger than 7000 K for the [Fe/H] = −1.0 models, where the deviations can become as large as 1000 K or more. The deviations in $\log g$ are of the order of 0.5 dex. The deviations in [Fe/H] are also around 0.5 dex, specifically in the regions where $\log g$ is also strongly deviating. These deviations are as large as the separation of the grid points. If it is already problematic to get the correct parameters of spectra exactly on the grid points, it will also be very difficult to find reliable parameters interpolating between grid points. It appears from our self-inversion test that we cannot trust the PHOENIX interpolator to produce atmospheric parameters with better precisions than the step sizes in the grid.

Prugniel also made a version of the PHOENIX interpolator that is just for dwarf stars. This interpolator is fixed to a smaller local region of the parameter space, and it is a less global interpolator. We use this interpolator to compute stellar atmospheric parameters for the PHOENIX spectra that have $\log g \geq 3.0$. The dwarf interpolator produces better results for the dwarfs in the self-inversion test than the global interpolator for the [Fe/H] = 0.0 case; for [Fe/H] = −1.0 it only seems better below 6000 K. It is not strange that the dwarf interpolator works better, because it is an interpolator that has the same number of terms in the polynomial as the global interpolator, but it describes a smaller part of the parameter space. The dwarf interpolator is effectively using a higher order polynomial, which might not be a good solution for getting better parameters. The number of terms in the polynomial decomposition of the interpolators was chosen carefully, and it is not clear whether it wise to increase this, although, it might be possible that the optimal number of terms in the polynomial for a theoretical interpolator is different from the number in an empirical interpolator.

[1] http://phoenix.astro.physik.uni-goettingen.de/

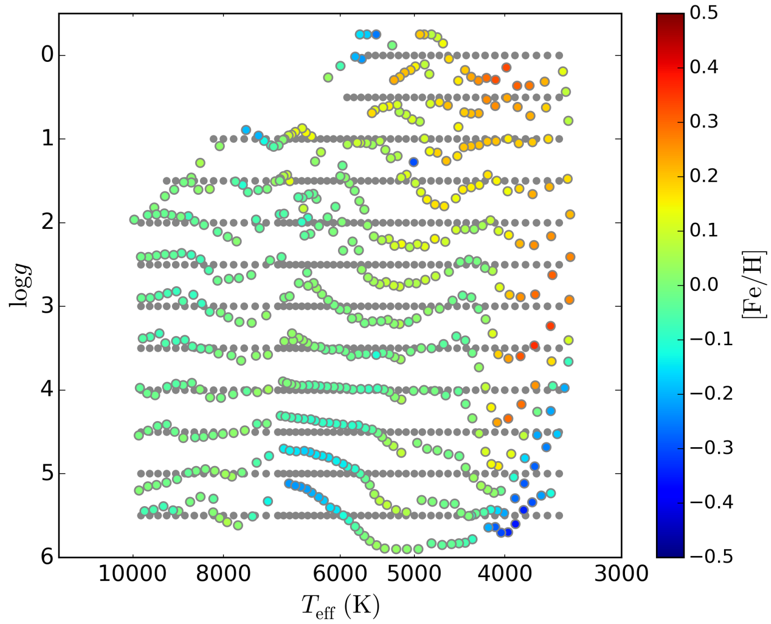

Figure 4.10 - Comparison of stellar atmospheric parameters for the [Fe/H] = 0.0 PHOENIX models (grey points) with the result of the self-inversion test of the PHOENIX interpolator (colored points). The colored points are color-coded by their interpolated [Fe/H].

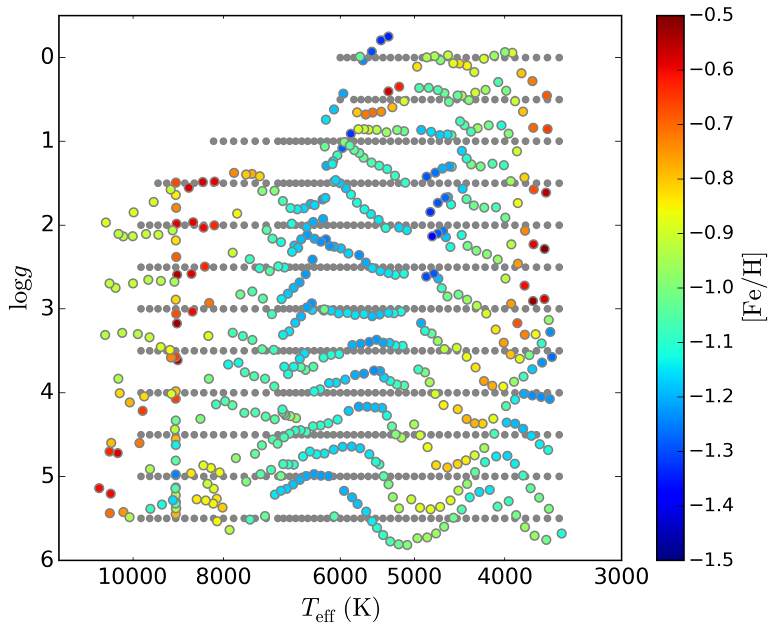

Figure 4.11 - The same as Figure 4.10, but now for models of [Fe/H] $= -1.0$.

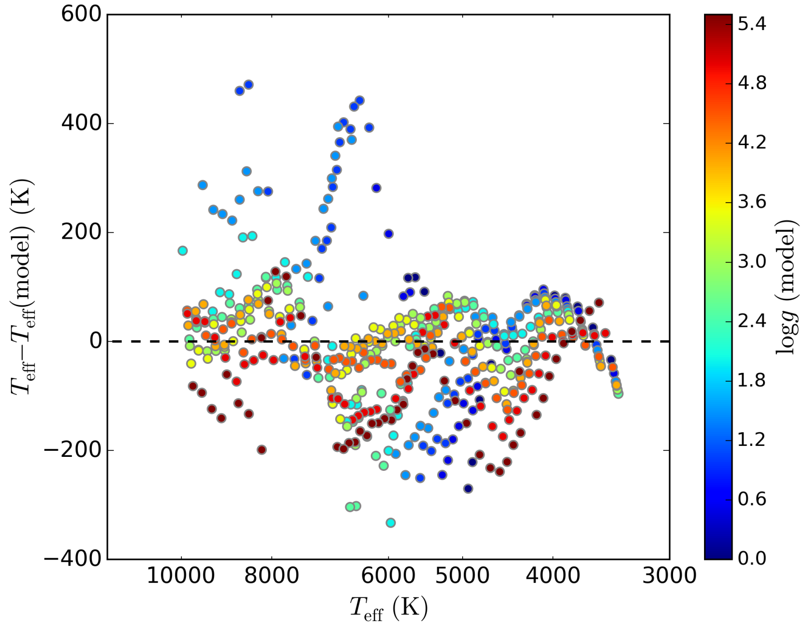

Figure 4.12 - Comparison of $T_{\rm eff}$ for the [Fe/H] = 0.0 PHOENIX models with the result of the self-inversion test of the PHOENIX interpolator. The colored points are color-coded by their model $\log g$.

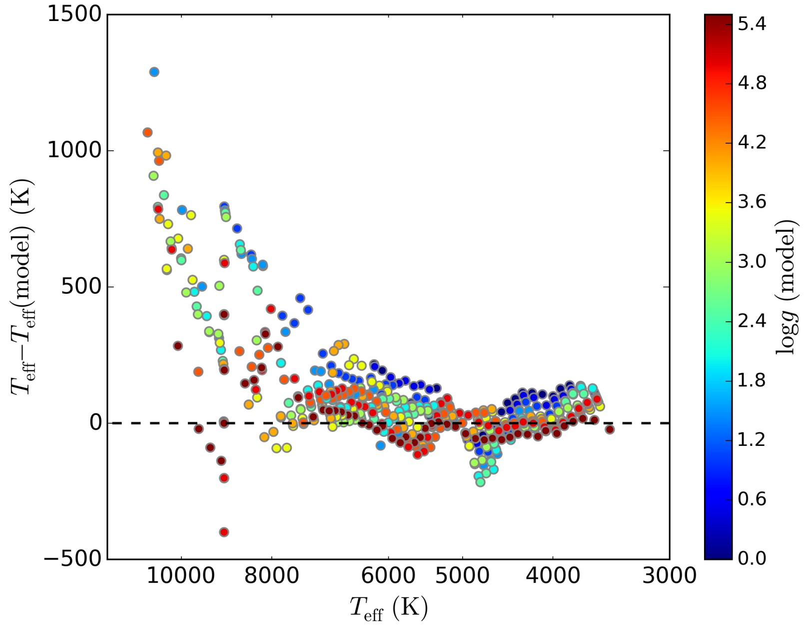

Figure 4.13 - The same as Figure 4.12, but now for models of [Fe/H] $= -1.0$.

4.5.1.2 PHOENIX models with MILES interpolator

The PHOENIX interpolator does not seem to produce good stellar atmospheric parameters. One reason could be that the PHOENIX spectra themselves are not accurately representing real stellar spectra over a large range of the parameter space. Naturally, an interpolator made from such models would not produce good stellar atmospheric parameters for real stars like those in XSL. An external check could be made to test whether this is the case by fitting the PHOENIX spectra with a method that we know produces reliable stellar atmospheric parameters. The computed and model parameters should not differ significantly from each other if the PHOENIX models represent real spectra well.

We performed such a test and fit the PHOENIX spectra with the MILES interpolator. The MILES interpolator has been extensively tested and we assume that it is able to reproduce stellar atmospheric parameters well (Prugniel et al. 2011, Sharma et al. 2016). There will be some regions in the theoretical model grid where the MILES interpolator will not find good parameters, because MILES does not cover everything (see Figure 4.14). But in the regions where the MILES interpolator is valid, it should find good stellar atmospheric parameters for the PHOENIX spectra. We present the stellar atmospheric parameters for the PHOENIX models computed with the MILES interpolator in Figures 4.15 and 4.16 for [Fe/H] = 0.0 and −1.0 respectively. The MILES library does not contain many stars with $\log g$ below 4.5, and we see that the interpolator indeed does not place many of the PHOENIX stars in that region. Similarly, there are few stars placed at a high temperature and a low surface gravity. But we also find that the PHOENIX model parameters differ significantly from the MILES results in regions where we do expect good results from the MILES interpolator, namely on the main sequence and the giant branch. It might therefore be the case that the PHOENIX models themselves are untrustworthy over a wide range, which implies that it might not be possible to build a good interpolator with them.

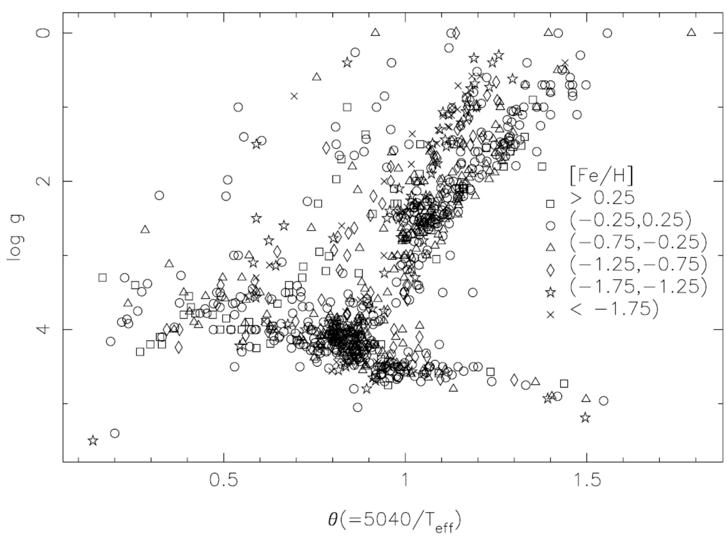

Figure 4.14 - Coverage of the parameter space by MILES. Different symbols indicate different metallicities (Figure taken from Sánchez-Blázquez et al. 2006).

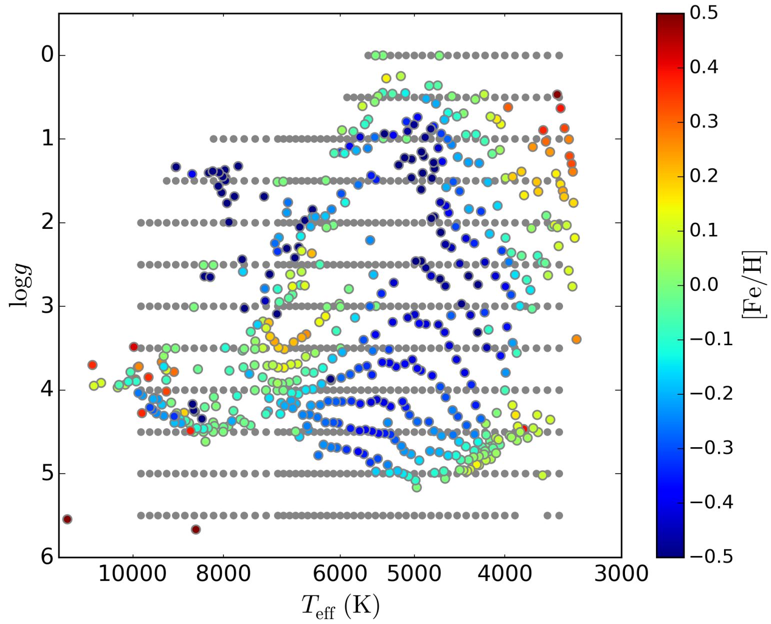

Figure 4.15 - Comparison of stellar atmospheric parameters for the [Fe/H] = 0.0 PHOENIX models (grey points) with the result of fitting the PHOENIX models with the MILES interpolator (colored points). The colored points are color-coded by their interpolated [Fe/H].

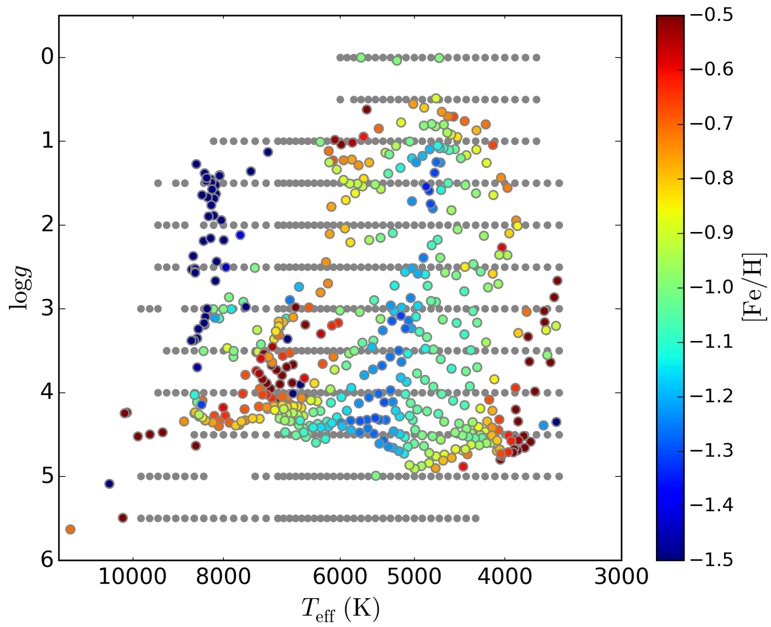

Figure 4.16 - The same as Figure 4.15, but now for models of [Fe/H] = −1.0.

Table 4.2. Comparison of the atmospheric parameters of FGK[a] stars with Prugniel et al. (2011).

Comparison		N^{b}	T_{eff} (K)		$\log g$ (dex)		[Fe/H] (dex)	
			Δ	σ	Δ	σ	Δ	σ
MILES - literature	Prugniel et al. (2011)	773	46	120	0.04	0.28	0.05	0.13
	This work	244/242/238	49	233	0.08	0.44	0.04	0.23
MILES - ELODIE	Prugniel et al. (2011)	332	12	60	0.01	0.08	0.04	0.06
	This work	338	21	72	0.08	0.15	−0.06	0.09

Note. — For each parameter, the Δ column gives the mean difference between the two samples in the first column. The σ column gives the dispersion between the two. Both were computed with the IDL command `BIWEIGHT_MEAN` to discard outliers.

[a]FGK stars: $4000 < T_{\mathrm{eff}} \leq 8000$ K

[b]Number of compared stars. If there is more than one number, a different number of stars is used for every parameter.

4.5.1.3 Discontinuities around 5000 K

In several of the self-inversion plots (especially Figures 4.10 and 4.11), discontinuities can be seen around $T_{\mathrm{eff}} = 5000\,\mathrm{K}$. We note that the location of the discontinuities overlaps with the problematic regions around 5000 K (at high and low surface gravity) in the HR diagram of XSL stars fitted with the PHOENIX interpolator (Figure 4.2). It is unclear what causes the discontinuities. One explanation could possibly be found on the website of the PHOENIX models. There, it is indicated that in February 2016 a new version of the models was uploaded to their website. Improved in this version is that some models were added to fill holes in the grid, specifically at 5000 K. In the previous version of the library, these holes were filled up with interpolated models. The PHOENIX interpolator was made with this previous version of the PHOENIX library. It could be that the missing models have influenced the interpolator in such a way that it produces these discontinuities.

4.5.2 ELODIE & MILES results

When we inspect the HR diagrams of the results from the ELODIE and MILES interpolators (Figures 4.4 and 4.6), it appears to be the case that they reproduce the literature parameters relatively well. Unlike with the PHOENIX interpolator, there are no obvious regions on this diagram where one of the interpolators fails, except at the highest effective temperatures (above 10 000 K). But stars with such high temperatures are difficult to fit, because they have very few metal lines. The difference plots (Figures 4.5 and 4.7) also show less "structure" than the difference plots of the PHOENIX interpolator (Figure 4.3). Instead, the differences appear to be mainly random.

Prugniel et al. (2011) (henceforth P11) use an earlier version of the MILES interpolator to compute stellar atmospheric parameters, which they compare to the uniform literature sample of Cenarro et al. (2007). They also compare their results from the MILES interpolator to the values in ELODIE 3.2. We perform similar comparisons, and show our results together with the comparison from P11 in Table 4.2. Our dispersions are generally somewhat less than twice as big as the dispersions in P11. The comparison between our results and theirs is not completely fair, as they use a uniform literature sample and we do not, and they use the values for ELODIE from the literature, while we compute values for our own spectra with the ELODIE interpolator. They also performed the fit in a slightly different wavelength region; they used 4200 − 6800 Å while we used 4000 − 5500 Å, and they used an older version of the MILES interpolator. Furthermore, we present stellar atmospheric parameters for all stars with spectra that have automatically gone through the fitting process, and we have not carefully examined all our fits to discard outliers. For these reasons, the comparison in Table 4.2 is only meant for global comparison, to check if we are in the same ballpark as similar previous work.

Which one of the MILES and ELODIE interpolators is the best to use is not obvious from our results. Compared to the literature, the dispersions from the MILES interpolator are slightly smaller. The ELODIE interpolator has a higher resolution and therefore has more information in the spectrum that can be fit. One would expect that this might increase its precision. In P11 it is concluded that there is no significant degradation of the precision when calculating parameters for MILES and CFLIB, which has a higher resolution than MILES. It is possibly the case that in this method of full-spectrum fitting a higher resolution does not necessarily increase the quality of the fit. Additionally, P11 find that the MILES interpolator is better than the ELODIE interpolator at the lowest and highest temperatures. The MILES interpolator is also the interpolator that has been updated most recently (Sharma et al. 2016), specifically for stars with lower effective temperatures.

From the comparison of the mean differences and dispersions for the MILES UV, VB and VIS results, it is clear that the quality of the resulting stellar atmospheric parameters depends on which wavelength range is used. It appears that from these three regions, the UV and VB regions perform best and the VIS region the worst. The UV and VB are most consistent with each other, which is not surprising since they are regions in the same spectrum, whereas the VIS regions comes from a different spectrum, taken with a different spectral arm. Sharma et al. (2016) also fit their spectra in different spectral ranges and they compare the results from the fit in the blue (3600 − 5500 Å) and red (5600 − 7400 Å). They find no indication that one of the two segments produces better stellar atmospheric parameters than the other. We find a different result, possibly because we use smaller regions than they do, but also because their regions are in the same spectrum, while we have two different spectra for the UVB and VIS.

It appears to be that the VB region performs better than the UV region in the comparison with the VIS results, since the dispersions are smaller. Sharma et al. find that excluding the blue range of their spectra (3600 − 4200 Å) improves the dispersion of the computed parameters with respect to their compiled literature sample. They claim that this is likely due to the fact that the bluer region is more sensitive to various abundances of different chemical elements in the library stars (Marcum et al. 2001; Koleva & Vazdekis 2012). They reject the possibility that excluding this region improves the fit because of a low signal-to-noise ratio (S/N) at shorter wavelengths, because their S/N is still reasonable at these wavelengths. We cannot exclude the possibility that the S/N in our spectra at shorter wavelengths is so low that it influences the results.

4.6 Conclusion

The fact that ULySS can run ~ 350 stars within 2 hours makes it suitable to use for the mass-production of stellar atmospheric parameters. This relatively short computing time allowed us to try different settings.

We tested the theoretical PHOENIX interpolator in ULySS on XSL stars and we performed a self-inversion test with the PHOENIX models. From the results of these tests we conclude that the PHOENIX interpolator is not good enough to use for the determination of reliable stellar atmospheric parameters. A better investigation of the way this theoretical interpolator works is necessary to understand how it can be improved.

The results from the MILES and ELODIE interpolators suggest that we can use them with $4000 - 5500$ Å to determine relatively reliable parameters. The results do depend slightly on which interpolator and which wavelength range is used.

In the next chapter we will present final stellar atmospheric parameters for the stars in XSL, using ULySS with the MILES interpolator in the wavelength range $4000 - 5500$ Å, on the basis of our analysis in this chapter. Following this analysis and keeping to a single method, we will be able to derive uniform stellar atmospheric parameters.

Chapter 5

Parameters

In this chapter we present uniform stellar atmospheric parameters for XSL.

5.1 Method

We run ULySS on the Large Program (LP) and Pilot Program (PP) spectra of P3. We use the MILES interpolator from Sharma et al. (2016) with the wavelength range $4000 - 5500$ Å. We use the settings described in Section 4.3. For stars with multiple spectra, we usually used the most recent spectrum. For all stars we use exactly the same method, so that the derived stellar atmospheric parameters will be uniform.

5.2 Results

The resulting parameters are shown on the HR diagram in Figure 5.1. We present the values for the stellar atmospheric parameters for 417 stars in Table 6.1 in the Appendix. The uncertainties we present for the parameters are the values ULySS that computes. All stars that had spectra that did not fail in the automatic parameter determination have computed stellar atmospheric parameters in this list. Failing can happen in two ways. First, it is possible that ULySS cannot find a fit at all and crashes, which happened for 18 LP and 41 PP stars. Second, it can be that ULySS does find a fit but that it failed for one of the three stellar atmospheric parameters. The other parameters also cannot be trusted if this is the case. This second type of fail occurred for 12 LP and 18 PP stars, and we flag the stars in the table with *fail*. We also flag stars that had bad fits because of a bad LSF determination over the full spectral range, based on visual inspection. We show an extreme example in Figure 5.2 for the star HD172488. These stars with bad LSF determinations are flagged with *lsf* in the last column of the table. The parameters of these stars should be used with more caution.

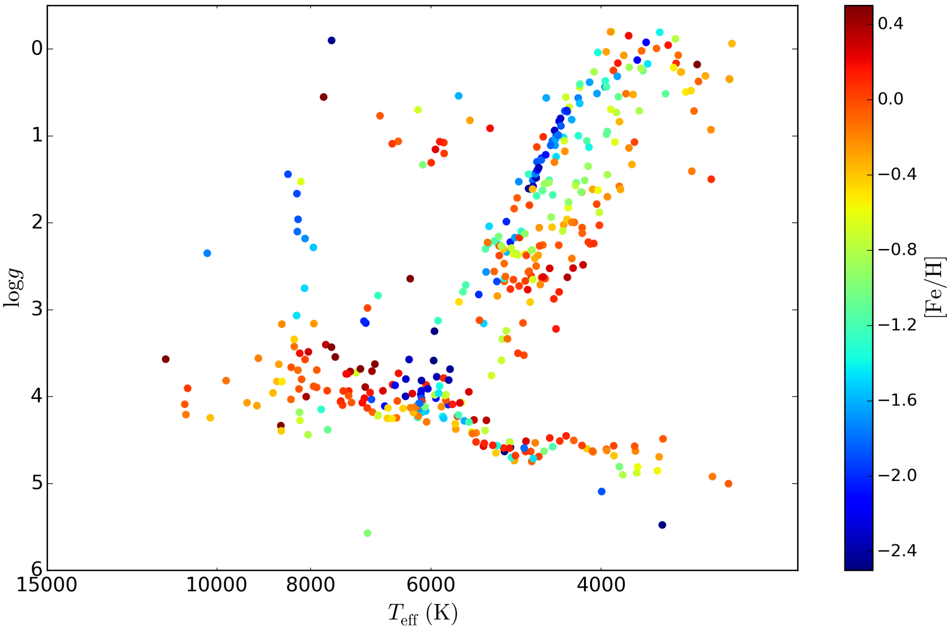

Figure 5.1 - Stellar atmospheric parameters for XSL, color coded by [Fe/H].

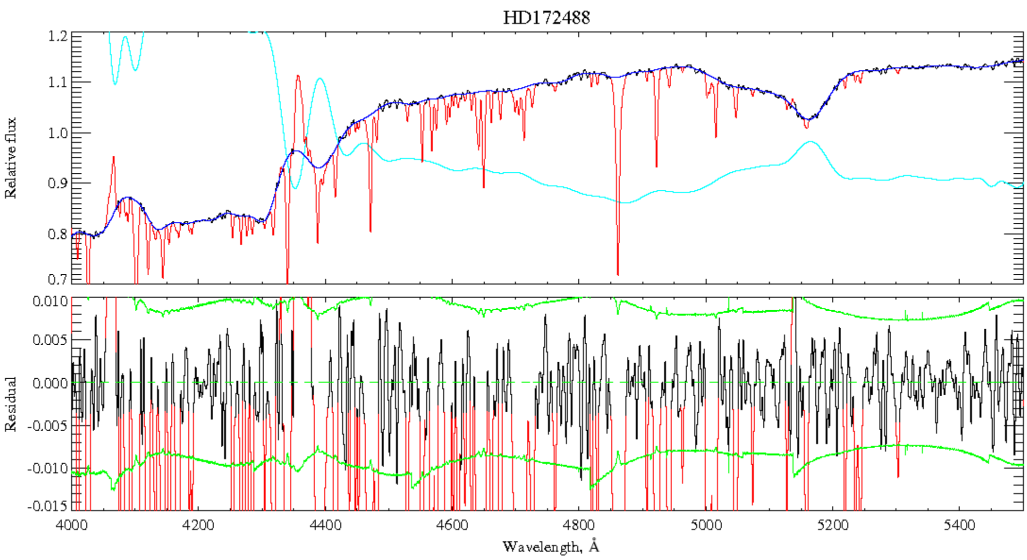

Figure 5.2 - Example of a fit with a bad LSF determination. In the top plot, the black line (almost invisible) indicates the XSL spectrum, the red regions are regions excluded in the fit by the `/CLEAN` option, the dark blue line is the fitted model convolved with the fitted LSF and the cyan line shows the multiplicative polynomial. The bottom panel shows the residuals in black and red, and the green lines marks the 1-σ deviation.

5.3 Discussion

The uncertainties we present in Table 6.1 are the values ULySS calculates for the error of the fit. It gives an indication of the precision of the fitting procedure and represents a random error. However, this uncertainty highly underestimates the real uncertainty of the computed stellar atmospheric parameters. A comparison with the literature gives an idea of the global accuracy of the parameters and our systematic errors. For the 129 stars we have in common with MILES, we compare our results to the literature results of Cenarro et al. (2007). This is the largest uniform sample of literature parameters in our literature compilation. For $T_{\rm eff}$ we find a mean difference of 50 K and a dispersion of 175 K, for $\log g$ the mean difference is 0.06 dex and the dispersion 0.31 dex and for [Fe/H] we find a mean difference of 0.03 dex and a dispersion of 0.20 dex. There are several reasons why these errors are much bigger than the fitting errors. Several things are not taken into account in the fitting error. First of all, it is a simplistic assumption that a stellar spectrum can be modeled with just three parameters. There are more parameters such as rotation, detailed chemical abundances and chromospheric activity that could be taken into account. Second, the polynomial form of the interpolator cannot reproduce the spectra perfectly. Finally, there are also uncertainties in the stellar atmospheric parameters of the stars that have been used to create the MILES interpolator, which propagate to our results.

The *lsf* flag in Table 6.1 is based on visual inspection of the spectra, and indicates that there were clear mismatches between the observed and the modeled spectrum in terms of the LSF over the full spectral range. There are also stars that we did not flag, which had partial bad LSF determinations. We determined the LSF in chunks of 300 Å shifting them every 100 Å so that they partially overlap, and from the visual inspection it is clear that the automatic LSF determination sometimes fails in one or more of these chunks, especially at shorter wavelengths. Because of this, the model spectrum is smoothed to a very low resolution in these regions, which makes an accurate fit more difficult. If we could somehow improve the automatic determination of the LSF, it would increase the quality of the fit for a large number of spectra. We note that many of the flagged stars are either hot or cool evolved stars. These kinds of stars are difficult to fit because they have either very few metal lines or lots of molecular lines.

Of the fits that failed completely, there are many stars from the PP sample. We can see this when comparing Figure 5.1 with Figure 2.1: we are missing the clump of evolved stars at cool temperatures. The PP targeted variable cool giants in particular (long-period variables and Mira-type stars), and also included many stars lacking from current libraries, for example red super giants and AGB stars in the Milky Way and the Magellanic Clouds and metal-rich stars from the Galactic Bulge (Chen et al. 2014). It is not surprising that these stars fail in the automatic stellar atmospheric parameter determination. These are hard stars to fit, since they have spectra quite different from the "normal" spectra, and they are not yet in existing stellar libraries. The interpolator made from such an existing library is therefore not able to reproduce their spectra.

There are several stars that have good fits and no clear mismatches between observed and model spectrum, for which two or three of the computed stellar atmospheric parameters are further than one $\sigma_{\rm lit}$ away from the literature parameters. This could indicate that the stellar atmospheric parameters from the literature are not good for these stars, or it could also indicate a misidentification of a star. A misidentification means that the parameters that we have in our literature list are not actually the parameters for the given star but for another star. This is probably the case for at least some of our cluster stars. In clusters it can be difficult to know exactly which star was targeted because of the high density of stars.

In the remainder of this discussion we will discuss the impact of the new data release on the parameter determination, discuss possible improvements of our current method and discuss possible extra methods to increase the quality of the stellar atmospheric parameters for XSL.

5.3.1 XSL Data Release 2

In Chapter 2 we mentioned that we use an intermediate version of the XSL library for our determination of stellar atmospheric parameters in this Thesis. Soon there will be a new version of the library available in the form of Data Release 2 (DR2). DR2 will have spectra in all arms for all the stars in the library, and multiple spectra for some variable stars. The spectra will be organized by observation, and each observation will have a unique number. Currently the file names of the spectra are not all in a uniform format. All of the spectra will also have gone through the newest version of the data reduction pipeline, which will fix some of the current problems with the spectra. Among other things, the telluric correction and the flux calibration will be improved, and a correction for shifts in wavelength will be applied. There will also be merged versions of the spectra in DR2.

Once DR2 is available, the determination of the stellar atmospheric parameters will profit from many of the above-mentioned points. The new file names will lead to a better match between data files and the list of all XSL stars with literature parameters. Matching the correct star to the right file is sometimes problematic in the current version of the library, for example different names for the same star are sometimes used. With DR2 we will be able to compute parameters for more spectra of more stars, since the library will be complete. We can also use the merged spectra to increase the wavelength coverage of a single fit, and we can use them to make more uniform comparisons between different wavelength ranges. Also, the results for the stellar atmospheric parameters using the VIS arm could improve since the telluric correction improves in the new data reduction.

5.3.2 Improvements of current method

There are several things that can still be improved about the method that we used. These were not carried out for this thesis, but they should be taken into account in future work on the stellar atmospheric parameters for XSL.

First of all, we could follow Wu et al. (2011) and use a grid of stellar atmospheric parameter guesses in the determination of the stellar atmospheric parameters. ULySS performs a local minimization between data and model, and sometimes gets trapped in a local minimum. Using different initial guesses for the parameters, one could find multiple results for the parameters and select the best solution, which represents the global minimum. Implementing this might improve our results.

Second, a more detailed investigation of the effect of the LSF on the final determination of the stellar atmospheric parameters should be made. We found that the automatic determination of the LSF quite often did not result in a smooth LSF that represented the actual broadening of the spectral lines well. Some tests should be conducted that vary the size of the chunks of wavelength that are used and the separation of the chunks, to find the optimal parameters for determining a good LSF. It is known that there are currently some issues with the wavelength calibration for XSL (XSL Busy Week 4, 2016), which might also influence the determination of a good LSF.

Another point that should be addressed is how to deal with multiple spectra that have been taken per star for some variable stars. We currently used the most recent spectrum per star, which was the most convenient with the way that our files were named and organized, but this is not necessarily the best spectrum to use. A more careful investigation of this could result in more useful spectra for the determination of stellar atmospheric parameters. This will be easier with the new data release for XSL, since that will have fits file names with the names for unique observations, instead of names of stars. The parameters can then be calculated for every unique observation, and results for different observations of the same star can be compared and combined.

Additionally, in future work a more careful treatment of the outliers should be done. For every spectrum it should be investigated why a fit failed, why it was bad or why its computed parameters lie so far from the literature stellar atmospheric parameters. This can be done by studying the residuals better, by checking the signal-to-noise ratio of the spectra, by comparing solutions in the red and blue part of the spectrum and by checking the origin of the literature parameters. While studying the fits carefully, one could also investigate what regions in the spectrum are more often problematic than others. This could, for example, give insight into where the models have difficulty representing the spectra.

Finally, what could also be valuable is a more careful comparison of our computed stellar atmospheric parameters with a uniform literature sample. We used the uniform MILES literature sample from Cenarro et al. (2007), and we had 129 stars in our current sample in common. In the complete sample of XSL stars there are 167 stars in common with MILES, so when the new data release comes out we will have some more stars. It could also be useful to follow Prugniel et al. (2011) in their literature comparison, by comparing stars in three categories (M, FGK and OBA stars). This comparison could also result in a better determination of the errors.

5.3.3 New methods

To improve the quality of the stellar atmospheric parameters for XSL further, one could search for other spectra of the XSL stars and analyse them with the same method and interpolator. For example, one could use spectra from MILES, ELODIE, UVES-POP and search the archives for more. This will especially help for the stars in XSL with low S/N, and it can help to solve the identification problems for certain stars.

Some stars are difficult to fit with ULySS, for example the hottest stars and the cool evolved stars. We might have to set aside our requirement of a completely uniform determination of the stellar atmospheric parameters for all stars in XSL, and use a different method for these stars. We could for example follow Chen (2013) and use pPXF (Cappellari & Emsellem 2004) with a theoretical grid of models to calculate stellar atmospheric parameters for the cool evolved stars. If we were to do this, we should also investigate how we could homogenize parameters from different methods as much as possible.

5.4 Conclusion

In this Chapter, we have derived stellar atmospheric parameters for XSL in a uniform manner using ULySS with the empirical MILES interpolator. For many of the stars, this determination resulted in acceptable stellar atmospheric parameters. There are some points for improvement, which will be implemented when the parameters for the second data release will be computed.

Chapter 6

Summary and conclusions

In this Thesis, we have looked for a uniform method to determine stellar atmospheric parameters $T_{\rm eff}$, $\log g$ and [Fe/H] from spectra for stars in the X-shooter Spectral Library.

The first method we investigated is a Bayesian inference code called Starfish that uses full-spectrum fitting to determine (among other things) stellar atmospheric parameters. Starfish can make precise measurements of the parameters and attempts to derive a reasonable uncertainty in those measurements. We used Starfish in combination with the PHOENIX theoretical grid of model spectra to derive parameters for some stars in XSL. We concluded that the run-time of Starfish is too long for a good automatic determination of stellar atmospheric parameters for $\sim$900 spectra, and additionally we decided that we do not need the high precision that Starfish claims to give. Therefore we do not use Starfish as main inference method for stellar atmospheric parameters for XSL.

The second investigated method is ULySS, a full spectrum fitting software package that performs χ^2 minimization between an observed spectrum and an interpolated theoretical or empirical model spectrum. ULySS is suitable for the mass-production of stellar atmospheric parameters. We tested a new theoretical model interpolator based on the PHOENIX models, and we found that it is currently not yet good enough to use. We also ran ULySS on stars in XSL with two established empirical model interpolators. The results from that indicate that the determination of stellar atmospheric parameters is reasonably good using these interpolators, but depends on the chosen wavelength range and on the different models that are used.

We decided that we would use ULySS with the MILES empirical model interpolator to determine stellar atmospheric parameters for XSL, and we studied the results. For many stars this resulted in a good fit between models and data, and we adopted stellar atmospheric parameters for these stars. We looked at the outliers, but those should be studied in more detail in the future. We gave some recommendations for improvement and further investigation of our method. When the next XSL data release is available, we can apply our method to the new spectra and derive stellar atmospheric parameters for as many stars in XSL as possible.

The determination of stellar atmospheric parameters is not a trivial task. Different methods and different types of models result in stellar atmospheric parameters with large dispersions and average shifts, and uncertainties are difficult to estimate. A lesson to be learned from this: when using stellar atmospheric parameters from any source, it is wise to not use them blindly but to investigate where they come from, how they were determined, how the uncertainties are determined and what kinds of biases are present that could be reflected in any future results that use the parameters.

Acknowledgements

During the two years of my masters, I was supported by the NOVA MSc Fellowship. I thank NOVA for awarding me this fellowship.

I am very thankful to Scott, who believed that I could do this project and invited me to work with XSL. The project went a bit differently than initially planned and we had some setbacks, but I learned that this is part of doing science and I will take these experiences with me. Thank you for being a good supervisor, helping me out and guiding me where it was necessary, but letting me figure things out by myself most of the time. Thank you for giving me a pep talk every now and then when I needed it, it helped me get through some difficult parts of the project! I also want to thank you for giving me the opportunity to be part of the XSL Busy Week. It was a fun, good and interesting experience and I learned a lot about XSL and the people behind XSL, which I think is very valuable for the project.

Additionally, I would like to thank Mariya. I could always come to you with questions about XSL and you were always very helpful! Usually the conversations lasted a lot longer than necessary for the question that I asked, but I enjoyed them very much :) Among other things I learned more about life as a scientist, and I really appreciate that you were always interested in what was going on with me and the project, and enthusiastic about the things that were happening. Thanks for your encouragements!

My thanks also go out to the people in our group. I have enjoyed the group meetings a lot! Matthijs, thanks for helping me sometimes with stuff for XSL, it was nice that there was another XSL student in the group, especially during the Busy Week :) Gerjon and Shoko, thanks for proof-reading my thesis!

I would also like to thank Philippe Prugniel, who made the PHOENIX interpolators for ULySS and shared them with us. He also gave some very helpful comments on the results we found with the PHOENIX interpolator on the XSL stars early on, and he suggested we should try the self-inversion test. During the Busy Week we also had some more discussions about the results with the empirical interpolators, which were helpful for the remainder of the project.

Furthermore, I would like to thank Ariane Lançon, who looked through the list of literature stellar atmospheric parameters that I made and identified some errors and added parameters for several more stars.

I want to end on a more personal note. Pap en mam, bedankt dat jullie zo nu en dan de ellenlange verhalen over mijn onderzoek hebben aangehoord! Ik vond het leuk jullie uit te leggen waar het over ging, en misschien heeft dat me ook af en toe weer meer gemotiveerd. Sietske, wat heerlijk om een vriendin te hebben die ook sterrenkunde doet en die exact met je kan meeleven met het doen van onderzoek en het zoeken naar een PhD plek! Ik zie uit naar de komende drie jaar als we ook in Potsdam bij elkaar in de buurt blijven :) Verder was ik afgelopen jaar ook heel erg blij met mijn huisgenoten Femke en Aline, we hebben veel goede gesprekken gehad

tijdens bijvoorbeeld het eten, en jullie hebben niet gezeurd als ik met mijn burgerritme elke dag weer redelijk vroeg op stond om naar de universiteit te gaan :) Ik wil mijn kring ook bedanken, jullie hebben gedurende het jaar interesse getoond in de status van mijn project en met me meegeleefd! Tot slot bedank ik de meiden van mijn gebedsgroepje, Aline, Petra, Maaike, Ruth, Iris en Iris: jullie zijn echt geweldig! Jullie hebben me door het jaar heen gesleept, twee keer per week een goed begin van de studiedag met jullie was een voorrecht! We hebben samen gelachen en gehuild, gebeden en gekletst, advies gegeven en advies aangehoord, en ontzettend veel gedeeld. Thanks meiden!

Anke Arentsen
September 8, 2016

Bibliograpy

Allard, F., Homeier, D., & Freytag, B. 2011, in Astronomical Society of the Pacific Conference Series, Vol. 448, 16th Cambridge Workshop on Cool Stars, Stellar Systems, and the Sun, ed. C. Johns-Krull, M. K. Browning, & A. A.West, 91

Allende Prieto, C. Beers, T. C., Wilhelm, R., et al. 2006, ApJ, 636, 804

Bagnulo, S., Jehin, E., Ledoux, C., et al. 2003, The Messenger, 114, 10

Blackwell, D. E. & Lynas-Gray, A.E. 1998, A&AS, 129, 505

Buchhave, L. A., Latham, D. W., Johansen, A., et al. 2012, Nature, 486, 375

Cappellari, M. & Emsellem, E. 2004, PASP, 116, 138

Castelli, F. & Kurucz R. L. 2004 [arXiv:astro-ph/0405087]

Cenarro, A. J., Peletier, R. F., Sánchez-Blázquez, P., et al. 2007, MNRAS, 374, 664

Chen, Y.-P. 2013, PhD Thesis, University of Groningen

Chen, Y.-P., Trager, S. C., Peletier, R. F., et al. 2014a, The Messenger, 158, 30C

Chen, Y.-P., Trager, S. C., Peletier, R. F., et al. 2014b, A&A, 565A, 117

Coelho, P., Barbuy, B., Meléndez, J., Schiavon, R. P., & Castilho, B.V. 2005, A&A, 443, 735

Coelho, P. 2014, MNRAS, 440, 1027C

Czekala, I., Andrews, S. M., Mandel, K. S., et al. 2015, ApJ, 812, 128

Gelman, A., Carlin, J., Stern, H., et al. 2013, Bayesian Data Analysis (3rd ed.; London: Taylor and Francis)

Gregg, M. D., Silva, D., Rayner, J., et al. 2006, The 2005 HST Calibration Workshop: Hubble After the Transition to Two-Gyro Mode, p. 209

Husser, T.-O., Wende-von Berg, S., Dreizler, S., et al. 2013, A&A, 553, A6

Jofré, P., Panter, B., Hansen, C. J., & Weiss, A. 2010, A&A, 517, A57

Katz D., Soubiran C., Cayrel R., Adda M., Cautain R., 1998, A&A, 338, 151

Koleva, M., Prugniel, P., Bouchard, A., & Wu, Y. 2009, A&A, 501, 1269

Koleva, M., & Vazdekis, A. 2012, A&A, 538, A143

Lançon, A. & Wood, P. R. 2000, A&AS, 146, 217

Le Borgne, J.-F., Bruzual, G., Pelló, R., et al. 2003, A&A, 402, 433

Le Borgne, D., Rocca-Volmerange, B., Prugniel, P., et al. 2004, A&A, 425, 881

Lee, Y. S., Beers, T. C., Sivarani, T., et al. 2008a, AJ, 136, 2022

Lee, Y. S., Beers, T. C., Sivarani, T., et al. 2008b, AJ, 136, 2050

Marcum, P. M., O'Connell, R. W., Fanelli, M. N., et al. 2001, ApJS, 132, 129

Percival, S. M., & Salaris, M. 2009, ApJ, 703, 1123

Pickles, A. J. 1998, PASP, 110, 863

Prugniel, P. & Soubiran, C. 2001, A&A, 369, 1048

Prugniel, P., Koleva, M., Ocvirk, P., Le Borgne, D., & Soubiran, C. 2007a, in IAU Symp. 241, eds. A. Vazdekis & R. F. Peletier, 68

Prugniel, P., Soubiran, C., Koleva, M., & Le Borgne, D. 2007b, unpublished [arXiv:astro-ph/0703658]

Prugniel, P., Vauglin, I., & Koleva, M. 2011, A&A, 531, A165

Rayner, J. T., Cushing, M. C., & Vacca, W. D. 2009, ApJS, 185, 289

Sánchez-Blázquez, P., Peletier, R. F., Jiménez-Vicente, J., et al. 2006, MNRAS, 371, 703

Sharma, K., Prugniel, P. & Singh, H. P. 2016, A&A, 585, A64

Sneden, C. A. 1973, PhD thesis, The Univ. Texas

Soubiran C., Katz D., Cayrel R., 1998, A&AS, 133, 221

Tinsley B. M., 1972, ApJ, 178, 319

Trager, S. C. 2012, in International Workshop on Stellar Libraries, eds. Prugniel, P. & Singh, H. P., Astr. Soc. India Conf. Ser., 6, 1

Valdes, F., Gupta, R., Rose, J. A., Singh, H. P., & Bell, D. J. 2004, ApJS, 152, 251

Valenti, J. A., & Piskunov, N. 1996, A&AS, 118, 595

Vazdekis A., Sánchez-Blázquez P., Falcón-Barroso J., et al. 2010, MNRAS, 404, 1639

Vernet, J., Dekker, H., D'Odorico, S., et al. 2011, A&A, 536, A105

Worthey, G. & Ottaviani, D. L. 1997, ApJS, 111, 377

Wu, Y., Singh, H. P., Prugniel, P., Gupta, R., & Koleva, M. 2011, A&A, 525, A71

XSL Busy Week 4, 2016, internal notes

Appendix

Table 6.1. XSL stars with literature and computed stellar atmospheric parameters

Name[a]	Literature compilation				This work			
	$T_{\rm eff}$ (K)	$\log g$ (dex)	[Fe/H] (dex)	catalog[b]	$T_{\rm eff}$ (K)	$\log g$ (dex)	[Fe/H] (dex)	flag[c]
ABC89Cir18								
ABC89Pup17								
ABC89Pup42								
[B86] 133	4800	2.5	−0.81	PASTEL				
LMC143035								*fail*
LMC148035					3503 ± 1	-0.007 ± 0.011	-0.108 ± 0.012	
LMC150040					3630 ± 1	0.021 ± 0.007	-0.099 ± 0.006	
[M2002] LMC157533								
[M2002] LMC158646								
[M2002] LMC159974								
[M2002] LMC162635								
[M2002] LMC168757								
[M2002] LMC170452								
SMC046662					3788 ± 1	0.073 ± 0.006	-0.27 ± 0.005	
SMC052334					3950 ± 2	0.032 ± 0.006	-0.287 ± 0.005	
SMC055188					3578 ± 3	0.171 ± 0.023	-1.446 ± 0.032	
SMC083593					3617 ± 2	0.249 ± 0.014	-1.017 ± 0.019	
PHS2008-RGB533	4188	0.96	−0.77	AL				
PHS2008-RGB512	4128	0.88	−0.91	AL	4137 ± 19	1.057 ± 0.059	-1.147 ± 0.042	
PHS2008-RGB522	4101	0.91	−0.67	AL				
W65_c2					3901 ± 25	-0.198 ± 0.101	-0.713 ± 0.087	
[W71b]008-03								
2MASS-J15065441+1321060								
2MASS-J17535707-2931427								
2MASS-J18024572-3001120								
2MASS-J18024611-3004509								
2MASS-J18025277-2954335								
2MASS-J18032525-2959483	4690	2.4	0.47	PASTEL				
2MASS-J18033716-2954227								
2MASS-J18040638-3010497								
2MASS-J18042244-3000534								
2MASS-J18042265-2954518								
2MASS-J18080765-3142020								
2MASS-J18083220-3201531								
2MASS-J18351799-3428093								
2MASS-J18352206-3429112								
2MASS-J18352834-3444085								
2MASS-J18355679-3434481								
2MASS-J22244381-0158521								
BBB_SMC_104					4350 ± 3	0.554 ± 0.005	-0.716 ± 0.004	
BBB_SMC_148					4209 ± 11	0.439 ± 0.021	-0.696 ± 0.017	
BD-011792	4948	3.05	−1.05	MILES				
BD-095831	4575	1.12	−1.94	PASTEL	4707 ± 15	1.511 ± 0.037	-1.801 ± 0.019	
BD-114126	5000	4.3	0.2	MILES	4730 ± 4	4.631 ± 0.006	-0.017 ± 0.003	
BD-145890	4891	2.03	−2.16	PASTEL	4966 ± 12	2.222 ± 0.032	-2.052 ± 0.013	
BD-16 1934								
BD+012916	4238	0.35	−1.47	MILES	4335 ± 11	0.721 ± 0.025	-1.907 ± 0.018	
BD+023375	5944	3.97	−2.29	ELODIE	5920 ± 50	3.772 ± 0.075	-2.354 ± 0.061	
BD+032688	4300	0	−1.42	PASTEL	4649 ± 4	1.387 ± 0.009	-1.443 ± 0.005	
BD+042466	5223	2.02	−1.95	PASTEL	5013 ± 11	1.986 ± 0.027	-2.019 ± 0.012	
BD+060648	4400	1.02	−2.1	MILES	4611 ± 18	1.256 ± 0.042	-1.964 ± 0.024	

Table 6.1 (cont'd)

Name[a]	Literature compilation $T_{\rm eff}$ (K)	$\log g$ (dex)	[Fe/H] (dex)	catalog[b]	This work $T_{\rm eff}$ (K)	$\log g$ (dex)	[Fe/H] (dex)	flag[c]
BD+062986	4450	4.8	−0.3	MILES	3877 ± 6	4.68 ± 0.009	-0.41 ± 0.013	
BD+090352	5894	4.25	−2.12	MILES				
BD+092190	6270	4.11	−2.86	MILES	6149 ± 18	3.975 ± 0.029	-2.317 ± 0.026	
BD+092860	5298	2.98	−1.99	NGSL	5262 ± 19	2.565 ± 0.049	-1.686 ± 0.019	
BD+092870	4632	1.3	−2.37	PASTEL	4669 ± 21	1.482 ± 0.058	-2.366 ± 0.024	
BD+093223	5350	2	−2.26	MILES	5355 ± 9	2.825 ± 0.022	-2.002 ± 0.01	
BD+17_4708	5993	3.94	−1.65	ELODIE	6191 ± 7	4.14 ± 0.011	-1.5 ± 0.008	
BD+182890	4957	2.2	−1.61	MILES	5011 ± 11	2.335 ± 0.029	-1.582 ± 0.012	
BD+195116B	2950	5.06	0.1	MILES	3065 ± 24	4.92 ± 0.038	-0.162 ± 0.046	
BD+203603	6121	4.32	−2.09	MILES	6175 ± 14	4.08 ± 0.02	-2.032 ± 0.02	
BD+241676	6201	4.38	−2.45	MILES	6141 ± 7	3.932 ± 0.011	-2.24 ± 0.01	
BD+251981	6798	4.25	−1.26	MILES				
BD+292091	5780	4.46	−1.8	ELODIE	5761 ± 8	4.092 ± 0.013	-2.021 ± 0.012	
BD+302034	4500	0.4	−1.5	PASTEL	4452 ± 14	1.004 ± 0.03	-1.965 ± 0.021	
BD+302611	4311	0.94	−1.36	MILES	4374 ± 4	1.018 ± 0.01	-1.481 ± 0.007	
BMB 162								
BMB 300								
BS3923								
BS4104	3990	1.77	−0.39	PASTEL				
BS4432	3939	1.8	−0.31	MILES				
BS4463								
BS4517								
CD-2415398	6269	2.93	−1.14	MILES	8116 ± 11	2.753 ± 0.025	-1.486 ± 0.014	
CD-2610417	4570	4.5	0.06	MILES	4719 ± 3	4.746 ± 0.006	-0.08 ± 0.004	
CD-2809374	5000	3.4	−1.18	MILES	5061 ± 6	3.338 ± 0.012	-0.769 ± 0.006	
CD-3018140	5965	3.34	−2.15	PASTEL	6139 ± 4	4.019 ± 0.007	-1.917 ± 0.006	
CD-314916					3744 ± 2	-0.154 ± 0.008	0.19 ± 0.005	
CD-4911404	4676	2.88	0.23	PASTEL	4609 ± 7	2.63 ± 0.02	0.035 ± 0.008	
CD-603621					3842 ± 1	0.162 ± 0.004	0.158 ± 0.003	
CD-603636								
CD-621346	5300	1.7	−1.59	PASTEL	5224 ± 7	2.04 ± 0.017	-1.492 ± 0.008	
CD-691618	29000	3.7	−0.3	NGSL	5952 ± 20	3.247 ± 0.054	-2.53 ± 0.032	*lsf*
CL_NGC_121_T_V1					3739 ± 8	0.209 ± 0.061	-0.877 ± 0.062	*lsf*
Cl_NGC_121_T_V8					4206 ± 19	0.403 ± 0.04	-1.168 ± 0.033	
ClNGC1978_LE09	3750	0.3	−0.82	PASTEL	3827 ± 18	0.836 ± 0.116	-0.353 ± 0.079	
Cl_NGC_2324_BSV_10828	4750	1.7	−0.1	PASTEL				
Cl_NGC_288_OCH_531	3780	0.1	−1.31	PASTEL				
ClNGC330_ROBA3					5469 ± 15	0.821 ± 0.019	-0.291 ± 0.014	
ClNGC330_ROBB38	17000	2.3		PASTEL	8188 ± 12	1.525 ± 0.007	-0.644 ± 0.008	
N371R20					3909 ± 2	-0.198 ± 0.006	-0.252 ± 0.005	
Cl_NGC_371_LE_31								*fail*
CL_NGC_419_LE_27					10239 ± 2984	2.35 ± 0.719	-1.737 ± 0.771	
CL_NGC_419_LE_35					4558 ± 195	0.562 ± 0.262	-1.628 ± 0.203	
Cl_NGC_5139_SAW_V_1	5200	1	−1.77	PASTEL	6120 ± 11	1.332 ± 0.017	-0.998 ± 0.009	
Cl_NGC_5904_Arp_III-03_	4818	2.15	−1.51	PASTEL				
Cl_NGC_5904_Arp_IV-19	4845	2.2	−1.46	PASTEL	4221 ± 13	0.998 ± 0.037	-1.322 ± 0.027	
Cl_NGC_6121_LEE_2303	6190	2.75	−1.52	PASTEL	7176 ± 19	3.725 ± 0.029	-0.664 ± 0.014	
Cl_NGC_6121_LEE_2626	4625	1.5	−1.2	PASTEL	4488 ± 40	1.678 ± 0.123	-1.191 ± 0.063	
Cl_NGC_6121_LEE_4302	4775	1.45	−1.19	PASTEL	4754 ± 27	1.44 ± 0.062	-1.279 ± 0.036	
ClNGC6121_LEE4611	3725	0.3	−1.16	PASTEL	3948 ± 2	0.98 ± 0.011	-1.087 ± 0.008	
ClNGC6121_LEE4613	3750	0.2	−1.17	PASTEL	3940 ± 3	0.949 ± 0.016	-1.095 ± 0.011	

Table 6.1 (cont'd)

Name[a]	Literature compilation $T_{\rm eff}$ (K)	$\log g$ (dex)	[Fe/H] (dex)	catalog[b]	This work $T_{\rm eff}$ (K)	$\log g$ (dex)	[Fe/H] (dex)	flag[c]
CL_NGC_6522_ARP_1021	4750	1.2	−0.9	PASTEL	4521 ± 5	2.524 ± 0.015	0.267 ± 0.005	
CL_NGC_6522_ARP_1073	4750	1.2	−0.9	PASTEL	3828 ± 2	1.58 ± 0.014	-0.149 ± 0.007	
CL_NGC_6522_ARP_3190	4990	2	−1.12	PASTEL	3818 ± 3	1.616 ± 0.016	-0.304 ± 0.01	
CL_NGC_6522_ARP_3213	4220	1.9	−0.49	PASTEL	3962 ± 10	0.435 ± 0.052	-1.644 ± 0.049	*lsf*
CL_NGC_6522_ARP_4126	4900	2.7	−0.81	PASTEL	4288 ± 10	2.411 ± 0.04	-0.151 ± 0.015	
Arp4329	4690	2.4	0.47	PASTEL	4244 ± 34	1.541 ± 0.123	-1.084 ± 0.072	
Cl_NGC_6838_AH_A2	4100	0.8	−0.59	PASTEL				
Cl_NGC_6838_AH_A9	4200	1.2	−0.82	PASTEL				
CM Car								
CPD-5307400f	5389	1.6	0.12	PASTEL	5820 ± 4	1.077 ± 0.006	0.064 ± 0.004	
CPD-573502								
CS30336-049	4725	1.19	−4.1	AL	5036 ± 101	4.631 ± 0.343	-2.579 ± 0.247	*lsf*
EV Car								
Feige110	38905	6		PASTEL				
G012-021	5940	4.32	−1.43	MILES				
G013-035	6065	4.26	−1.68	MILES	6102 ± 5	4.12 ± 0.008	-1.696 ± 0.007	
G018-039	6130	4.15	−1.46	PASTEL	6139 ± 12	4.166 ± 0.018	-1.395 ± 0.014	
G019-013	4581	4.17	−0.62	PASTEL	4136 ± 4	4.6 ± 0.006	-0.421 ± 0.008	
G021-024	3906			PASTEL	4076 ± 3	4.636 ± 0.005	-0.194 ± 0.006	
G024-003	6180	4.62	−1.4	PASTEL	6078 ± 10	4.166 ± 0.014	-1.531 ± 0.012	
G029-023	6046	3.74	−1.82	ELODIE	6211 ± 12	4.108 ± 0.016	-1.658 ± 0.015	
G063-026	6175	4.17	−1.58	PASTEL	6148 ± 8	4.139 ± 0.013	-1.564 ± 0.011	
G169-28	3995	4.49	−0.44	NGSL	5836 ± 14	4.228 ± 0.023	-1.407 ± 0.018	
G187-40	6037	5	−1.27	PASTEL	5823 ± 10	4.249 ± 0.016	-1.523 ± 0.012	
G188-22	5890	3.9	−1.5	PASTEL	6197 ± 11	4.24 ± 0.015	-1.271 ± 0.012	
G20-15	6162	4.32	−1.5	PASTEL	6142 ± 16	4.186 ± 0.023	-1.469 ± 0.019	
Gl109	3462	4.87	−0.2	NGSL				
GL644C								
GL752B								*fail*
GL866	2747	5.09		MILES				*fail*
HD101712								
HD16031	6030	4.05	−1.72	MILES	6143 ± 10	4.095 ± 0.015	-1.719 ± 0.013	
HD16160	4829	4.6	−0.16	PASTEL	4679 ± 2	4.532 ± 0.003	-0.182 ± 0.002	
HD1638					4250 ± 7	1.57 ± 0.024	-0.777 ± 0.014	
HD17072	5428	2.65	−0.98	PASTEL	5271 ± 4	2.3 ± 0.012	-1.162 ± 0.005	
HD18191	3250	0.3		MILES	3203 ± 0	0.713 ± 0.002	-0.115 ± 0.002	
HD18769					8210 ± 6	3.501 ± 0.007	0.189 ± 0.003	
HD18907	5009	3.6	−0.75	MILES	5073 ± 3	3.583 ± 0.007	-0.711 ± 0.004	
HD19019	6063	4	−0.17	ELODIE	6065 ± 4	4.291 ± 0.007	-0.159 ± 0.004	
HD191709	6824	4.2	−0.04	ELODIE	6732 ± 4	3.933 ± 0.006	0.254 ± 0.003	
HD19445	5918	4.35	−2.05	MILES	5932 ± 12	4.018 ± 0.019	-2.093 ± 0.018	
HD019787	4940	2.92	0.12	PASTEL				
HD201237	4829	4.14	0	PASTEL	4789 ± 3	4.632 ± 0.005	0.077 ± 0.003	
HD215578	5136	3.37	0.43	PASTEL				
HD218566	4808	4.09	0.17	PASTEL	4784 ± 2	4.513 ± 0.003	0.246 ± 0.002	
HD221149	6144			PASTEL	5824 ± 3	3.786 ± 0.006	0.112 ± 0.002	
HD224926	15273	4.08	1	PASTEL	7013 ± 17	3.153 ± 0.05	-2.073 ± 0.024	*lsf*
HD25329	4787	4.58	−1.72	MILES	4972 ± 12	4.524 ± 0.022	-1.579 ± 0.02	
HD27295	11704	3.93	−0.74	MILES				
HD284248	6025	4.2	−1.6	MILES	6169 ± 16	4.137 ± 0.025	-1.674 ± 0.02	
HD2857	7450	2.6	−1.6	MILES				

Table 6.1 (cont'd)

Name[a]	Literature compilation				This work			
	$T_{\rm eff}$ (K)	$\log g$ (dex)	[Fe/H] (dex)	catalog[b]	$T_{\rm eff}$ (K)	$\log g$ (dex)	[Fe/H] (dex)	flag[c]
HD28978	9164	3.7	0.14	MILES	9063 ± 11	3.559 ± 0.007	-0.179 ± 0.005	
HD29391	7256	4.11	−0.1	ELODIE	7413 ± 5	4.098 ± 0.004	0.059 ± 0.002	
HD031421	4400	2.56	−0.1	PASTEL				
HD33299	4626	1.5	0.26	PASTEL	4591 ± 2	1.01 ± 0.004	0.08 ± 0.002	
HD34797	15988			PASTEL	8107 ± 9	2.181 ± 0.012	-1.703 ± 0.009	*lsf*
HD034816	30400	4.3	0.04	PASTEL				
HD035601	4000	0.7	−0.24	PASTEL				
HD000358	14007	3.77	−0.47	ELODIE				
HD037763	4630	3.15	0.33	PASTEL				
HD37828	4296	1.14	−1.38	MILES	4452 ± 4	1.239 ± 0.009	-1.49 ± 0.006	
HD038237	8110	3.69	−1.94	ELODIE				
HD039587	5918	4.36	−0.03	ELODIE				
HD039801	3550		0.03	MILES				
HD44007	4969	2.26	−1.47	MILES	4913 ± 13	2.17 ± 0.034	-1.663 ± 0.015	
HD45282	5348	3.24	−1.44	MILES	5292 ± 10	3.158 ± 0.023	-1.512 ± 0.011	
HD4813	6185	4.45	−0.15	ELODIE	6187 ± 3	4.224 ± 0.005	-0.168 ± 0.003	
HD050877	3900	0.65	−0.32	PASTEL				
HD052005	4117	0.2	−0.2	MILES				
HD052298	6072	4.6	−0.84	PASTEL				
HD052973	5659	1.37	0.34	MILES				
HD057060	35950	3.2		MILES				
HD58790	5300	3.4	0.3	PASTEL	4669 ± 7	2.498 ± 0.018	-0.107 ± 0.007	
HD061064	6495	3.2	0.4	MILES				
HD062164								
HD6229	5133	2.39	−1.08	MILES	5112 ± 15	2.243 ± 0.04	-1.172 ± 0.017	
HD063302	4500	0.2	0.12	MILES				
HD064332	3500	0.5	−0.34	MILES				
HD065354								
HD070138								
HD072968								
HD074088	7500	4	−1.04	PASTEL				
HD076221	2625		−0.3	PASTEL				
HD079349								
HD081797	4120	1.54	−0.06	MILES				
HD82395	4730	2.97	−0.17	PASTEL	4748 ± 2	2.557 ± 0.004	-0.085 ± 0.002	
HD082734	4709	2.65	0.3	MILES				
HD083212	4600	1.3	−1.4	MILES				
HD8724	4688	1.49	−1.69	MILES	4734 ± 11	1.614 ± 0.027	-1.712 ± 0.014	
HD093813	4435	2.2	−0.25	PASTEL				
HD96446					5964 ± 10	3.585 ± 0.022	-2.514 ± 0.015	*lsf*
HD098817								
HD099648	4850	1.9	0.36	MILES				
HD002796	4945	1.36	−2.31	MILES	4754 ± 11	1.606 ± 0.03	-2.453 ± 0.013	
HD003008	4331	0.84	−1.87	MILES	4361 ± 5	0.713 ± 0.01	-1.855 ± 0.007	
HD003883	7777	3.65	0.48	MILES	7542 ± 7	3.544 ± 0.007	0.629 ± 0.003	
HD004539	25200	5.4	0.16	MILES	6702 ± 79	4.109 ± 0.084	-2.121 ± 0.081	*lsf*
HD004893	4057	1.8	0.2	PASTEL	4104 ± 6	2.243 ± 0.023	0.023 ± 0.008	
HD004906	5068	3.47	−0.84	MILES	5195 ± 8	3.758 ± 0.016	-0.689 ± 0.009	
HD005544	4655	2.26	−0.04	NGSL	4595 ± 7	2.255 ± 0.02	-0.09 ± 0.008	
HD005857	4520	2.8	−0.3	ELODIE	4623 ± 2	2.711 ± 0.006	-0.222 ± 0.002	
HD006268	4740	1.2	−2.32	MILES	4674 ± 15	1.425 ± 0.038	-2.463 ± 0.018	

Table 6.1 (cont'd)

Name[a]	Literature compilation				This work			
	$T_{\rm eff}$ (K)	$\log g$ (dex)	[Fe/H] (dex)	catalog[b]	$T_{\rm eff}$ (K)	$\log g$ (dex)	[Fe/H] (dex)	flag[c]
HD007595	4345	1.5	−0.8	MILES	4325 ± 8	1.825 ± 0.027	-0.621 ± 0.014	
HD009051	4949	2.3	−1.57	PASTEL				
HD009356	6282	2.77	−1.38	MILES				
HD011397	6074	5.15	0.09	MILES				
HD014625	4513	2.42	0	ELODIE	4765 ± 5	2.769 ± 0.013	0.208 ± 0.005	
HD014829	8666	3.1	−1.25	MILES				
HD014938	6153	4.04	−0.35	MILES	6259 ± 4	4.182 ± 0.007	-0.345 ± 0.004	
HD016232	6346	4.54	0.03	MILES				
HD016456	6750	2.8	−1.7	PASTEL	7947 ± 8	2.283 ± 0.012	-1.529 ± 0.008	
HD016673	6253	4.28	0.05	MILES				
HD019304	6860	3.88	−0.9	ELODIE	6661 ± 6	4.25 ± 0.008	-0.446 ± 0.005	
HD020619	5652	4.48	−0.28	MILES	5657 ± 4	4.374 ± 0.007	-0.28 ± 0.004	
HD021197	4616	4.59	0.3	MILES	4347 ± 3	4.452 ± 0.005	0.121 ± 0.003	
HD023924	8000	4	−0.3	MILES				
HD024616	4954	3.2	−0.75	MILES	5013 ± 7	3.243 ± 0.015	-0.757 ± 0.007	
HD025532	5525	2.2	−1.2	MILES	5561 ± 7	2.793 ± 0.018	-1.145 ± 0.007	
HD025673	5150	4.5	−0.6	MILES	5140 ± 5	4.648 ± 0.008	-0.422 ± 0.006	
HD026297	4316	1.06	−1.67	MILES	4492 ± 6	1.056 ± 0.012	-1.791 ± 0.008	
HD027771	5143	4.5	0.07	MILES	5295 ± 3	4.57 ± 0.006	0.242 ± 0.003	
HD030328	3925	1.4	0	PASTEL	4725 ± 2	2.612 ± 0.004	0.064 ± 0.002	
HD030743	6411	4.12	−0.34	MILES				
HD033793	3570	4.96	−0.99	PASTEL	3672 ± 5	4.878 ± 0.008	-0.709 ± 0.016	
HD035179	4720	1.6	−0.67	MILES	4930 ± 6	2.358 ± 0.016	-0.608 ± 0.007	
HD036395	3737	4.9	−1.5	MILES				
HD036702	4337	0.88	−2.12	PASTEL				
HD038145	7256	3.78	−1.72	ELODIE				
HD038769	6942	3.7	−2.1	ELODIE	7035 ± 3	4.018 ± 0.004	0.205 ± 0.002	
HD038856	16901	4.32	0	ELODIE				
HD039833	5761	3.85	0.29	MILES				
HD039949	5316	1.72	−0.01	PASTEL				
HD039970	9400	1.43		MILES				
HD041433	4837	2.62	−0.2	ELODIE	5099 ± 4	2.265 ± 0.01	-0.018 ± 0.004	
HD041661	6200	4.22	0	ELODIE	6578 ± 4	3.862 ± 0.006	0.16 ± 0.003	
HD041667	4581	1.8	−1.07	PASTEL	4664 ± 6	1.69 ± 0.016	-1.215 ± 0.008	
HD041770	6800	3.85	0.36	ELODIE	7103 ± 4	3.681 ± 0.005	0.519 ± 0.002	
HD042143	9190	3.96	0.06	ELODIE				
HD042182	5117	4.54	0.11	MILES	5046 ± 3	4.591 ± 0.006	0.103 ± 0.003	
HD042256	4597	2.58	−0.3	ELODIE	4683 ± 3	2.409 ± 0.008	-0.326 ± 0.003	
HD042597	24530	3.64	0	ELODIE	6373 ± 6	3.798 ± 0.011	-2.292 ± 0.01	*lsf*
HD042983	4633	3.23	0	ELODIE	4808 ± 5	3.523 ± 0.01	-0.015 ± 0.005	
HD043021	7822	3.85	−0.63	ELODIE	8205 ± 7	4.274 ± 0.005	-0.688 ± 0.006	
HD043286	15518	3	0	ELODIE	6918 ± 30	4.032 ± 0.04	-1.891 ± 0.033	*lsf*
HD044285	4595	1.47	−0.2	ELODIE	4263 ± 3	1.994 ± 0.013	-0.1 ± 0.005	
HD044391	4672	1.38	0.11	PASTEL	4662 ± 9	1.127 ± 0.018	0.009 ± 0.01	
HD044515	4346	1.53	−0.03	ELODIE	4122 ± 3	2.222 ± 0.014	0.054 ± 0.005	
HD044770	7300	3.57	−2.64	ELODIE	6517 ± 5	4.244 ± 0.007	-0.112 ± 0.004	
HD045196	7060	3.83	−0.5	ELODIE	7349 ± 6	3.739 ± 0.008	0.172 ± 0.003	
HD045507	4925	2.66	−0.13	ELODIE	5039 ± 8	2.469 ± 0.02	-0.114 ± 0.008	
HD046454	4328	1.6	−0.2	ELODIE	4187 ± 3	1.648 ± 0.011	-0.315 ± 0.005	
HD048616	6100	3.61	0.4	ELODIE	6490 ± 4	1.062 ± 0.005	-0.07 ± 0.003	
HD049068	4381	1.73	−0.2	PASTEL				

Table 6.1 (cont'd)

Name[a]	Literature compilation				This work			
	$T_{\rm eff}$ (K)	$\log g$ (dex)	[Fe/H] (dex)	catalog[b]	$T_{\rm eff}$ (K)	$\log g$ (dex)	[Fe/H] (dex)	flag[c]
HD049739	7150	3.79	−0.5	ELODIE	7450 ± 12	4.061 ± 0.012	-0.106 ± 0.006	
HD050372	4970	2.2	−0.1	ELODIE	4745 ± 5	1.797 ± 0.012	0.015 ± 0.006	
HD050819	5500	2.71	−0.04	ELODIE				
HD053003	5500	1.41	0	ELODIE	5816 ± 5	1.202 ± 0.008	0.041 ± 0.005	
HD053927	4811	4.5	−0.74	MILES	4918 ± 6	4.736 ± 0.011	-0.318 ± 0.007	
HD054828	5020	2.43	−0.61	ELODIE	4894 ± 7	2.354 ± 0.019	-0.737 ± 0.009	
HD055583	4482	2.36	−0.17	ELODIE	4569 ± 5	2.642 ± 0.013	-0.035 ± 0.005	
HD055693	5845	0.26	0.02	MILES	5701 ± 3	4.089 ± 0.005	0.155 ± 0.003	
HD056448	4801	2.68	0	ELODIE	5037 ± 5	2.674 ± 0.013	-0.093 ± 0.005	
HD057132	4390	1.47	−0.2	ELODIE	4080 ± 4	1.615 ± 0.015	-0.291 ± 0.007	
HD057707	4602	2.8	−0.3	ELODIE	4818 ± 4	3.152 ± 0.008	-0.038 ± 0.004	
HD058051	4202	1.63	−0.03	ELODIE	4015 ± 4	2.028 ± 0.016	0.029 ± 0.006	
HD058072	5500	2.62	−0.2	ELODIE	5099 ± 4	2.377 ± 0.01	0.007 ± 0.004	
HD058455	4334	1.47	−0.2	ELODIE	4184 ± 6	2.055 ± 0.023	-0.042 ± 0.009	
HD058554	4337	2.03	−0.2	ELODIE	4373 ± 5	2.025 ± 0.018	-0.289 ± 0.008	
HD059295	4437	2.76	0.1	ELODIE	4631 ± 3	2.266 ± 0.009	-0.022 ± 0.004	
HD059984	6000	4.31	−0.68	MILES	5947 ± 3	3.98 ± 0.006	-0.786 ± 0.003	
HD060319	6012	4.16	−0.84	PASTEL				
HD062968	4758	2.58	0.07	ELODIE				
HD064630	7754	3.62	−2.3	ELODIE				
HD065372	8142	3.61	−0.82	ELODIE				
HD065583	5268	4.44	−0.56	MILES	5275 ± 5	4.39 ± 0.009	-0.759 ± 0.007	
HD066776	4645	2.73	0.07	ELODIE	4792 ± 4	2.669 ± 0.011	0.026 ± 0.004	
HD069701	3910	0.5	−0.12	PASTEL	3741 ± 1	1.139 ± 0.004	-0.223 ± 0.003	
HD071160	4097	1.87	0.07	NGSL	4041 ± 4	1.785 ± 0.014	-0.005 ± 0.006	
HD071310								
HD071497	4558	2.76	0.1	ELODIE				
HD073665	4965	2.35	0.16	MILES				
HD074000	6166	4.19	−2.02	MILES				
HD074166	4300	1.8	−0.05	PASTEL				
HD074721	8560	3.57	−1.42	MILES	10166 ± 69	4.244 ± 0.024	-0.385 ± 0.026	
HD075318	5422	4.5	−0.04	MILES	5389 ± 7	4.417 ± 0.012	-0.185 ± 0.008	
HD076780	5869	4.8	0.21	MILES	5633 ± 3	4.225 ± 0.005	0.087 ± 0.003	
HD078737	6350	3.8	−0.6	MILES	6585 ± 5	4.253 ± 0.007	-0.501 ± 0.004	
HD083632	4198	1	−1	MILES	4124 ± 2	1.349 ± 0.008	-0.896 ± 0.005	
HD084937	6228	4.01	−2.17	MILES				
HD085380	6037	4.07	0.084	PASTEL				
HD085773	4463	0.97	−2.19	MILES				
HD088737	5994	3.92	0.17	MILES	6071 ± 3	3.866 ± 0.006	0.126 ± 0.003	
HD090862	4129	1.7	−0.39	NGSL	4028 ± 3	1.624 ± 0.012	-0.595 ± 0.006	
HD093329	8075	2.8	−1.48	MILES	8272 ± 8	3.067 ± 0.02	-1.447 ± 0.009	
HD093487	5250	1.8	−1.05	MILES	5160 ± 10	2.209 ± 0.027	-1.181 ± 0.012	
HD098468					4495 ± 11	2.05 ± 0.037	-0.394 ± 0.017	
HD099109	5400	4.2	0.45	MILES	5258 ± 3	4.273 ± 0.006	0.355 ± 0.003	
HD099329	7005	3.75	−1.9	ELODIE	7071 ± 6	4.071 ± 0.006	0.172 ± 0.003	
HD099491	5456	4.34	0.24	ELODIE	5416 ± 3	4.268 ± 0.005	0.318 ± 0.003	
HD100906	4980	2	−1.02	MILES	5049 ± 5	2.304 ± 0.014	-0.421 ± 0.006	
HD102634	6344	4.12	0.27	MILES	6132 ± 4	4.056 ± 0.008	0.077 ± 0.004	
HD103877	7341	4	0.4	MILES	6862 ± 5	3.626 ± 0.007	0.619 ± 0.003	
HD103932	4510	4.57	0.16	MILES	4413 ± 2	4.511 ± 0.003	0.057 ± 0.002	
HD104307	4451	2	−0.01	MILES	4424 ± 2	2.257 ± 0.006	-0.039 ± 0.002	

Table 6.1 (cont'd)

Name[a]	Literature compilation				This work			
	$T_{\rm eff}$ (K)	$\log g$ (dex)	[Fe/H] (dex)	catalog[b]	$T_{\rm eff}$ (K)	$\log g$ (dex)	[Fe/H] (dex)	flag[c]
HD104893	4500	1.1	−1.97	PASTEL	4420 ± 7	0.831 ± 0.015	-2.222 ± 0.009	
HD105262	8542	1.5	−1.37	MILES	8444 ± 7	1.441 ± 0.004	-1.914 ± 0.004	
HD105740	4700	2.5	−0.51	MILES	4706 ± 6	2.653 ± 0.015	-0.684 ± 0.007	
HD106304	8675	2.85	−1.63	NGSL				
HD108564	4594	4.67	−1.09	MILES	4582 ± 2	4.628 ± 0.003	-0.988 ± 0.003	
HD108915				MILES	5000 ± 2	3.335 ± 0.005	-0.115 ± 0.002	
HD109307	8396	4.1	0.05	PASTEL	8318 ± 12	3.424 ± 0.014	-0.127 ± 0.008	
HD109443	6632	4.2	−0.65	MILES	6818 ± 6	4.221 ± 0.008	-0.618 ± 0.005	
HD109871				MILES	3939 ± 4	1.7 ± 0.019	-0.215 ± 0.009	
HD110184	4336	0.54	−2.38	ELODIE	4468 ± 8	0.937 ± 0.019	-2.33 ± 0.01	
HD110885	5253	2.4	−1.53	MILES	5525 ± 6	2.717 ± 0.015	-1.177 ± 0.006	
HD111515	5364	4.46	−0.62	PASTEL	5446 ± 4	4.406 ± 0.007	-0.641 ± 0.005	
HD111631	3748	4.75	0.1	MILES	3880 ± 1	4.566 ± 0.002	0.012 ± 0.002	
HD111721	5212	2.6	−1.11	PASTEL	5037 ± 5	2.638 ± 0.013	-1.366 ± 0.006	
HD111786	7450	3.93	−1.6	MILES	8051 ± 7	4.439 ± 0.004	-0.807 ± 0.006	
HD112374	6629	2.35	−0.59	PASTEL	6191 ± 5	0.7 ± 0.005	-0.692 ± 0.004	
HD113002	5152	2.53	−1.08	NGSL	5106 ± 10	2.156 ± 0.028	-1.002 ± 0.012	
HD114606	5523	4.12	−0.69	MILES	5581 ± 8	4.068 ± 0.015	-0.625 ± 0.009	
HD114960					4069 ± 5	2.237 ± 0.021	0.084 ± 0.007	
HD116114	8020	4.18	0.48	MILES	8589 ± 10	4.334 ± 0.009	0.781 ± 0.004	
HD116544	4400	4.5	−0.2	MILES	4453 ± 7	3.221 ± 0.02	0.159 ± 0.007	
HD116745	4500	1	−1.97	PASTEL	6811 ± 14	2.836 ± 0.034	-1.26 ± 0.014	
HD117880	9300	3.3	−1.64	PASTEL				
HD118055	4202	0.71	−1.91	MILES	4401 ± 7	0.885 ± 0.015	-1.863 ± 0.01	
HD118100	4179	4.5	−0.07	MILES	4268 ± 3	4.504 ± 0.005	-0.08 ± 0.004	
HD119802	4763	4	−0.05	ELODIE	4640 ± 4	4.69 ± 0.008	0.021 ± 0.004	
HD119850	3623	4.8	−0.1	ELODIE	3481 ± 5	4.693 ± 0.012	-0.27 ± 0.015	
HD122956	4635	1.49	−1.75	MILES	4677 ± 14	1.438 ± 0.032	-1.743 ± 0.018	
HD124292	5391	4.5	−0.19	MILES	5436 ± 7	4.425 ± 0.012	-0.127 ± 0.008	
HD126053	5662	4.5	−0.45	MILES	5663 ± 6	4.313 ± 0.01	-0.419 ± 0.007	
HD126661	7514	3.13	0.31	PASTEL	7715 ± 5	3.402 ± 0.006	0.326 ± 0.002	
HD126681	5536	4.65	−1.25	MILES	5621 ± 6	4.212 ± 0.012	-1.214 ± 0.008	
HD126778	4847	2.34	−0.61	MILES	4791 ± 6	2.358 ± 0.015	-0.549 ± 0.007	
HD128429	6266	4.12	−0.13	MILES	6302 ± 5	4.127 ± 0.008	-0.187 ± 0.004	
HD128801	10250	3.4	−1.2	MILES				
HD130095	8656	3.47	−1.65	MILES				
HD130322	5349	4.72	0.04	MILES	5390 ± 4	4.522 ± 0.007	0.074 ± 0.004	
HD13043	5695	3.68	0.1	MILES	5792 ± 8	4.04 ± 0.014	-0.019 ± 0.007	
HD134063	4885	2.34	−0.68	MILES	4879 ± 10	2.37 ± 0.025	-0.701 ± 0.012	
HD134439	4950	4.57	−1.49	MILES	5125 ± 4	4.563 ± 0.008	-1.385 ± 0.007	
HD134440	4740	4.5	−1.48	MILES	4953 ± 5	4.699 ± 0.01	-1.33 ± 0.009	
HD138290	6872	4.59	−0.05	MILES	6901 ± 5	4.179 ± 0.005	-0.09 ± 0.003	
HD138776	5700	4.2	0.48	MILES	5483 ± 3	3.945 ± 0.007	0.257 ± 0.003	
HD139717	5426	1.4	0.15	PASTEL	6583 ± 4	1.09 ± 0.006	0.045 ± 0.003	
HD140232	7754	4.44	0.52	PASTEL	8085 ± 19	4.001 ± 0.017	0.39 ± 0.009	
HD140283	5687	3.55	−2.53	MILES	5735 ± 7	3.684 ± 0.013	-2.439 ± 0.009	
HD141531	4335	1.11	−1.62	PASTEL	4457 ± 6	1.035 ± 0.012	-1.648 ± 0.008	
HD142575	6550	3.6	−1	MILES	6807 ± 6	4.213 ± 0.008	-0.735 ± 0.005	
HD142703	7220	3.89	−1.02	MILES	7681 ± 9	4.381 ± 0.006	-1.078 ± 0.008	
HD143459	8842	3.55	−1.26	MILES	10774 ± 20	4.207 ± 0.009	-0.166 ± 0.007	
HD144172	6302	4.02	−0.46	MILES	6416 ± 6	4.135 ± 0.009	-0.449 ± 0.005	

Table 6.1 (cont'd)

Name[a]	Literature compilation $T_{\rm eff}$ (K)	$\log g$ (dex)	[Fe/H] (dex)	catalog[b]	This work $T_{\rm eff}$ (K)	$\log g$ (dex)	[Fe/H] (dex)	flag[c]
HD144921	4165	0.2	−1.8	PASTEL	4110 ± 7	0.382 ± 0.017	-1.652 ± 0.015	
HD147550	10506	3.63	0	ELODIE				
HD149382	36000	5.5	−1.3	MILES	6378 ± 23	3.997 ± 0.041	-2.347 ± 0.034	*lsf*
HD150281	4863	4.26	−0.29	MILES	5179 ± 4	4.56 ± 0.006	0.132 ± 0.003	
HD157089	5785	4.12	−0.56	MILES	5805 ± 7	3.987 ± 0.014	-0.616 ± 0.008	
HD160346	4983	4.3	−0.1	ELODIE	4906 ± 3	4.679 ± 0.005	0.038 ± 0.003	
HD160365	6009			PASTEL	6485 ± 5	3.732 ± 0.009	0.175 ± 0.004	
HD161149	6600	2.95	0.55	MILES	7022 ± 4	3.89 ± 0.005	0.403 ± 0.002	
HD161227	7522	3.5		MILES	7278 ± 5	3.711 ± 0.006	0.397 ± 0.003	
HD161370	9743	3.78	−1.04	ELODIE	8385 ± 16	4.032 ± 0.015	-0.086 ± 0.01	
HD161677	13962	3	0	ELODIE	6539 ± 70	3.87 ± 0.137	-2.106 ± 0.105	*lsf*
HD161770	5709	3.67	−1.57	PASTEL	5892 ± 12	3.961 ± 0.02	-1.441 ± 0.013	
HD161817	7636	2.93	−0.95	MILES	8214 ± 12	4.18 ± 0.01	-0.916 ± 0.012	
HD162652	9652	3.64	0.19	ELODIE	4930 ± 3	2.654 ± 0.007	0.005 ± 0.003	
HD163346	8478	3.24	0.2	ELODIE				
HD163641	10789	3.88	0	ELODIE				
HD163810	5424	4.43	−1.34	PASTEL				
HD164115	6938	3.74		ELODIE	6941 ± 7	3.953 ± 0.009	0.152 ± 0.005	
HD164257	9449	3.92	0.46	ELODIE	11307 ± 19	3.569 ± 0.01	0.808 ± 0.004	
HD164432	21311	3.65	−0.33	MILES	6324 ± 7	3.573 ± 0.015	-2.347 ± 0.012	*lsf*
HD164967	8742	3.98	−0.07	ELODIE	9093 ± 27	4.104 ± 0.014	-0.294 ± 0.014	
HD165195	4471	1.11	−2.15	MILES	4405 ± 6	0.798 ± 0.014	-2.292 ± 0.008	
HD165438	4862	3.4	0.02	MILES	4877 ± 2	3.501 ± 0.005	0.037 ± 0.002	
HD165887	8451	3.65	−2.03	ELODIE	8246 ± 10	3.696 ± 0.011	-0.121 ± 0.006	
HD166161	4905	2.31	−1.25	MILES	5233 ± 14	2.241 ± 0.034	-1.238 ± 0.015	
HD166283	8092	3.71	−1.31	ELODIE	8225 ± 13	3.912 ± 0.013	-0.033 ± 0.008	
HD166991	9011	3.92	−0.43	ELODIE	8631 ± 12	3.628 ± 0.014	-0.29 ± 0.009	
HD167278	6350	4.04	−0.18	ELODIE				
HD167946	9941	3.84	0.03	ELODIE	10804 ± 36	4.088 ± 0.017	-0.062 ± 0.011	
HD169032	7879	3.91	−0.5	ELODIE	8379 ± 24	3.663 ± 0.026	-0.049 ± 0.014	
HD170413	4413	2.51	−0.03	ELODIE	4757 ± 8	2.565 ± 0.02	-0.066 ± 0.008	
HD170756								
HD170783	15241	3	0	ELODIE	7043 ± 18	3.132 ± 0.056	-2.009 ± 0.029	*lsf*
HD170820	4489	1.41	0.1	PASTEL	4470 ± 11	1.302 ± 0.03	-0.175 ± 0.015	
HD170899	5265	2.55	−0.05	ELODIE	4635 ± 4	2.056 ± 0.012	-0.259 ± 0.005	
HD171234	7856	3.86	−0.77	ELODIE	7943 ± 9	3.881 ± 0.009	-0.031 ± 0.005	
HD171367	4511	2.8	−0.3	ELODIE	4383 ± 4	2.094 ± 0.015	-0.743 ± 0.007	
HD171496	4700	1.6	−0.91	MILES	4954 ± 8	2.291 ± 0.023	-0.717 ± 0.01	
HD172230	7100	3.62	0.31	ELODIE	7611 ± 9	3.431 ± 0.01	0.505 ± 0.004	
HD172365	5800	2.12	−0.36	MILES	5999 ± 3	1.308 ± 0.006	0.085 ± 0.003	
HD172472	4693	2.47	−0.02	ELODIE	4886 ± 9	1.713 ± 0.022	-0.073 ± 0.011	
HD172488	30031	3.71	0	ELODIE	4965 ± 75	4.584 ± 0.243	-2.584 ± 0.133	*lsf*
HD172506	6650	4.38	0	ELODIE	7257 ± 9	4.068 ± 0.01	-0.045 ± 0.005	
HD172522	8985	3.76	−1	ELODIE	8569 ± 24	3.166 ± 0.023	-0.213 ± 0.015	
HD173073	8384	3.76	−0.96	ELODIE	8320 ± 12	3.341 ± 0.017	-0.43 ± 0.009	
HD173158	4688	1.47	0.1	ELODIE	5212 ± 14	0.912 ± 0.021	0.185 ± 0.014	
HD173369	8212	3.52	0	ELODIE	8043 ± 8	3.485 ± 0.009	0.294 ± 0.004	
HD173669	9811	3.88	−0.59	ELODIE	8751 ± 15	3.957 ± 0.013	-0.356 ± 0.01	
HD174240	9437	3.98	−0.13	ELODIE	9788 ± 34	3.816 ± 0.018	-0.136 ± 0.013	
HD174350	4537	2.56	−0.02	ELODIE	4780 ± 5	2.375 ± 0.014	0 ± 0.006	
HD174512	11406	2.72	0	ELODIE	6984 ± 10	2.98 ± 0.018	-0.002 ± 0.007	

Table 6.1 (cont'd)

Name[a]	Literature compilation $T_{\rm eff}$ (K)	$\log g$ (dex)	[Fe/H] (dex)	catalog[b]	This work $T_{\rm eff}$ (K)	$\log g$ (dex)	[Fe/H] (dex)	flag[c]
HD174866	7200	3.88	−0.61	ELODIE	7885 ± 13	3.894 ± 0.012	-0.032 ± 0.007	
HD174966	7653	3.68	−2.04	ELODIE	7689 ± 18	3.932 ± 0.017	0.025 ± 0.01	
HD175058	7026	3.68	−1.94	ELODIE	7938 ± 8	3.16 ± 0.011	-0.26 ± 0.005	
HD175181	5082	2.69	−0.06	ELODIE	5024 ± 5	2.619 ± 0.013	-0.094 ± 0.005	
HD175376	4577	1.16	−0.2	ELODIE	4275 ± 4	2.521 ± 0.016	0.287 ± 0.005	
HD175545					4476 ± 6	2.875 ± 0.018	0.107 ± 0.007	
HD175640	12050	3.9	−0.43	MILES	8257 ± 17	2.101 ± 0.013	-1.797 ± 0.014	*lsf*
HD175805	6300	4.09	0.18	ELODIE	6275 ± 5	3.965 ± 0.01	0.253 ± 0.005	
HD175892	8816	4.22		MILES	8670 ± 14	3.825 ± 0.015	-0.372 ± 0.01	
HD176301	13100	3.5		MILES	8266 ± 9	1.664 ± 0.005	-1.903 ± 0.006	*lsf*
HD176698	4711	2.71	0	ELODIE	4966 ± 7	2.762 ± 0.017	0.072 ± 0.007	
HD176851	6500	3.95	−0.69	ELODIE	6910 ± 5	3.707 ± 0.007	0.416 ± 0.003	
HD178287	5600	1.4	0	ELODIE	5877 ± 8	1.066 ± 0.012	0.143 ± 0.007	
HD179315	5800	1.39	0.06	ELODIE	5938 ± 7	1.155 ± 0.011	0.235 ± 0.006	
HD179821	6997	0.62	0.44	PASTEL	7755 ± 26	0.552 ± 0.028	0.739 ± 0.017	
HD179870					4859 ± 9	2.169 ± 0.023	0.094 ± 0.01	
HD180086	6800	3.75	−1.7	ELODIE	7303 ± 8	3.936 ± 0.01	0.122 ± 0.005	
HD183085	7000	3.76	−1.69	ELODIE	7306 ± 9	3.989 ± 0.01	-0.043 ± 0.005	
HD184266	5780	1.85	−1.75	PASTEL	5901 ± 10	3.126 ± 0.023	-1.25 ± 0.009	
HD184571	6676	3.57	−0.5	ELODIE	6504 ± 6	4.05 ± 0.011	-0.031 ± 0.005	
HD185094	7089	4.32	−0.04	ELODIE	6989 ± 5	4.13 ± 0.005	0.049 ± 0.003	
HD186478	4540	0.65	−2.75	PASTEL	4704 ± 12	1.58 ± 0.034	-2.325 ± 0.014	
HD187111	4259	0.58	−1.83	MILES	4462 ± 5	1.108 ± 0.011	-1.666 ± 0.007	
HD188262	6199			PASTEL	5244 ± 15	2.226 ± 0.036	-0.134 ± 0.017	
HD188510	5490	4.69	−1.59	MILES	5543 ± 6	4.279 ± 0.011	-1.602 ± 0.009	
HD189511	5059	2.93	0.2	ELODIE	4921 ± 6	1.837 ± 0.015	-0.051 ± 0.007	
HD190073	8330			ELODIE				
HD190390	6440	1.55	−1.05	MILES				
HD190404	5051	4.45	−0.17	MILES	4970 ± 5	4.527 ± 0.009	-0.701 ± 0.007	
HD193225	7458	3.72	−1.86	ELODIE	7443 ± 7	4.051 ± 0.007	0.104 ± 0.004	
HD193281	8080	3.58	−1	MILES	8567 ± 21	3.828 ± 0.024	-0.498 ± 0.017	
HD193326	5129	2.65	−0.2	ELODIE	5123 ± 6	2.842 ± 0.015	-0.281 ± 0.006	
HD193896					5161 ± 6	2.56 ± 0.014	-0.09 ± 0.006	
HD194453	9950	3.69	0.1	ELODIE	10730 ± 35	3.904 ± 0.016	0.053 ± 0.011	
HD195729	8001	3.62	−2.28	ELODIE	8107 ± 13	3.573 ± 0.015	0.008 ± 0.007	
HD196125	7562	3.96	−0.71	ELODIE	7400 ± 8	3.935 ± 0.009	0.043 ± 0.005	
HD196218	6463	4.2	−0.15	ELODIE	6215 ± 5	4.12 ± 0.008	-0.161 ± 0.004	
HD196426	13050	3.85	0.05	ELODIE	8243 ± 12	1.96 ± 0.008	-1.869 ± 0.009	
HD196892	5670	3.85	−1.38	PASTEL	6090 ± 12	4.116 ± 0.02	-1.002 ± 0.014	
HD_198140					4709 ± 5	1.612 ± 0.013	-0.367 ± 0.007	*lsf*
HD200081	5260	2.79	−0.17	ELODIE	5346 ± 13	3.121 ± 0.026	-0.021 ± 0.012	
HD200494	4457	2.5	0.06	ELODIE	4420 ± 4	2.795 ± 0.013	0.126 ± 0.005	
HD200779	4252	4.63		MILES	4185 ± 3	4.562 ± 0.006	0.021 ± 0.006	
HD201053	4596	2.38	−0.05	ELODIE	4863 ± 5	2.727 ± 0.013	0.039 ± 0.005	
HD201377	8193	3.93	−0.47	ELODIE	8174 ± 10	3.801 ± 0.011	-0.04 ± 0.006	
HD201626	4550			PASTEL	4867 ± 16	1.526 ± 0.036	-1.704 ± 0.019	*lsf*
HD_202851					4599 ± 6	1.628 ± 0.017	-1.105 ± 0.009	*lsf*
HD204041	8100	4.03	−0.98	MILES	8582 ± 14	4.394 ± 0.009	-0.421 ± 0.012	
HD204155	5608	4.24	−0.9	MILES	5789 ± 11	3.979 ± 0.02	-0.737 ± 0.012	
HD204543	4617	1.31	−1.76	MILES	4660 ± 10	1.298 ± 0.024	-1.885 ± 0.014	
HD204587	4035	4.67		MILES	4082 ± 3	4.627 ± 0.006	-0.091 ± 0.007	

Table 6.1 (cont'd)

Name[a]	Literature compilation $T_{\rm eff}$ (K)	$\log g$ (dex)	[Fe/H] (dex)	catalog[b]	This work $T_{\rm eff}$ (K)	$\log g$ (dex)	[Fe/H] (dex)	flag[c]
HD205202	6498			PASTEL	6650 ± 9	4.131 ± 0.012	-0.478 ± 0.007	
HD205555	7186	3.81	−1.65	ELODIE	7325 ± 9	3.737 ± 0.011	0.203 ± 0.005	
HD205734	7828	3.91	−0.5	ELODIE	7883 ± 14	3.694 ± 0.016	-0.06 ± 0.008	
HD207222	8542	3.5	−1.15	MILES	9311 ± 54	4.07 ± 0.026	-0.282 ± 0.025	
HD207795	5126	4.46	0	ELODIE	5285 ± 4	4.537 ± 0.007	0.114 ± 0.004	
HD209290	3580			PASTEL	3684 ± 12	4.626 ± 0.025	-0.194 ± 0.027	
HD210295	4769	2.2	−1.39	MILES	4838 ± 12	2.098 ± 0.031	-1.316 ± 0.014	
HD211075	4350	1.5	−0.54	MILES	4338 ± 4	1.96 ± 0.013	-0.407 ± 0.006	
HD212516	3709	1.54	−0.24	NGSL	3715 ± 4	1.329 ± 0.027	-0.329 ± 0.018	
HD213042	4760	4.58	0.25	MILES	4520 ± 3	4.476 ± 0.007	0.136 ± 0.004	
HD214080	22186	3.3	−0.2	MILES	6984 ± 111	5.571 ± 0.089	-0.969 ± 0.173	*lsf*
HD216143	4496	1.27	−2.15	MILES	4656 ± 13	1.393 ± 0.033	-2.056 ± 0.017	
HD216219	5727	3.36	−0.39	MILES	5614 ± 13	2.91 ± 0.03	-0.483 ± 0.015	
HD217357	4125			PASTEL	3948 ± 3	4.605 ± 0.004	-0.062 ± 0.005	
HD217877	6021	4.35	−0.1	PASTEL	5855 ± 9	4.116 ± 0.015	-0.235 ± 0.01	
HD218502	6030	3.76	−1.84	MILES	6163 ± 6	4.075 ± 0.01	-1.813 ± 0.009	
HD218857	5082	2.41	−1.93	MILES	5128 ± 10	2.675 ± 0.028	-1.916 ± 0.011	
HD220662	4512	1.16	−1.79	PASTEL	4612 ± 11	1.277 ± 0.025	-1.825 ± 0.014	
HD220838	4450	1.2	−1.65	PASTEL	4436 ± 8	0.993 ± 0.018	-1.761 ± 0.012	
HD221170	4465	1.04	−2.1	MILES	4564 ± 16	1.217 ± 0.038	-2.087 ± 0.02	
HD222434	4499	1.33	−1.69	PASTEL	4510 ± 6	1.109 ± 0.012	-1.826 ± 0.008	
HD232078	3983	0.3	−1.73	MILES	4038 ± 13	0.512 ± 0.041	-1.65 ± 0.034	
HD250792	5440	4.29	−1.21	MILES	5481 ± 7	4.293 ± 0.011	-1.176 ± 0.008	
HD270110	5200	−0.5	−0.4	PASTEL				
HD271018	6200	0.1	−0.33	PASTEL	6778 ± 6	0.768 ± 0.006	-0.062 ± 0.004	
HD271182	6000	0.5	−0.53	PASTEL				
HD345957	5702	3.87	−1.51	MILES	5880 ± 11	3.879 ± 0.021	-1.384 ± 0.011	
HE0146-1548	4636	0.99	−3.46	AL				
HE1142-1422	6238	2.8	−2.84	PASTEL	6047 ± 13	3.91 ± 0.019	-2.277 ± 0.017	
HE1201-1512	5725	3.39	−3.92	PASTEL				
HE1204-0744	6500	4.3	−2.71	AL	6139 ± 60	3.815 ± 0.086	-2.389 ± 0.068	*lsf*
HE1207-3108	5294	2.85	−2.7	PASTEL	5753 ± 9	3.81 ± 0.013	-2.369 ± 0.011	
HE1346-2410								
HE1428-1950					4796 ± 4	2.125 ± 0.01	-0.929 ± 0.005	*lsf*
HIP100047								
HIP103039					3591 ± 3	-0.077 ± 0.021	-2.168 ± 0.022	
HIP66993					3665 ± 2	4.809 ± 0.004	-0.6 ± 0.006	
HIP70472					3945 ± 2	4.62 ± 0.003	-0.193 ± 0.003	
HIP75423					3449 ± 2	4.486 ± 0.006	-0.054 ± 0.005	
HIP84123					3668 ± 1	0.127 ± 0.009	-2.167 ± 0.009	
HIP96710					3691 ± 2	4.571 ± 0.005	-0.049 ± 0.005	
HIP064965	4888	4.78	−1.03	PASTEL	4489 ± 4	4.577 ± 0.009	-1.175 ± 0.01	
HV2555								
HV12149								
HV2255								*fail*
HV2360					3428 ± 4	0.515 ± 0.035	-1.112 ± 0.044	
HV2446								*fail*
IRAS06404+0311					3883 ± 12	0.246 ± 0.054	0.025 ± 0.033	
IRAS06498-1102								
IRAS09484-6242								
IRAS10019-6156								

Table 6.1 (cont'd)

Name[a]	Literature compilation				This work			
	$T_{\rm eff}$ (K)	$\log g$ (dex)	[Fe/H] (dex)	catalog[b]	$T_{\rm eff}$ (K)	$\log g$ (dex)	[Fe/H] (dex)	flag[c]
IRAS10151-6008					3692 ± 2	1.071 ± 0.015	0.011 ± 0.009	
IRAS14303-1042								
IRAS15060+0947								*fail*
J004900.4-732224								
J004932.4-731753								
J004950.3-731116					3855 ± 6	0.73 ± 0.036	-0.77 ± 0.029	
J005059.4-731914					3837 ± 4	0.549 ± 0.027	-1.073 ± 0.024	
J005101.9-731607					4314 ± 5	0.668 ± 0.01	-0.656 ± 0.007	
J005304.7-730409								
J005307.8-730747								
J005314.8-730601								
J005332.4-730501					4366 ± 10	1.055 ± 0.026	-0.677 ± 0.017	
J005422.8-730105								*fail*
J005531.0-731018								
J005622.2-730334					3907 ± 21	0.693 ± 0.103	-0.656 ± 0.075	
J005638.9-730452								
J005644.8-731436					3455 ± 2	5.477 ± 0.003	-2.795 ± 0.007	*lsf*
J005700.7-730751								
J005712.2-730704								*fail*
J005714.4-730121								*fail*
J005716.5-731052					3959 ± 8	0.367 ± 0.033	-1.303 ± 0.026	
J010031.5-730724					3947 ± 8	0.435 ± 0.051	-1.183 ± 0.033	
Kelu-1								
LHS320	3600	4.6	-0.6	PASTEL	3495 ± 2	4.854 ± 0.004	-0.559 ± 0.007	
LHS0318	3690	5.4	-1.26	PASTEL	3797 ± 16	4.9 ± 0.025	-0.805 ± 0.044	
LHS0343	4110	5.1	-1.74	PASTEL	3828 ± 2	4.806 ± 0.004	-1.004 ± 0.006	
LHS1841	4440	5.13	-1.47	PASTEL	4701 ± 4	4.712 ± 0.006	-1.453 ± 0.006	
LHS2065								*fail*
LHS2463	4540	5	-1.89	PASTEL	4805 ± 3	4.592 ± 0.006	-1.815 ± 0.006	
NGC_1904_153	4270	0.75	-1.37	PASTEL	4223 ± 6	0.563 ± 0.014	-1.727 ± 0.012	
NGC_1904_160	4270	0.75	-1.37	PASTEL	4289 ± 7	0.812 ± 0.017	-1.615 ± 0.013	
NGC_1904_223	4250	0.75	-1.36	PASTEL	4208 ± 3	0.626 ± 0.007	-1.53 ± 0.006	
NGC_2682_108	6213	3.93	-0.05	PASTEL	4183 ± 3	2.12 ± 0.013	-0.093 ± 0.005	
NGC_4147_230	4383	1.1	-1.3	PASTEL	4429 ± 9	0.989 ± 0.019	-1.799 ± 0.013	
NGC_5139_1627	4400	1.6	-1.45	PASTEL	4526 ± 15	1.51 ± 0.038	-1.193 ± 0.021	
NGC_5139_3812	3850	0.5	-1.1	PASTEL	3651 ± 4	0.711 ± 0.033	-0.825 ± 0.041	
NGC6397_211	4150	0.6	-2.1	PASTEL	4340 ± 5	0.707 ± 0.011	-2.022 ± 0.007	
NGC6838_1009	4350	1.45	-0.7	PASTEL	4531 ± 11	1.537 ± 0.031	-0.866 ± 0.016	
NGC6838_1037	4350	1.45	-0.7	PASTEL	4505 ± 11	1.934 ± 0.037	-0.897 ± 0.017	
NGC6838_1039	4050	0.8	-0.67	PASTEL	5075 ± 31	2.266 ± 0.08	-0.859 ± 0.035	
NGC6838_1053	4300	1.4	-0.68	PASTEL	4158 ± 6	1.512 ± 0.021	-0.925 ± 0.012	
NGC6838_1063	3950	0.7	-0.71	PASTEL	4576 ± 19	1.551 ± 0.055	-0.893 ± 0.029	
NGC6838_1066	4200	1	-0.87	PASTEL	4194 ± 22	1.645 ± 0.081	-0.959 ± 0.046	
NGC6838_1071	3950	0.7	-0.71	PASTEL	4321 ± 13	1.761 ± 0.048	-0.938 ± 0.025	
NGC6838_1073	4200	1	-0.87	PASTEL	4715 ± 18	2.312 ± 0.052	-0.888 ± 0.023	
NGC6838_1075	4100	0.95	-0.66	PASTEL	4722 ± 39	2.32 ± 0.106	-0.87 ± 0.05	
NGC6838_1077	4100	0.95	-0.66	PASTEL	3939 ± 1	1.446 ± 0.007	-0.846 ± 0.005	
NGC6838_1078	4100	0.95	-0.66	PASTEL	4288 ± 5	1.994 ± 0.019	-0.167 ± 0.008	
NGC_7078_1079	4695	1.55	-2.37	PASTEL	4641 ± 22	1.365 ± 0.058	-2.36 ± 0.026	
OGLE204664c4					4977 ± 5	4.594 ± 0.009	0.169 ± 0.005	
OGLE212654c8					4592 ± 16	2.623 ± 0.046	0.253 ± 0.016	

Table 6.1 (cont'd)

Name[a]	Literature compilation $T_{\rm eff}$ (K)	log g (dex)	[Fe/H] (dex)	catalog[b]	This work $T_{\rm eff}$ (K)	log g (dex)	[Fe/H] (dex)	flag[c]
OGLE6263C6					4174 ± 6	2.484 ± 0.024	0.303 ± 0.007	
OGLE-101167c8					4646 ± 86	2.373 ± 0.252	-0.3 ± 0.106	
OGLE-27350c4					4737 ± 39	2.912 ± 0.18	-0.415 ± 0.084	
OGLE-63839					4016 ± 34	1.88 ± 0.155	-0.732 ± 0.087	
OGLE-75382c8					4334 ± 34	2.627 ± 0.128	0.367 ± 0.038	
OGLE-82717					5602 ± 36	4.072 ± 0.068	0.258 ± 0.03	
BUL-SC01-0235								*fail*
BUL-SC01-1821								
BUL-SC03-1890								
BUL-SC03-3941								
BUL-SC04-1709								
BUL-SC04-4628								
BUL-SC04-9008								
BUL-SC06-2525								*fail*
BUL-SC08-1687								
BUL-SC13-0324								
BUL-SC13-1542								
BUL-SC15-1379	6836			PASTEL				
BUL-SC15-2106								
BUL-SC16-1428								
BUL-SC17-1595								
BUL-SC19-2302								*fail*
BUL-SC19-2332								
BUL-SC19-2948								
BUL-SC22-1319								
BUL-SC24-0989								
BUL-SC26-0532								
BUL-SC30-0707								*fail*
BUL-SC33-0357								
BUL-SC33-4149								
BUL-SC36-2158								
BUL-SC41-3304								
BUL-SC41-3443								
R Cha								
RU Pup								
SHV0448341-691510								
SHV0452361					2940 ± 86	0.351 ± 0.696	-0.785 ± 0.314	*lsf*
SHV0500412-684054					4030 ± 71	0.04 ± 0.203	-1.352 ± 0.169	*lsf*
SHV0501215								
SHV0502469-692418								
SHV0503595					3847 ± 7	0.314 ± 0.067	-1.639 ± 0.067	*lsf*
SHV0504353								
SHV0506368								
SHV0510004								*fail*
SHV0515313-694303					3348 ± 12	-0.118 ± 0.092	-0.8 ± 0.129	
SHV0515461					3074 ± 18	1.498 ± 0.066	0.072 ± 0.086	*lsf*
SHV0517337-725738								*fail*
SHV0518161-683543								
SHV0518222								
SHV0518331-685102					3326 ± 12	0.071 ± 0.107	-0.132 ± 0.121	
SHV0518570								

Table 6.1 (cont'd)

Name[a]	Literature compilation				This work			
	$T_{\rm eff}$ (K)	$\log g$ (dex)	[Fe/H] (dex)	catalog[b]	$T_{\rm eff}$ (K)	$\log g$ (dex)	[Fe/H] (dex)	flag[c]
SHV0518571-690729								*fail*
SHV0520036-692817								
SHV0520261-693826					4360 ± 7	1.177 ± 0.017	-0.25 ± 0.01	
SHV0520342-693911					3302 ± 9	0.264 ± 0.094	-0.303 ± 0.113	
SHV0520427-693637								*fail*
SHV0520498-692715								
SHV0520505								
SHV0522380								
SHV0523357								
SHV0523371-713351					3868 ± 11	1.07 ± 0.074	-0.64 ± 0.048	
SHV0525012-694829					3705 ± 4	0.524 ± 0.031	-0.315 ± 0.025	
SHV0525478								
SHV0525543					3220 ± 41	1.406 ± 0.206	-0.161 ± 0.173	
SHV0526364					3768 ± 4	0.514 ± 0.027	-0.133 ± 0.02	
SHV0527058-693746								
SHV0527072-701238								*fail*
SHV0527122-695006								
SHV0528537					7800 ± 348	4.147 ± 0.317	-1.301 ± 0.36	*lsf*
SHV0529222-684846								
SHV0529355-694037								
SHV0529467					6307 ± 1	2.643 ± 0.702	0.865 ± 0.13	*lsf*
SHV0530380-702618					3343 ± 15	0.165 ± 0.161	0.092 ± 0.14	
SHV0531398-701050								
SHV0531582-701623								
SHV0533015								*fail*
SHV0533130-702409								
SHV0534578-702532								
SHV0535237-700720								
SHV0536139								
SHV0542111-683837					4116 ± 94	1.13 ± 0.441	-1.397 ± 0.303	*lsf*
SHV0543367					3407 ± 9	-0.045 ± 0.104	0.16 ± 0.088	
SHV0549503					3117 ± 5	0.309 ± 0.036	-0.31 ± 0.028	
SHV0606101								*fail*
SV_HV_11223	3500	0	−0.38	PASTEL	3635 ± 6	0.223 ± 0.065	-0.839 ± 0.078	
SV_HV_11366	3450	0	−0.42	PASTEL				
SV_HV_12179	3400	0	−0.34	PASTEL				*fail*
SV_HV_1963	3350	−0.27	−0.43	PASTEL	3306 ± 7	0.265 ± 0.072	-0.345 ± 0.089	
TCae					7609 ± 18	-0.099 ± 0	-2.456 ± 0.054	*lsf*
TLE NGC 6522 435								
SgrI11								
SgrI117								
SgrI55								
TUCar								*fail*
UCrt					3266 ± 1	0.494 ± 0.014	-0.517 ± 0.016	
V_AL_Mon					3226 ± 9	0.479 ± 0.088	-0.464 ± 0.087	
VBHTel					2950 ± 5	5.002 ± 0.006	-0.07 ± 0.009	*lsf*
V_CI_Vel					4067 ± 14	0.262 ± 0.038	-0.838 ± 0.044	*lsf*
V_DG_Peg					2926 ± 13	-0.063 ± 0.06	-0.362 ± 0.048	
V_EY_Eri								
VFRHer					3169 ± 8	0.373 ± 0.062	-0.081 ± 0.055	
V_RR_Ara								*fail*

Table 6.1 (cont'd)

Name[a]	Literature compilation $T_{\rm eff}$ (K)	$\log g$ (dex)	[Fe/H] (dex)	catalog[b]	This work $T_{\rm eff}$ (K)	$\log g$ (dex)	[Fe/H] (dex)	flag[c]
V_RY_CrA					3476 ± 3	-0.193 ± 0.016	-1.401 ± 0.029	*lsf*
VSYPav								*fail*
V_U_Psc					3363 ± 1	0.214 ± 0.015	-0.542 ± 0.023	
V_UZ_Cen	5845	1.86	0.02	PASTEL				
V_V_CrA					5618 ± 1633	0.539 ± 1.81	-1.605 ± 1.88	*lsf*
VVCrv					3993 ± 13	5.092 ± 0.014	-1.884 ± 0.016	*lsf*
V_V335_Aql								*fail*
V_V5475_Sgr	4900	2.7	−0.81	PASTEL	3179 ± 6	0.178 ± 0.056	0.617 ± 0.033	
VXLib								*fail*
V_XZ_Her								*fail*
V_Y_Sge								
V348Sco					2944 ± 17	0.344 ± 0.132	-0.277 ± 0.045	
V354Cen					3076 ± 10	0.928 ± 0.063	-0.22 ± 0.048	
V874_Aql								
WX_Psc								
YHya	2769		−0.1	PASTEL				*fail*

[a]The name of the star, in the form that they match the file names of the spectra. This can deviate slightly from the form that Simbad recognizes.

[b]References as described in Section 2.3.

[c]The flag *fail* indicates a star for which the fit failed for one or more of the three stellar atmospheric parameters, the flag *lsf* indicates fits with bad LSF determinations.